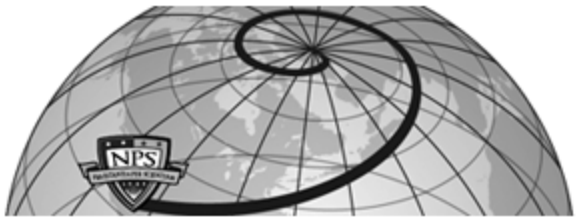

PROPERTIES OF SOME ENERGY LEVELS IN PHOSPHORUS - 30

PHARO A. PHELPS

PROPERTIES OF SOME ENERGY LEVELS IN PHOSPHORUS-30

* * * * *

Pharo A. Phelps

PROPERTIES OF SOME ENERGY LEVELS IN PHOSPHORUS-30

by

Pharo A. Phelps

Lieutenant Commander, Civil Engineer Corps

United States Navy

Submitted in partial fulfillment of
the requirements for the degree of

DOCTOR OF PHILOSOPHY
IN
PHYSICS

United States Naval Postgraduate School
Monterey, California

1963

PROPERTIES OF SOME ENERGY LEVELS IN PHOSPHORUS-30

by

Pharo A. Phelps

This work is accepted as fulfilling
the dissertation requirements for the degree of
DOCTOR OF PHILOSOPHY
IN
PHYSICS
from the
United States Naval Postgraduate School

ABSTRACT

The excitation function for the $Si^{29}(p, \gamma)P^{30}$ reaction has been experimentally determined in the proton energy range from 1420 kev through 2160 kev. Unreported resonances in this reaction have been identified at 1975, 2033, 2075, and 2117 kev with estimated errors of $\pm$ 4 kev. Gamma spectra at these resonances are obscured by contaminant radiation but suggest complex decay schemes. Double angular correlation measurements have been made at the 1470-kev resonance indicating a resonance level spin of 2+, or less probably, 2-. The level at 4.50 Mev is shown to probably have a spin of 2+, or less probably, 3+ rather than 0+ as has been predicted.

TABLE OF CONTENTS

		Page
I	INTRODUCTION	1
II	DESCRIPTION OF EQUIPMENT	5
	1. Experimental Layout	5
	2. Accelerator	5
	3. Target Assemblies	5
	4. Shielding	10
	5. Correlation Table	12
	6. Gamma-ray Detectors	12
	7. Electronics	12
III	EXPERIMENTAL PROCEDURE	18
	1. Target Preparation	18
	2. Excitation Function Measurements	19
	3. Measurement of Saturation Activity	20
	4. Gamma-ray Spectra	21
	5. Measurements at 1470 kev	23
IV	EXPERIMENTAL RESULTS	26
	1. Excitation Function	26
	2. Gamma-ray Spectra at 1975, 2033, 2075 and 2117 kev Resonances	32
	3. 1470-kev Resonance Decay and Intensities	36
	4. Angular Correlations at the 1470-kev Resonance	39
	5. Summary of Results	49
V	ACKNOWLEDGEMENTS	62
VI	APPENDICIES	63
	1. Theoretical Description of Double Angular Correlations	63
	2. Computer Programs and Analysis	73
VII	REFERENCES	116

LIST OF ILLUSTRATIONS

Figure		Page
1.	The Lower Energy Levels in P^{30}	3
2.	Experimental Layout	6
3.	Photograph of Target Area	7
4.	Target Assembly Details	8
5.	Photograph of Cold Trap Area	11
6.	Photograph of Correlation Table	13
7.	Block Diagram of Electronics	14
8.	Gamma-ray Yield Curve	27
9.	Gamma-gamma Coincidence Yield Curve	28
10.	Gamma-ray Spectrum at 1470 kev	37
11.	Decay Scheme at 1470-kev Resonance	38
12.	Spectrum and Fit for Correlation Run number 3-5 at 90^{o}	40
13.	Distribution Coefficients for the 4.50-Mev Gamma Ray	42
14.	Fits of Combined Experimental Data to Theoretical Curves for 4.50-Mev Gamma Ray	43
15.	Contour Plots for $1+ \rightarrow 1+$ Transition	51
16.	Contour Plots for $2+ \rightarrow 1+$ Transition	52
17.	Contour Plots for $2- \rightarrow 1+$ Transition	54
18.	Contour Plots for $2+ \rightarrow 2+ \rightarrow 1+$ Transition	56
19.	Contour Plots for $2- \rightarrow 2+ \rightarrow 1+$ Transition	58
20.	Contour Plots for $2+ \rightarrow 3+ \rightarrow 1+$ Transition	60

LIST OF TABLES

Table		Page
1	Spectrometer Calibration Gamma rays	24
2	Resonances Observed in the $Si^{29}(p,\gamma)P^{30}$ Reaction	29
3	Half Life of Postbombardment Decay of P^{30}	30
4	Intensity of Postbombardment Annihilation Radiation	31
5	Gamma-ray Intensities at Resonance Energies of 1975, 2033, 2075, and 2117 kev	33
6	Relative Gamma-ray Intensities at the 1470-kev Resonance	34
7	Double Angular Correlation Coefficients at 1470-kev Resonance	35
8	Relative Penetration Factors for 1470-kev Protons	72
9	Coulomb Phase Factors for 1470-kev Protons	72

I. INTRODUCTION

As a result of successive refinements and extensions of the collective model of nuclear structure, it has been possible to extend its applicability into the region of intermediate mass nuclei ($20 \leqslant A \leqslant 40$). By considering the outer nucleons to be strongly coupled to the nuclear core, excited states in Al^{25}, Mg^{25}, Al^{28}, and Si^{29} have been interpreted as collective rotational excited states with considerable success.[1-4] More recently states in P^{31} and Si^{30} have been identified with collective vibrational states of a weakly coupled collective model.[5,6] The experimental collection of information on the states of intermediate mass nuclei serves to verify the theoretical models, to determine the parameters which enter into descriptions of the models, and to permit the extensions and refinements to theory necessary for a more adequate description of nuclei. Of particular relevance to the present investigation is the prediction based on the weakly coupled collective model applied to $A \approx 30$ nuclei that the 4.50-Mev level of P^{30} has a spin-parity of $0+$.[6] In the present work the experimental determination of this value has been the object of double angular correlation measurements performed on the gamma rays observed at the 1470-kev resonance in the $Si^{29}(p,\gamma)P^{30}$ reaction.

Determinations of resonance energies in the $Si^{29}(p,\gamma)P^{30}$ reaction have been carried out by numerous investigators since 1941.[7-15] The proton energies which have been employed in these investigations extend over the range 300 to 1950 kev.

In addition to detecting resonances and measuring the energies at which they occur, the allied problem of analyzing the associated gamma-ray spectra has been the object of an increasingly large amount of research commensurate with improvements in gamma-ray spectroscopy techniques and instrumentation.

Investigations of the gamma rays which arise from deexcitation of the excited states of P^{30} were begun in 1954 by Endt, Kluyver, and Van der Leun.[16] They studied the $Si^{29}(p,\gamma)P^{30}$ reaction at resonances occurring at proton energies of 414 kev and 326 kev and assigned spin, parity, and isotopic spin to the ground state and the first excited state of P^{30} premised on gamma-transition probabilities, shell model considerations and the isotopic spin multiplet formalism. In 1956 Broude et al.[17]

confirmed the assignments to the first excited level by measuring the angular distribution of the gamma-rays at the 414-kev resonance. They also detected five new states in P^{30} by examining gamma radiation arising from the same reaction at resonances occurring at proton energies of 696 kev and 737 kev.

Investigations by Lee and Mooring[17] and by Endt and Paris[18], who studied the $S^{32}(d,\alpha)P^{30}$ reaction, showed the first excited state to be in reality a close doublet. The latter investigators were able to accurately determine the energies of 30 excited levels of P^{30} up to excitation energies of 5.8 Mev by magnetic analysis of the alpha-particle groups from this reaction.

In 1958 Van der Leun and Endt[19] reinvestigated the four aforementioned resonances, studying the decay schemes by analysis of gamma-ray spectra, coincidence measurements, and angular distribution measurements. From this work came decay schemes, branching ratios, and assignment of spin-parities and isotopic spins to the four resonance levels and to five other excited levels of P^{30}, including the two states of the above mentioned doublet. During 1962 the gamma-ray spectra associated with the proton resonances at 1330 kev[20] and the resonances at 1375 kev and 1505 kev were investigated.[21] Proposed decay schemes were advanced for these resonances and spin-parity assignments made to three levels of P^{30}. One of the more comprehensive investigations of the $Si^{29}(p,\gamma)P^{30}$ reaction is that of Baart et al.[22], who studied six resonances and proposed decay schemes for them. Firm spin-parities were assigned to six low-lying levels and tentative assignments were made to four more levels. The most recent investigation of the reaction is that by Moore.[23] As a result of this work decay schemes were proposed for resonances at 1302, 1470, 1505, 1640, 1686, 1748, and 1772 kev, and spin-parities were determined for three resonance levels and two intermediate levels. The present knowledge of the quantum states of the lower P^{30} levels resulting from the above investigations is summarized in Fig. 1. Two compilations which summarize important experimental results of the above mentioned investigations are the Nuclear Data Sheets[24] and the compilation of information on the energy levels of nuclei with Z = 11 to Z = 20 by Endt and Van der Leun.[25]

Energies in MEV, T values are isotopic spins,
spin-parities in parentheses are less likely alternates.

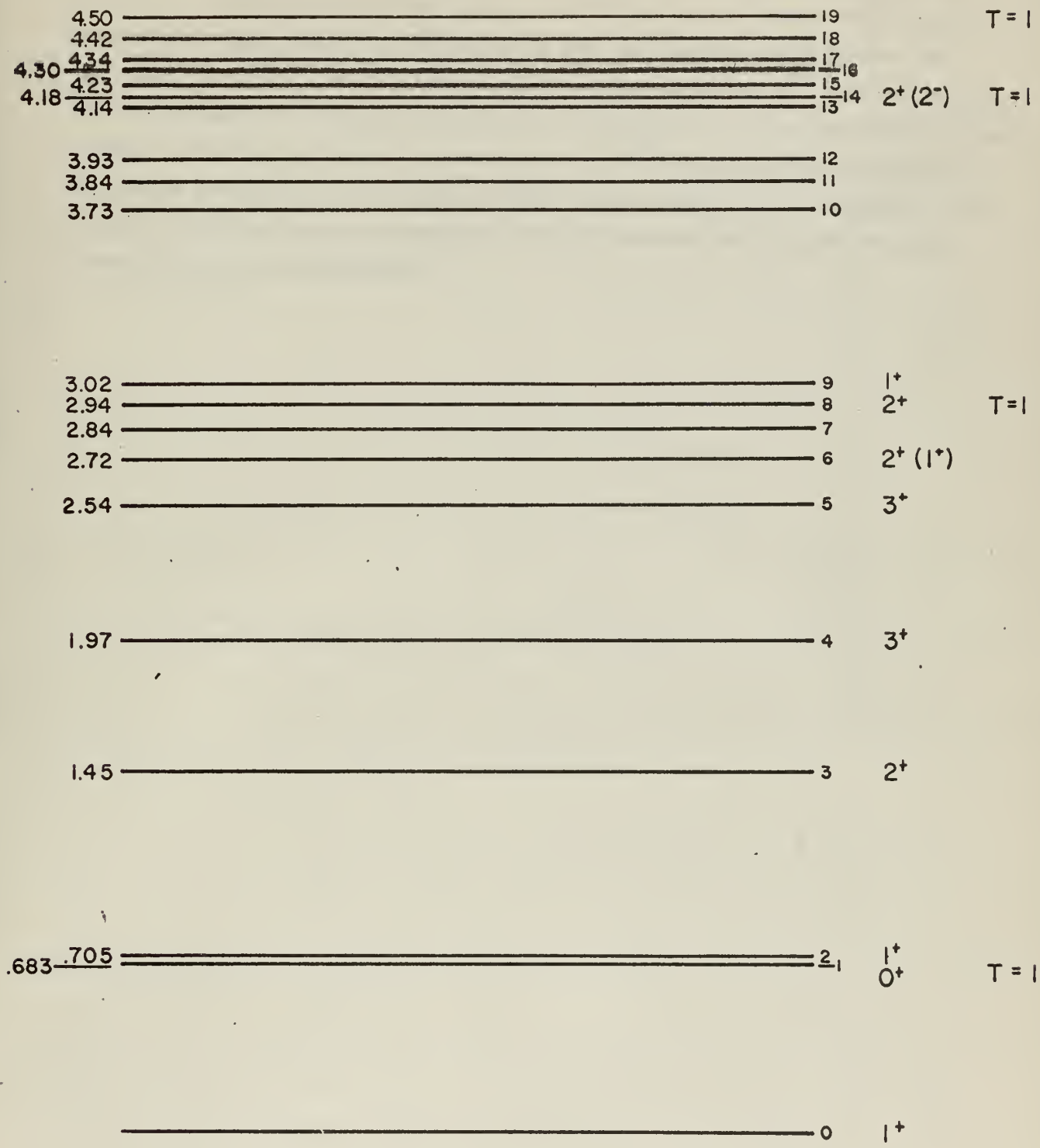

THE LOWER ENERGY LEVELS OF P^{30}

FIGURE 1.

The purpose of the present work has been to investigate resonances in the $Si^{29}(p,\gamma)P^{30}$ reaction in the proton energy range from 1950 kev to 2150 kev which has not previously been reported on, and to investigate the gamma-ray spectrum associated with the known resonance occurring at 1470 kev. In particular, the angular distributions of gamma rays at the latter resonance have been measured in a double angular correlation experiment to obtain information on the 4.50-Mev level in P^{30}. Additionally, some information has been obtained from examination of spectra taken at the higher resonances although contamination by F^{19} hampered this work. The following sections of this paper describe the experimental equipment, procedure, and data analysis employed, and the results which have been obtained from the investigation.

II. DESCRIPTION OF EQUIPMENT

1. Experimental Layout

Fig. 2 indicates the general arrangement of equipment used in this experiment. Fig. 3 is a photograph of the target area showing the correlation table tilted into a vertical plane.

2. Accelerator

The 2-Mev Van de Graaff horizontal electrostatic accelerator of the U.S. Naval Postgraduate School, manufactered by the High Voltage Engineering Corporation, was used in this work as a source of protons. The radio frequency ion source is of the type described by Moak.[26] A proton spin-resonance fluxmeter for accurately measuring the analyzing magnet's field was installed furing the course of the work. An error signal from the fluxmeter was used in a feed back loop to the power supply of the beam analyzing magnet to hold the field strength automatically at a set value. This feature simplified the maintenance of a given resonance energy for long bombardment times without "slipping off".

A current integrator of the vacuum tube electrometer type was used to measure beam current. High stability plastic insulated capacitors were used to collect the charge. The voltage across the capacitor in use was applied to the grid of a 954 acorn tube, whose output fired a Schmidt trigger circuit at a preselected voltage level. The trigger output actuated other circuitry to discharge the capacitor and advance a Veeder-Root cycle counter after each cycle.

3. Target Assemblies

Two types of targets and target mounts were developed and used in this experiment. These are shown in Fig. 4. For resonance and coincidence measurements, which were made in the plane perpendicular to the beam, the target backing consisted of a one-half-in.-diameter flanged copper hemisphere held against a flat copper boss on the mount by a threaded retaining ring. This assembly was designed with the beam direction as a symmetry axis so that it can be used for triple correlation experiments in the perpendicular plane with no perturbations from target geometry. For the double correlations, measured in the horizontal plane containing the beam, target backings were 0.046 cm thick copper strips clamped in a copper mount. Both types of backings and mounts were vacuum

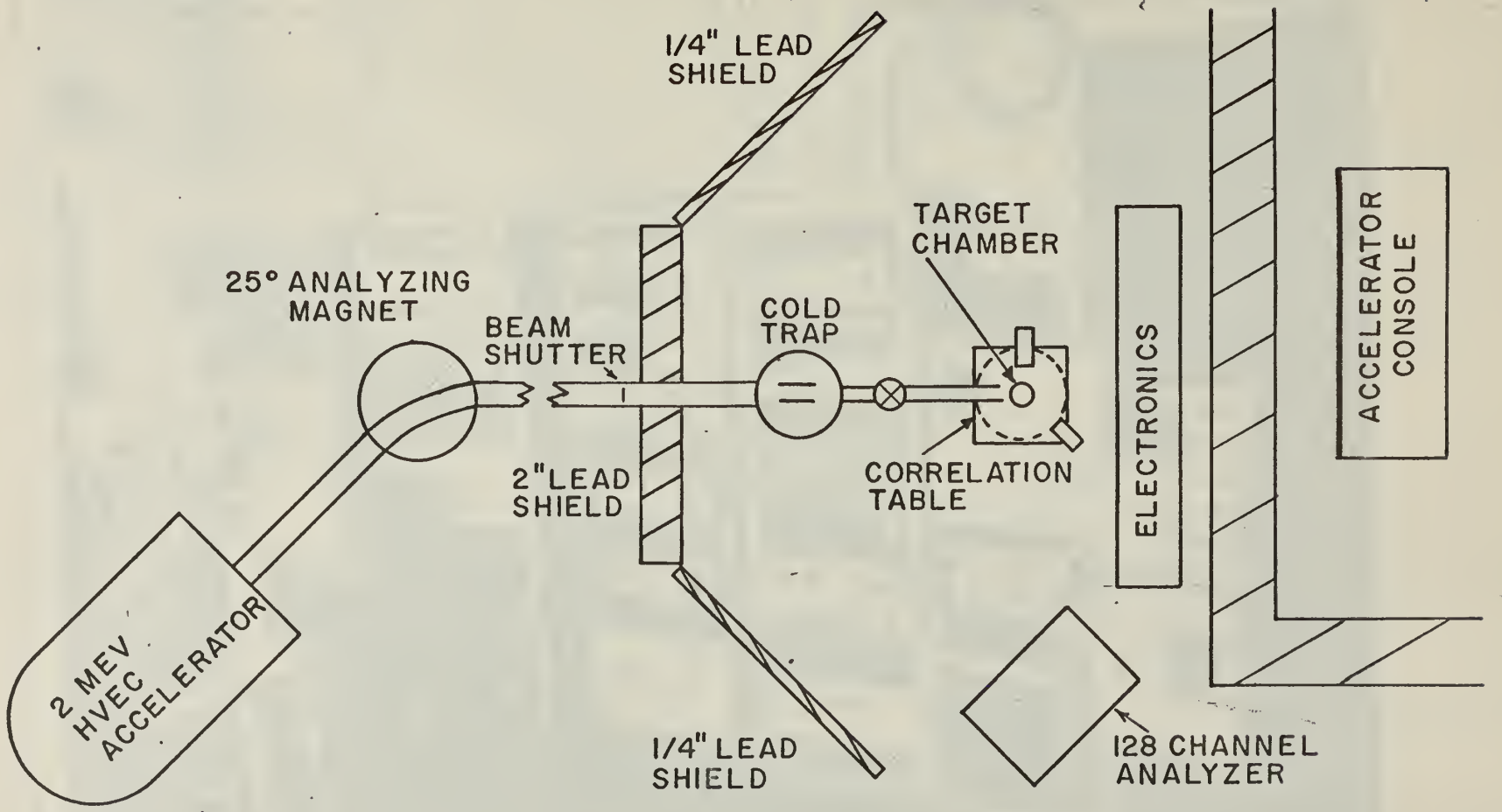

FIGURE 2. EXPERIMENTAL LAYOUT

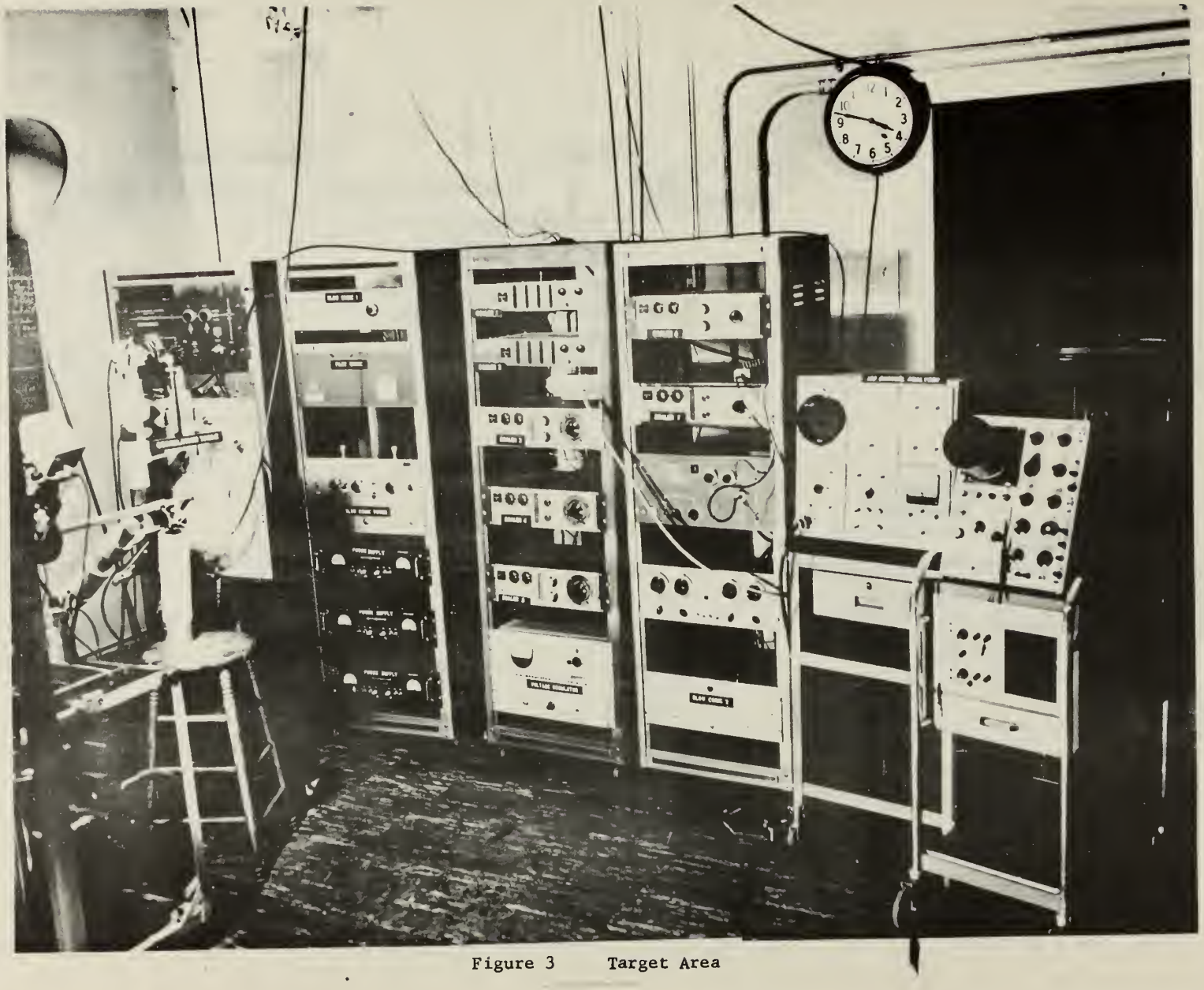

Figure 3 Target Area

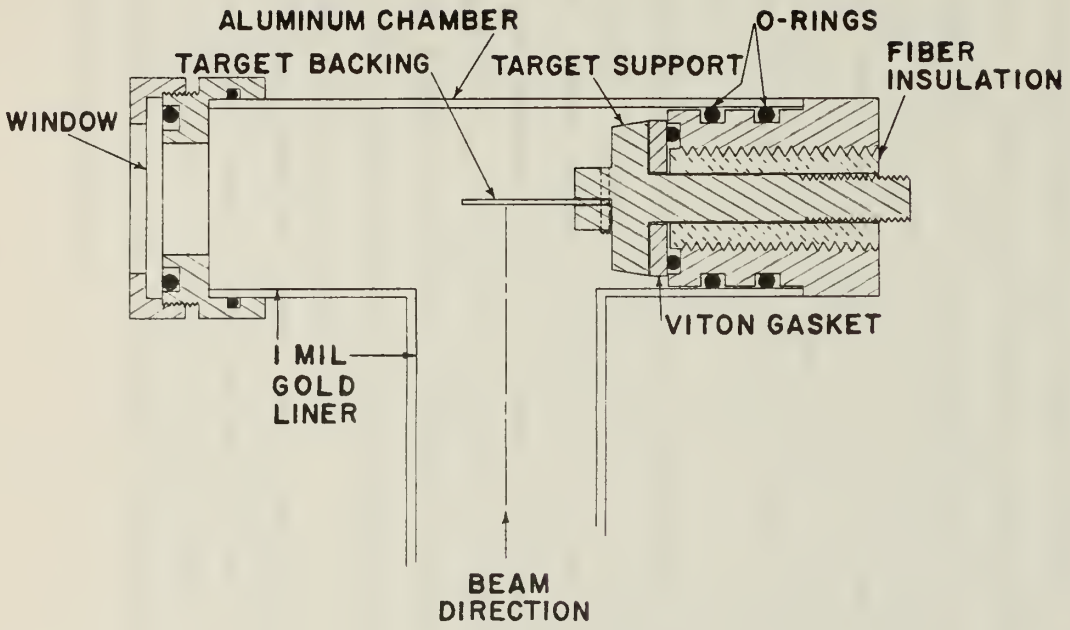

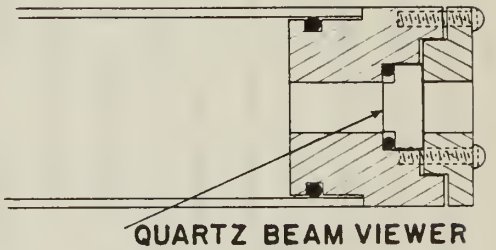

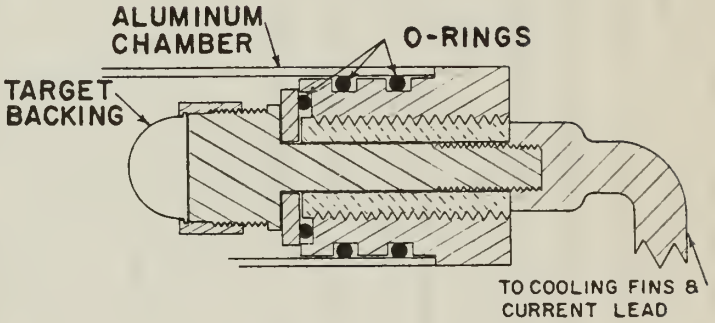

FIGURE 4. TARGET ASSEMBLY DETAILS

plated with a layer of gold thick enough to stop incident protons. For both geometries the target mount was fitted inside one end of a one-in. diameter tubular chamber, the axis of which coincided with the beam path. Both target assemblies were designed so as to keep mass in the target vicinity to a minimum. Competing with this requirement was the need to cool the target in order to prevent any appreciable target material evaporation. Maximum possible beam intensities were desired so as to take advantage of the better counting statistics which accompany high yields. Still another requirement of angular correlation measurements is a small target spot to approximate a point source of gamma rays. A beam collimator consisting of two five-mil tantalum discs separated by 0.4 in. was mounted in a brass holder 38 in. from the target. A 0.096-in. diameter collimating aperture was followed by a 0.098-in. hole in the second disc for the purpose of stopping protons scattered from the edge of the collimating disc. A cylindrical lead shield surrounded the collimator in order to attenuate any gamma rays produced here.

As is described in Chapter III, target material was evaporated directly onto the gold-plated copper backings to permit good heat conduction. Initially, a hollow copper target backing through which coolant could be circulated was tried, but was abandoned for a simpler solid copper backing cooled by conduction through a finned copper extension leading to an external Dewar flask. Liquid air in the Dewar proved to be convenient as a coolant at high beam powers and, below about ten watts, target power dissipation by forced air cooling of the target extension fins proved adequate.

After unsuccessful trials of Lucite and glass target tubes, aluminum was finally adopted for this purpose. An auxiliary target assembly with a quartz window target was used to accurately center the proton beam spot. The target chamber tube, which was insulated from ground at both ends, was maintained at a negative potential of 300 volts relative to ground in order to suppress secondary electrons from the target. In order to prevent recoil protons from exciting aluminum resonances, the target tube was lined with one-mil gold foil.

The hemispherical copper target backings for measurements in the plane perpendicular to the beam were needed in some quantity, so were "mass produced" in a small hand forge made for this purpose. A surface which needed only minor polishing and cleaning before gold plating was obtained in this manner.

A frequently troublesome feature of (p,γ) investigations is the gradual accumulation of carbon on the target as a result of cracking of pump oil vapor by particle bombardment. To reduce this difficulty, advantage was taken of an 8-in. glass cross which was mounted between the target diffusion pump and the target chamber as shown in Fig. 5. A special liquid air cold trap was constructed and installed in this cross to serve a dual purpose. First, it functioned as an ordinary cold trap with a large surface of copper vanes suspended from the coolant reservoir to provide an optically dense path from the diffusion pump thus permitting the vacuum to be routinely maintained close to 10^{-7} Torr. The second feature of the trap was a 1-in. diameter copper pipe piercing the vanes which the proton beam traversed. At high vacuum the proton beam functions effectively as a pump, transporting gases and vapor encountered in its path. When the beam passes through the restricted cold pipe for 6 in. before entering the target chamber, it was reasoned that its drifting retinue of condensable vapor contaminants would be largely trapped by the cold inner wall. The results from use of the trap support this idea since only minor discoloration was observed on targets compared with that which occurred when the trap was not used, and no increase in bombardment energy was found necessary as targets aged.

4. Shielding

To reduce the radiation level at the target resulting from bremsstrahlung and X-rays caused by electrons accelerated toward the high voltage accelerator terminal, a considerable amount of lead shielding was erected. A 2-in.-thick lead wall, 5 ft. high and 4 ft. wide, was placed between the energy control slits and the beam collimator. In addition, two lead screens 1/4-in. thick and each 5 ft. by 4 ft. were bolted onto a caster supported steel framework constructed for this purpose. The mobility of the screens permitted their placement to minimize the radiation level at the target and also allowed easy removal for access to the target area. Although the above-described shielding offered some reduction in natural background radiation, (notably the 1.46-Mev K^{40} gamma ray) it was not feasible to screen specifically against background without either increasing scattered target radiation at the detectors or utilizing an excessive amount of lead.

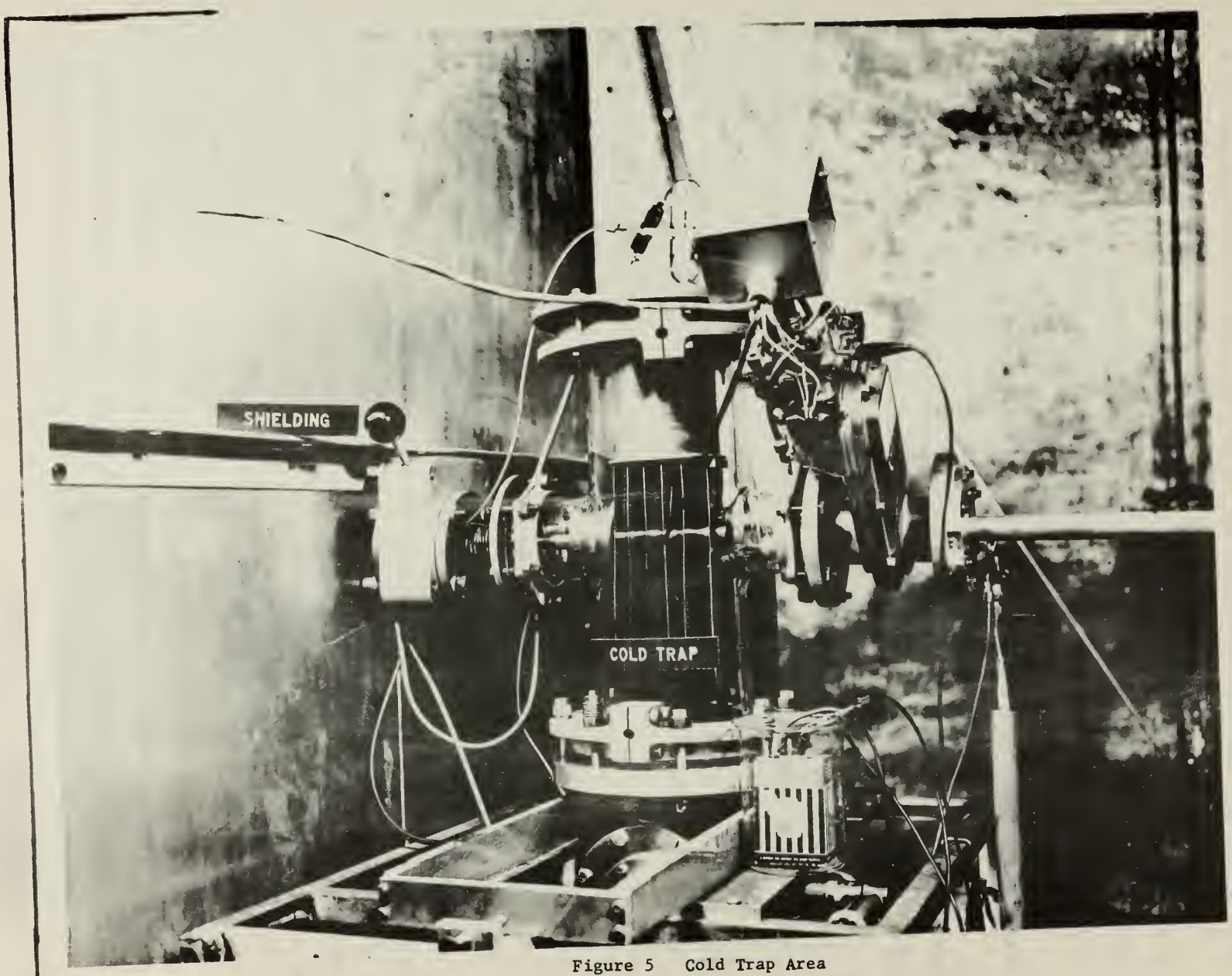

Figure 5 Cold Trap Area

5. Correlation table

A correlation table shown in Fig. 6 was built for this experiment to support the gamma-ray detectors and to permit their accurate positioning with respect to the target. A steel base plate mounted on casters supported a hollow magnesium column upon which the table was mounted. Screw jacks in the base plate were extended when the apparatus was in place to hold the table in position and to allow accurate vertical adjustment. The table itself consisted of a movable graduated aluminium disc which was mounted concentrically on a fixed aluminum support plate. Slides mounted on the disc and on the support plate held mounts for the two gamma-ray detection assemblies. The mounts were positioned in the slides by threaded rods which allowed the detectors to be set accurately at distances from 1/2 in. to 6 in. from the target position. The detection assembly mounted on the disc could be positioned in angle with respect to the fixed detector in 12 min. increments of arc by means of an adjusting gear meshing with gear teeth on the periphery of the disc. The entire table assembly was attached to the magnesium support column by a hinge so that it could be tilted into either a horizontal or vertical plane, permitting measurements to be taken in either the horizontal plane containing the proton beam or in the plane perpendicular to the beam. The first named arrangement is designated herein as geometry A and the latter as geometry B.

6. Gamma-ray detectors

The gamma-ray detection assemblies were supported with their centerlines 8 3/4 in. above the table. They each consisted of a 3 in. x 3 in. cylindrical sodium iodide (thallium activated) crystal integrally mounted with a Dumont 6363 photomultiplier tube supplied by the Harshaw Chemical Company. In the earlier phases of this work, similar 2 in. x 2 in. crystals mounted with Dumont 6292 tubes were used. The resolution of the 3-in. crystals, measured after the signal had traversed a 12-microsecond delay line input to the pulse height analyzer, was 9% for the 0.662-Mev Cs^{137} gamma ray. A 6AK5 cathode follower was constructed into each detector mount to serve as a preamplifier.

7. Electronics

The electronic equipment and circuitry for processing signals from the detectors were planned so as to permit considerable flexibility in experimental applications. A block diagram of the basic layout is shown in Fig. 7.

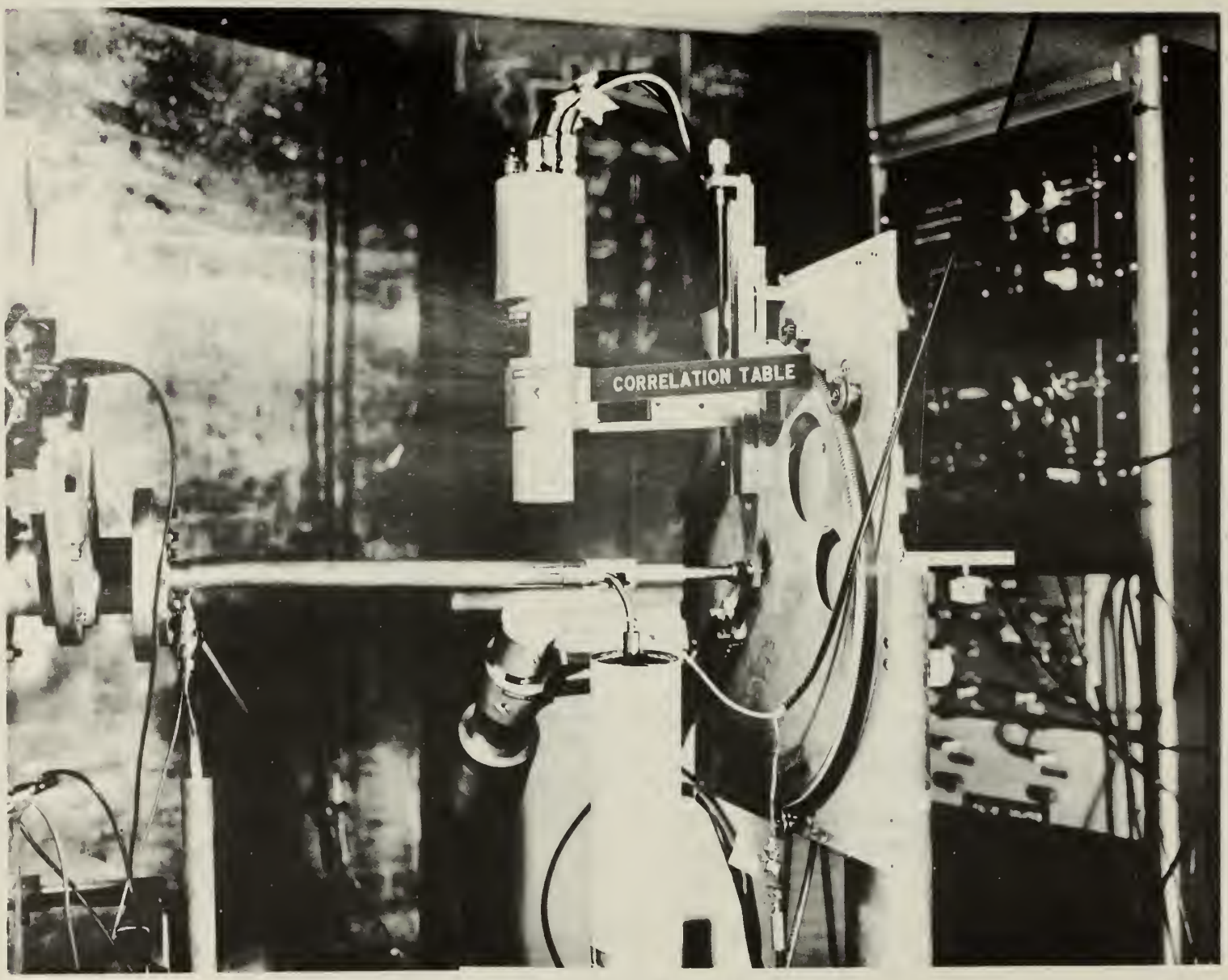

Figure 6 Correlation Table

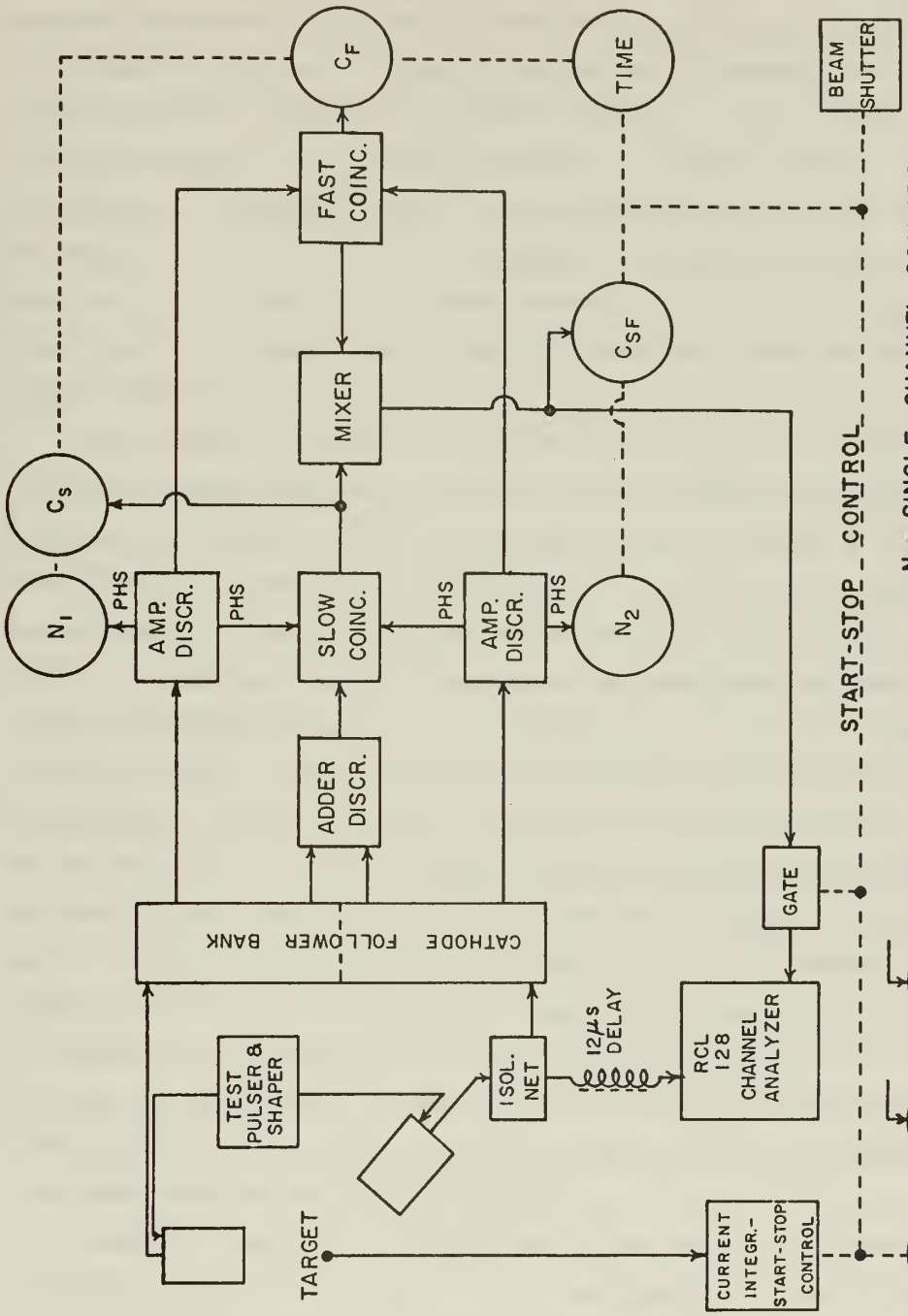

FIGURE 7. BLOCK DIAGRAM OF ELECTRONICS

The system is composed of an RCL 128-channel pulse height analyzer to record pulse height spectra, a slow-fast-sum coincidence analyzer, and scalers for recording various outputs.

It was found that requirements for the detector output signal by several components, including a monitor oscilliscope, tended to overload the preamplifiers and to permit unacceptable interaction of subsequent stages with each other through the coupling of their inputs. To avoid this problem a bank of six cathode followers was constructed. A bussing arrangement made it possible to feed the grids of the followers from either one of two busses or from an individual input, so that up to six pieces of equipment could be driven by the same input pulse with no interaction and with practically no signal loss. Each follower was provided with an individual output gain control.

The output of either detector as desired was also fed directly into the pulse height analyzer through a simple resistance isolation network. From the resistance network the signal passed through a terminated 1350-ohm delay line to allow time for formation of gating pulses needed for coincidence spectra. Several methods of injecting a signal into the analyzer were tried inasmuch as this equipment was designed to accept an input only from a photomultiplier tube connected directly into the preamplifier assembly provided. This was not an acceptable practice because there existed no convenient means of signal extraction for other purposes, and because the preamplifier utilized a high-voltage supply which required running the photomultiplier cathode at a high negative potential with respect to the tube shield with the attendant probability of tube damage. The procedure adopted as most successful was to apply the signal from the delay line to the anode pin of a 14-pin tube base which was connected directly into the analyzer preamplifier. It was also necessary to incorporate a gate pulse-forming network into the analyzer in order to meet the gating pulse specifications required by this equipment.

Gamma-ray spectra were obtained by gating the analyzer with the discriminator output pulses from the linear amplifier fed by the same detector. This procedure excluded a weak precursor pulse which was transmitted by the delay line input, by not gating the analyzer on until a few microseconds before arrival of the delayed pulse. No significant loss in detector resolution resulted from leaving the delay line in the input for

ordinary gamma-ray spectra, and it was found quite convenient to be able to switch from these singles spectra to coincidence spectra without change in analyzer calibration.

For the observation of coincidence spectra, the analyzer was gated by the slow-fast coincidence output. The basic slow-fast coincidence system assembled for this experiment has been described elsewhere.[27] In this system the output from an Atomic Instrument Company slow coincidence unit accepting up to four inputs was combined in a diode mixer with the fast coincidence unit output to obtain the slow-fast coincidence output signal. The fast unit, based on the circuit of Draper and Fleischer,[28] detects coincidences between amplified pulses from the scintillation detectors with a resolution time as low as ten ns. For pulses spanning a large amplitude range, however, more dependable operation was obtained when the resolving time was increased to about 80 ns. This was due to an observed amplitude dependence of the shape of the leading edge of the amplified pulse, to which the fast unit is sensitive.

Several modifications have been made to the coincidence system which do not appear in the previous description. The diode mixer unit for combining the slow and fast coincidence outputs has been modified by inserting a Schmidt trigger between the adding stage and the output stage in order to clip the sum pulse and improve output-pulse characteristics. The fast unit has been modified by providing a variable delay line in the input in order to permit accurate compensation for differences in time delays between the detectors and the coincidence unit. Finally, there has been added to the system a provision for obtaining sum-coincidence spectra as first described by Hoogenboom.[29] In this system the pulses from the two detectors are carefully matched in amplitude calibration, then summed in a pulse adding circuit. These summed pulses are analyzed in a differential discriminator set to accept pulses corresponding to the excitation energy of a resonance level. This output is then used as a third input to the slow coincidence unit so that its output represents coincidence between two completely absorbed gamma rays comprising a double cascade from the resonance level. This signal is then used to trigger the pulse height analyzer gate. The spectrum obtained from pulse height analysis of one detector output thus consists only of full energy peaks due to radiations which are members of a double cascade. The pulse height adder which has been constructed for this purpose employs the circuit used by Kantele and Fink in a somewhat different type of spectrometer.[30] The adder output was analyzed by a conventional linear amplifier and discriminator.

The scalers used to record single channel counts had dead times of one microsecond and those recording coincidences had dead times of approximately eight microseconds. Separate cathode-follower outputs to drive scalers were constructed for all coincidence stages so the relatively low scaler input impedances would not degrade coincidence pulses. The number of scalers provided, which exceeded the requirements for the present experimental measurements, permitted a continuous check on the performance of the coincidence system.

A double pulser with associated pulse shaping networks and an oscilloscope formed an integral part of the equipment and were used for all routine checks and adjustments. An additional slow coincidence unit of variable resolving time[31], which was constructed as part of the system, was used to check on the operation of the Atomic Instrument Company unit.

Control circuit relays were provided so that the pulse height analyzer and all scalers could be started and stopped simultaneously by the current integrator on-off switch.

III. EXPERIMENTAL PROCEDURE

1. Target preparation

The target material used in this experiment was isotopically enriched silicon in the dioxide form purchased from the Stable Isotopes Division of Oak Ridge National Laboratory. Relative percentages of the three stable silicon isotopes were 91.85 Si^{29}, 7.85 Si^{28}, and 0.30 Si^{30}. This material was evaporated onto prepared target backings in a vacuum evaporation apparatus under a chamber pressure of 10^{-5} to 10^{-6} Torr.

Beam power of as much as 20 watts was delivered to a target spot area of about 6 square millimeters during bombardment. Dissipation of this heat by 5-mil tantalum target backings, which had been used in previous work at this laboratory, was found insufficient to prevent local overheating of the target with an accompanying rapid loss of target material. This fact, and the fluorine contamination of the surface of all sheet tantalum examined, led to employment of the heavier target backings of copper described in Chapter II. While vacuum plating these copper backings with 60,000 Å or more of gold (99.999 percent purity) to completely stop 2-Mev protons, it was found that the plating tended to crack and spall off when the copper backings were maintained at ambient temperature during evaporation. This effect was caused chiefly by tensile stresses which have been found to be as much as 850 Kg/cm^2 in 2000 Å gold films deposited on copper.[32] This trouble was overcome by holding the copper backings at 400°C during evaporation by means of a resistance heater which was constructed for this purpose. The heater was made in the form of a 4-in. cylindrical section, to which the target backings were clamped. The cylindrical heater section was suspended in the vacuum coating chamber so that its axis coincided with the evaporant source. Heating the backings in this manner prior to evaporating both gold and SiO_2 also served to remove any residual volatile contaminants leaving a clean surface to receive the coating.

Evaporating boats were fabricated from 5-mil tungsten ribbon and, when cleaned by preheating before use, proved to be satisfactory for the evaporation of both gold and SiO_2. Temperature of the SiO_2 evaporant was monitored with an optical pyrometer to maintain an indicated evaporating temperature of 2130°C; at this temperature 4.0 mg of SiO_2 evaporated in

about two minutes. The temperature is not corrected for departure of the evaporant from an ideal black body inasmuch as reproducibility and temperature control were desired rather than an accurate measurement of true surface temperature. During the first five to ten seconds of all evaporations the evaporant was intercepted by a shutter, since the first part of an evaporant to boil off is known to carry a higher percentage of any contaminants present. Following evaporation, cooling of the heater and targets was accelerated by admitting pure helium to the chamber through a liquid air trap.

In practice, 2 gm or more of gold were evaporated at a distance of 5 cm from the target backings and exposed parts of target assemblies to produce the desired plating thickness. 4.1 mg of SiO_2 were evaporated at the same distance to give targets approximately 5-kev thick to 2-Mev protons for use in the excitation function runs. For the targets used to obtain gamma-ray spectra, and for angular correlation runs at 1470 kev, 5.2 mg of SiO_2 were evaporated to obtain targets 8-kev thick to 1470-kev protons.

Considerable care was used in an attempt to reduce the contamination by F^{19}. Evaporation boats were preheated to 2200°C before use, targets were stored in a vacuum (until this was found not to be of value), target chamber pressure was maintained at 10^{-7} Torr during runs, and possible sources of contamination in the vacuum systems such as Teflon were avoided. In preliminary bombardments at the F^{19} resonance energy of 1373 kev, the gold-plated copper target backings, which were washed in either pure ethanol or menthanol and rinsed in distilled water just prior to use, were found to be freer from F^{19} than backings of either Ta or W which had been cleaned by various methods. In spite of these precautions all targets which were prepared proved to be contaminated to some degree by F^{19}.

2. Excitation function measurements

The excitation function of the $Si^{29}(p,\gamma)P^{30}$ reaction has been measured by recording single gamma-ray yield and gamma-gamma coincidence yield at accelerator energy settings over a range of proton energies from 1420 kev to 2170 kev. The 2 in. x 2 in. NaI(Tl) scintillation detectors were used for this purpose. The output of one of the detectors was counted to obtain the gamma-ray yield at each proton energy, and the number of events in which gamma rays were detected simultaneously in each crystal was recorded by the use of the slow-fast coincidence system adjusted to a resolving time of 25 ns.

The two detectors were positioned in geometry B at angles of 0^{o} and 180^{o} relative to the vertical direction and at a distance of 0.6 in. from the beam spot. Integral discriminators in both channels were set so that counts would be recorded for gamma rays with energies exceeding 0.65 Mev, a setting chosen to exclude the 0.51-Mev annihilation radiation arising from the positron decay of P^{30}, while accepting the full energy peaks of the 0.68 and 0.71 Mev radiations which deexcite the first two excited states in P^{30}. The 7-microampere proton beam was collected by the current integrator which closed a beam shutter and stopped counters after collection of 84 microcoulombs at each energy step of approximately 3 kev. Background counts were made every 50 kev with the beam intercepted by a shutter in the beam tube outside of the shielded target area.

An auxiliary experiment was conducted to determine the energy calibration for the excitation curves. In this experiment the frequency of the NMR signal was measured to within one part in 10^{-6} as the 992-kev aluminum resonance [33] was traversed using a freshly prepared target about 10 kev in thickness. Runs with mass 2 beams were also made to check this calibration at a generator energy of 1984 kev. Immediately after calibration, the Si^{29} resonance energies above 1970 kev and the energy of the resonance at 1506 kev were carefully measured in a similar manner. Using these points as references it was then possible to calibrate the entire excitation curve in terms of magnet current, which was determined to a precision of one part in 10^{-5} at each energy step. This procedure gave a better calibration than that obtained using the fluxmeter logging dial readings, since calibration curves for converting these readings to magnetic field could not be read with adequate precision.

3. Measurement of saturation activity

In order to definitely identify resonances due to the $Si^{29}(p,\gamma)P^{30}$ reaction, measurements were made at the resonances above 1970 kev to determine the half life of decay radiation following bombardment. In these measurements Si^{29} targets were bombarded for ten minutes, then removed to a small cave of 2-in. lead brick where counting was started within 60 sec after cessation of bombardment. The positron annihilation radiation following beta decay of P^{30} was detected by a 3 in. x 3 in. crystal. Total counts above the noise threshold were recorded by the pulse height analyzer operated in a gross counting mode. In this mode the channel in which all counts are recorded is automatically shifted

ahead after a preset counting time. After counting for 3.1 sec per channel for a 6.46-minute total counting time, the target was removed from the cave and a background run made with the analyzer in the subtract mode.

Difficulty which was experienced in obtaining gamma-ray spectra recognizably due to Si^{29} at the upper resonances as a result of masking radiation from the $F^{19}(p,\alpha\gamma)O^{16}$ reaction caused some concern that the peaks observed in the excitation curve might have been due to other contaminants. Observance of the 2.5-min half life of P^{30} following bombardment could not entirely exclude this possibility since it is conceivable for P^{30} to be formed in a nonresonant direct capture process. For this reason it was desirable to compare the activity of the target observed after bombardment at energies corresponding to the peaks in the yield curves to the activity observed after bombardment at off-peak energies. In an experiment to do this, a proton bombardment time of ten minutes to obtain 94 percent of saturation activity was followed by a ten-minute counting period during which the pulse height spectrum was obtained. The target was then allowed to decay for an additional ten minutes before bombardment was resumed at the next energy. The number of counts observed in the 0.51-Mev annihilation radiation peak then served as a measure of the amount of P^{30} formed at each energy.

4. Gamma-ray spectra

All gamma-ray spectra were obtained using 3 in. x 3 in. NaI(Tl) crystals with no special shielding nor collimation. For most spectra the pulse height analyzer usable range extended from about channel 7 to channel 127 corresponding to gamma-ray energies from 0.7 to 7.7 Mev. For observation of annihilation radiation a higher gain was used so that these channels corresponded to energies from 0.18 to 1.92 Mev. The analysis of spectra for intensities was performed with a digital computer as described in Appendix 2. The particular method finally used to subtract background radiation from spectra varied according to the resonance being considered. When possible, backgrounds taken slightly above or below resonances were subtracted from spectra. This was not very successful for the resonances above 1950 kev where F^{19} contamination gave rise to the $F^{19}(p,\alpha\gamma)O^{16}$ reaction. This reaction is strongly resonant at 2030 kev with a width at half maximum of 120 kev[34] which effectively blankets the higher proton energy range considered in the present work. The 6-7 Mev

gamma rays occurring in this reaction are present in relative proportions which vary considerably with bombarding energy so that off-resonance background subtraction is not accurate. Bombardment of blank targets which had been processed identically to SiO_2 targets but using an empty evaporation boat gave a background measurement which was also rather unreliable because of individual variations among targets. A method of subtracting the background measured with the accelerator off was also used, in which case background radiation of specific energies due to contaminants was subtracted out in the spectrum analysis.

In order to circumvent radiation due to target contaminants efforts were exerted to obtain sum-coincidence spectra in the energy region above 1950 kev as a means of getting at decay schemes. The sum-coincidence spectra were, in general, measured with the slow-fast coincidence requirement also imposed, and with a coincidence resolving time of 110 ns. These runs were usually made in geometry B with counters positioned 1.6 in. from the beam spot at a 90° angle relative to each other. A 5/16-in. lead sheet between the counters served to minimize coincidences due to scattering or pair production in one crystal with the lost radiation being captured in the other crystal. The differential discriminator following the pulse adder was set with its lower level at the resonance energy and was adjusted to pass pulses in a band about 0.6 Mev in width. Settings were made by adjusting the discriminator so that the observed count rate of accepted pulses was equal to half the repetition rate of a test pulse. The proper test pulse amplitude was obtained by setting the pulser gain so that counts fell into the pulse height analyzer channel corresponding to the desired energy. Settings of integral discriminators in the two singles channels were adjusted to 0.62 Mev in a similiar manner. The pulse height analyzer was calibrated with Cs^{137} and Co^{60} sources and with the 5.31-Mev gamma ray which dominates the $Si^{29}(p,\gamma)P^{30}$ spectrum at the 414-kev resonance. It was found that the Dumont 6363 photomultiplier tubes experienced marked gain shifts as a function of count rate amounting to several percent, an effect which has been attributed to changes in the dynode surfaces[35]. Attempts to allow this shift to stabilize before commencing counts were only partially effective. The overall result of this phenomenon was to vitiate the results of a large number of sum-coincidence spectra.

5. Measurements at 1470 kev

Since the 4.50-Mev level in P^{30} has been shown to be most strongly excited at the 1470-kev resonance, this proton energy was a logical choice for angular correlation measurements which could lead to determination of the spin-parity for the level. The resonance is rather weak so it was decided to take five sets of data to improve the counting statistics and to permit a check of the consistency of results. Each set of data consisted of five spectra taken with the movable detector set to angles of 0°, 30°, 45°, 60°, and 90° relative to the proton beam. In geometry A with the 3 in. x 3 in. movable detector positioned with its face 4.125 in. from the target, runs were made using a 7-microampere beam for counting times of approximately one hour at each angular setting. The same target was used for each set of runs and the order of the angular settings was varied in different sets so as to minimize differences in the gamma-ray spectra due to any contaminant buildup or target erosion. The fixed 3 in. x 3 in. detector was positioned at 270° relative to the beam and 4.125 in. from the target for use as a monitor counter. Each run was terminated when 30,000 monitor counts had been recorded. A 2 in. x 2 in. detector was also used as a secondary monitor counter. The integral discriminator in each monitor channel was adjusted to a valley in the gamma-ray spectrum at 4.75 Mev so that the effect of gain shifts in these channels would be minimized. Before and after each run the discriminator levels were checked and adjusted with the aid of a Co^{60} source which was precisely and reproducibly located relative to the counters. For this check the gain in the monitor channels was increased by a factor of 4 by means of the gain multiplier switch so that the discriminator setting was equivalent to 1.14 Mev. At this setting, near the 1.17-Mev peak in Co^{60}, the count rate observed with the Co^{60} source was quite sensitive to the discriminator setting so that accurate adjustment was possible.

The unfolding of gamma-ray spectra and the determination of angular distribution coefficients was programed and analyzed on a CDC-1604 computer as described in Appendix 2. The radiations which have been used as spectrometer calibration curves in this analysis are listed in Table 1. These spectra were measured in experimental geometry A, backgrounds were subtracted, and any remaining contaminating gamma rays were subtracted off. Each of these monoenergetic spectrograms was plotted, hand smoothed, and redivided into 525 channels to reduce any interpolation errors in the

TABLE 1

Gamma Rays Used for Spectrometer Calibration

E_γ(Mev)	Radiation Source	E_p(kev)
0.662	Cs^{137}	-
1.63	$Na^{23}(p,\alpha\gamma)Ne^{20}$	1252
2.37	$C^{12}(p,\gamma)N^{13}$	460
2.75	Na^{24}	-
3.51	$C^{12}(p,\gamma)N^{13}$	1698
4.43	$B^{11}(p,\gamma)C^{12}$	675
5.31	$Si^{29}(p,\gamma)P^{30}$	414
6.135	$F^{19}(p,\alpha\gamma)O^{16}$	1374
8.06	$C^{13}(p,\gamma)N^{14}$	554

subsequent analysis. Energy calibration of each spectrum was made by equating distance in channels between the pair peak and the photopeak to 1.022 Mev. For the three lowest energy calibration curves, for which pair peaks are non-existent or poorly defined, an equivalent calibration was computed based on the pulse height analyzer calibration as determined in an auxiliary experiment.

All spectra were read out of the pulse height analyzer memory photographically. These data were then transcribed to punched cards and printed listings of the cards were carefully proofread against the photographs.

Gain drifts did not prove troublesome at the lower count rates observed during correlation runs at 1470 kev. To compensate for differences in calibration of the pulse height analyzer between successive runs, which were of the order of one percent, each spectrum was self-calibrated by the peaks at 7.00 Mev and at 1.45 Mev.

IV EXPERIMENTAL RESULTS

1. Excitation Function

The excitation function for $Si^{29}(p,\gamma)P^{30}$ as measured by gamma-ray yield is shown in Fig. 8, and as measured by gamma-gamma coincidence yield in Fig. 9. The energies at which resonances are observed are listed in Table 2, together with some of the results which have been obtained at proton energies below 1900 kev by other investigators.

In arriving at the uncertainty of 0.20% kev for the resonance energies, consideration has been given to errors arising from instability and inhomogeneity of the field of the analyzing magnet, the proton beam spread, possible surface contaminants, calibration drift, and the 0.5-kev estimated error for the 992-kev aluminum calibration point.[33]

Particular attention was given to the resonances above 1900 kev which have not previously been reported. The results of determinations of the half life of the post-bombardment activity of the targets at these energies are given in Table 3. The measurements are seen to agree with values for the half life of P^{30} reported in the literature, which range from 2.51 $\pm$ .02 min to 2.62 $\pm$ .02 min,[24] so that radiative capture by Si^{29} is clearly demonstrated. Table 4 shows the intensity of positron annihilation radiation observed after saturation at selected bombardment energies. These intensity values show distinct maxima at 1975, 2033, 2075, and 2117 kev and show that P^{30} is formed in a resonant reaction rather than by a non-resonant process. The peaks in the gamma-ray yield curves at these energies can therefore be positively ascribed to resonant proton reaction with Si^{29}.

The yield of 0.511-Mev radiation after bombardment at energies between resonances is probably due to a combination of off-resonant reaction with Si^{29} and to the 66-sec positron activity of F^{17} following the non-resonant $O^{16}(p,\gamma)F^{17}$ reaction. This hypothesis is supported by half life measurements of post-bombardment activity of the targets at two inter-resonance points at 1955 and 2007 kev. At those energies "half-lives" of the order of 1.6 $\pm$ .5 min are observed with the count rate 2 min after bombardment at 1955 kev a factor of ten lower than the count rate 2 min after bombardment at 1975 kev.

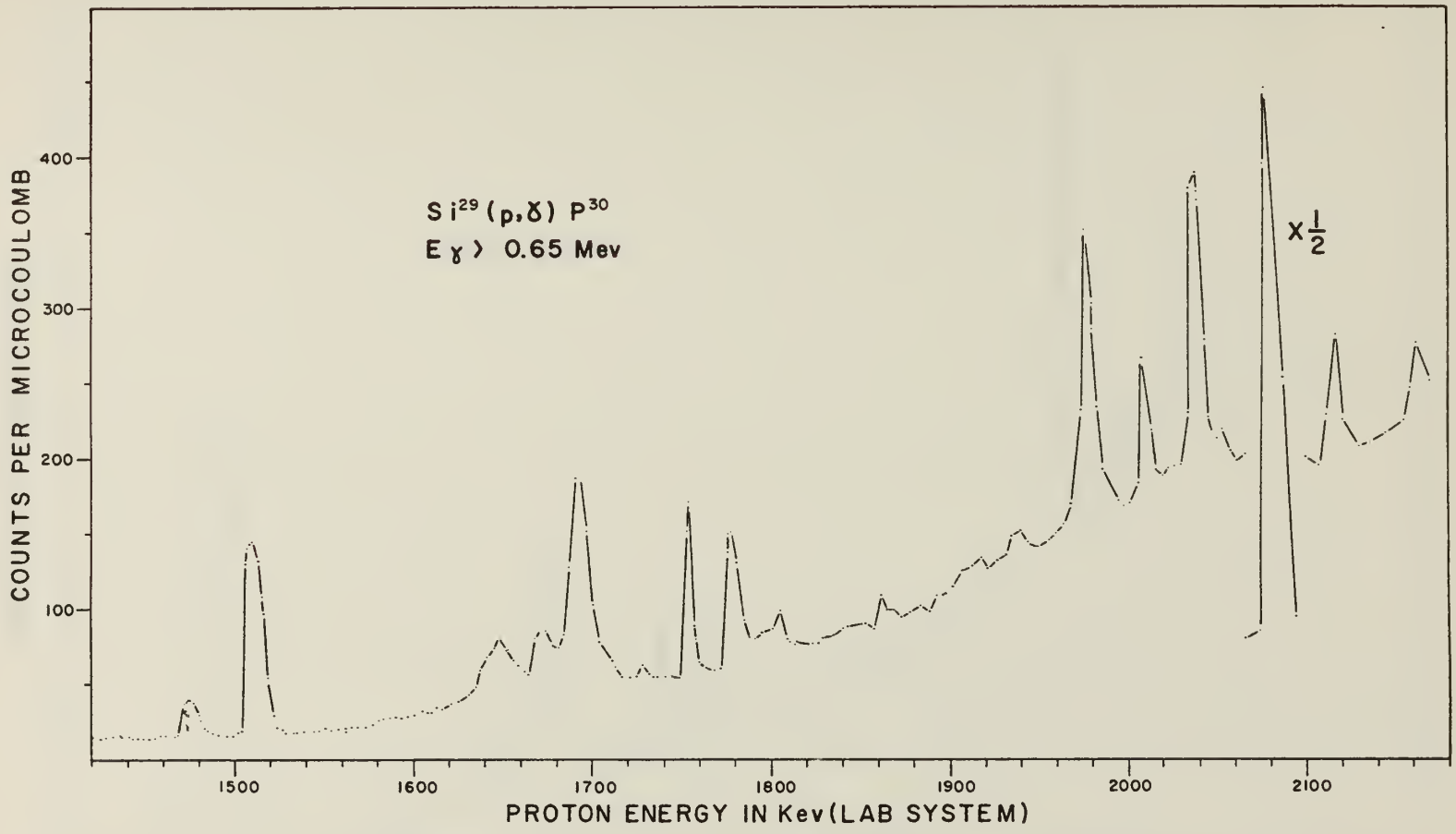

FIGURE 8. GAMMA-RAY YIELD

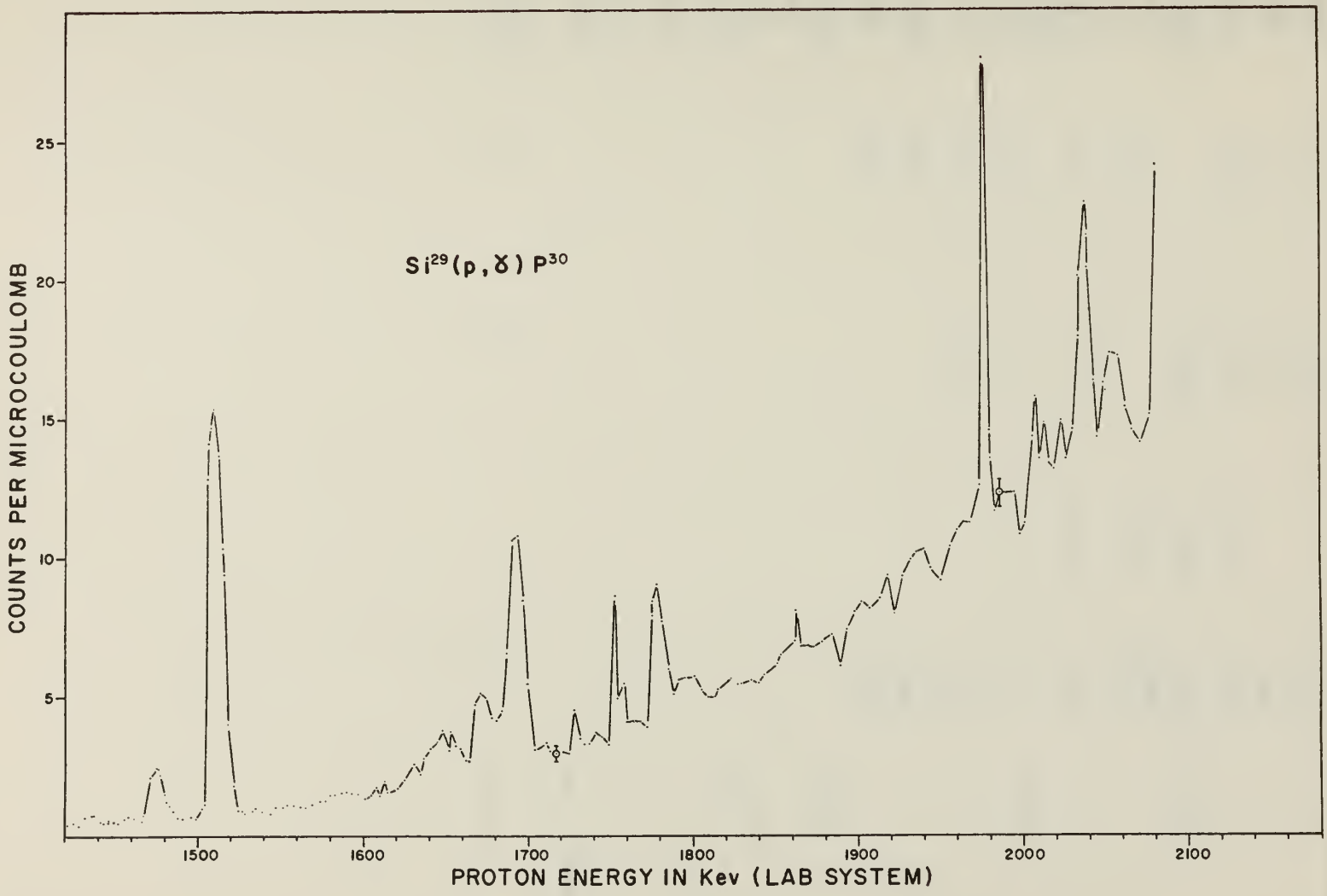

FIGURE 9. COINCIDENCE YIELD

TABLE 2

Resonances Observed in the $Si^{29}(p, \gamma)P^{30}$ Reaction

E_p from 1450 to 2170. Values in kev.

This work	Green[11]	Seagondollar[12]	Tsytko[10]	Wild[15]	Remarks
1470	1479	1479		1470	
1506	1515	1512		1505	
1637	1648	1643	1635	1638	
(1646)		(1653)	(1647)	(1650)	Si^{28}
1667	1671		1663	1665 1670	
1688	1692	1693	1680	1685	
(1726)					weak
1752	1752	1752		1749	
1775	1777	1775		1772	
(1803)	1811			1808	
1860	1857			1852	
(1933)					weak
1975					
(2007)					Si^{30}
2033					
2075					
2117					
(2159)					not identified
±0.20%	±2	±2		±3	Errors

TABLE 3

Half Life of Post-bombardment Decay of P^{30}

Bombardment Energy (kev)	Half life (min)
1975	2.42 ± .09
2033	2.45 ± .18
2075	2.51 ± .06
2117	2.47 ± .15

TABLE 4

Intensity of Post-bombardment Annihilation Radiation

Bombarding Energy (kev)	Excitation* Energy in P^{30} (Mev)	Relative Intensity
1506	7.04	19.3
1950	-	1.0
1975	7.49	4.1
1990	-	1.0
2033	7.55	7.9
2060	-	1.8
2075	7.59	12.4
2100	-	1.3
2117	7.63	8.1
2140	-	2.3

*Based on Q = 5.582, reference 24.

2. Gamma-ray Spectra at 1975, 2033, 2075 and 2117 kev Resonances

Gamma-ray spectra were obtained at the four resonances at proton energies of 1975, 2033, 2075 and 2117 kev. Masking radiation from the resonant reaction with the contaminant F^{19} dominates the upper energy region of these spectra so that a detailed analysis of the relatively weaker radiation from the $Si^{29}(p,\gamma)P^{30}$ reaction was not possible. However, the gamma-ray energies and intensities which could be determined with reasonable certainty from stripping and least squares analysis for intensities are given in Table 5. The 6-7 Mev gamma rays due to F^{19}, which are omitted in Table 5, were accounted for by inclusion in the least squares intensity analysis, since other background subtraction techniques did not work well at these energies as has been discussed in Chapter III. Also included in Table 5 are energies of sum-coincidence spectral peaks which were close to energies observed in the singles spectra. The good spectral resolution and discrimination against background radiation which are obtainable with the sum-coincidence method proved to be of only nominal assistance in analyzing the gamma-ray spectra. This was due in part to the relative weakness of radiative decay of these resonance levels in comparison with inelastic scattering, and in part due to photomultiplier gain drifts which blurred peaks in the sum-coincidence spectra. However, it is apparent from the large number of low intensity peaks observed in the sum-coincidence spectra at the higher-energy resonances that decay schemes from these levels are considerably more complex than decay from the 1752-kev resonance level,[23] where sum-coincidence spectra were recorded for the purpose of comparison.

The strong 1.28-Mev gamma ray observed at 1975, 2033, and 2075 kev is interpreted as deexcitation of the P^{30} compound nucleus by proton reemission to the first excited state of Si^{29} at 1.277 Mev.[25] The high intensity of this gamma ray is convincing evidence that this inelastic scattering process predominates over radiative capture and that the 128-Mev radiation is primarily responsible for the upper-energy peaks in the gamma-ray yield curve. Rather curiously, however, this gamma ray does not appear in the spectrum at the 2117-kev resonance.

The resonance at 2075 kev lies near the $Si^{28}(p,\gamma)P^{29}$ resonance reported at 2090 kev which has a half width of 16 kev.[25] The gamma-ray

TABLE 5

Gamma-ray Intensities at Resonance Energies of 1975, 2033, 2075, and 2117 kev

E_p (kev)	Singles Spectra E_γ (Mev)	Sum-Coincidence E_γ (Mev)	Intensity (quanta/μC)
1975	4.52	4.58	5
	4.19	4.07	2
	3.48	3.40	2
	3.33		2
	3.00	2.99	3
	2.44	2.50	3
	1.28	-	117
2033	5.10	-	8.6
	1.28	-	187.3
2075	7.59	-	14
	4.70	4.85	60
	2.98	2.95	55
	2.26	2.23	55
	1.36	-	303
	1.28	-	1360
2117	5.10	-	2
	2.55	-	3

Error in singles spectra E_γ estimated to be 1%

Error in sum-coincidence E_γ estimated to be 2%

Error in intensities estimated to be 30%

TABLE 6

Relative Gamma-ray Intensities at the 1470-kev Resonance

E_γ (Mev)	Transition	Observed* Intensity	Decay Scheme Intensity	Ref 23
7.00	R → 0	25.4	25.4	39.6
6.29	R → 2	9.6	9.6	6.3
4.50	19 → 0	14.6	14.3	13.2
4.14	13 → 0	10.7	10.7	11.1
3.98	R → 9	10.5	10.8	7.3
3.45	not accounted for	2.0	-	4.0
3.17	R → 11	3.0	1.5	2.0
3.17	11 → 1		1.5	2.0
3.07	R → 12	19.1	17.6	11.7
3.02	9 → 0		1.2	1.6
2.86	R → 13	13.7	13.7	13.0
2.69	13 → 3	2.8	2.8	-
2.50	R → 19	38.8	21.6	20.0
2.50	12 → 3		17.6	11.7
2.34	9 → 1	17.2	16.9	13.4
1.45	19 → 9	not analyzed+	7.3	6.8
1.45	3 → 0	"	20.3	11.7
.71	2 → 0	"	9.6	21.8
.68	1 → 0	"	18.4	

+ An intensity of approximately 34 is indicated for the 1.45 Mev radiation by observations at 90° with .6" crystal face to target distance.

* Relative intensities shown are also approximate absolute intensities in quanta per microcoulomb.

TABLE 7

Double Angular Correlation Coefficients at 1470-kev Resonance

E_γ (Mev)	P_2 highest term		P_4 highest term			
	A_2/A_o	Std. Dev.	A_2/A_o	Std. Dev.	A_4/A_o	Std. Dev.
7.00	-.42	.02	-.43	.03	.05	.03
6.29	-.47	.05	-.47	.06	.01	.06
4.50	.09	.02	.11	.02	-.07	.03
4.14	-.09	.04	-.08	.04	-.01	.05
3.98	-.35	.05	-.37	.06	.02	.07
3.45	.03	.22	-	-	-	-
3.17	-.09	.16	-	-	-	-
3.07-3.02	-.04	.07	-	-	-	-
2.86	.31	.03	.32	.04	-.03	.05
2.69	.39	.14	.50	.15	-.31	.19
2.50	-.22	.02	-.24	.02	.03	.02
2.34	-.24	.03	-.26	.03	.06	.04

Coefficients shown are corrected for finite angular resolution of detector.

spectrum at this resonance is characterized by a 4.76-Mev radiation to the ground state of P^{29}.[36] It seems probable, therefore, that the 4.70-Mev gamma ray seen in the spectrum at 2075 kev is due to the Si^{28} reaction. The observed intensity is in agreement with this explanation. Although the presence of 2.94-Mev and 2.24-Mev gamma rays in this spectrum suggest a cascade through level 8 at 2.94-Mev in P^{30}, the 1.45-Mev gamma ray known to occur in this cascade[22] is not seen and sum-coincidence work has not been able to confirm this possibility. It is possible, however, that the gamma rays due to Si^{29} reactions could be responsible for the anisotropy of the radiation from the 4.76-Mev level in P^{29} which has been observed by Newton,[37] since anisotropy is not expected to result from the spin assignment to this level of 1/2+ based on proton scattering experiments.[38]

The remaining weaker radiations seen at the four higher resonances are most probably due to radiative capture by Si^{29}, but the rather large errors, due chiefly to masking contaminant radiation, do not permit more than tentative postulation of decay modes. Gamma rays observed at the 1975-kev resonance suggest cascades through level 19 at 4.50 Mev and through level 14 at 4.18 Mev. No conclusions can be drawn for the 2033-kev resonance. At the 2075-kev resonance the 7.59-Mev radiation is readily recognized as a ground state transition but the other gamma rays are not identified. Finally, at the 2117-kev resonance, the two radiations observed nicely fit a decay through level 5 at 2.54 Mev which is known to decay 95% to the ground state.[22]

3. 1470-kev Resonance Decay and Intensities

The gamma-ray spectrum observed at the 1470-kev resonance with a crystal face to target distance of 0.6 in. and at an observation angle of 90^{o} is shown in Fig. 10. This spectrum has been least squares fitted by gamma rays with energies required by the decay scheme proposed in reference 23. Reanalyses with alternate energy choices in each instance gave a poorer fit in reassurance of the correctness of the decay modes proposed. This decay scheme, with intensities as found in the present analysis, is shown in Fig. 11. (Heavy dots indicate cascades confirmed in reference 23 by coincidence spectroscopy.) The branching ratio shown for the 4.50-Mev level is that given in reference 22. The assumed correctness of this ratio then requires branching ratios of 93:7 for level 9 and 80:20 for level 13 in order to fit the intensities of gamma rays which have been

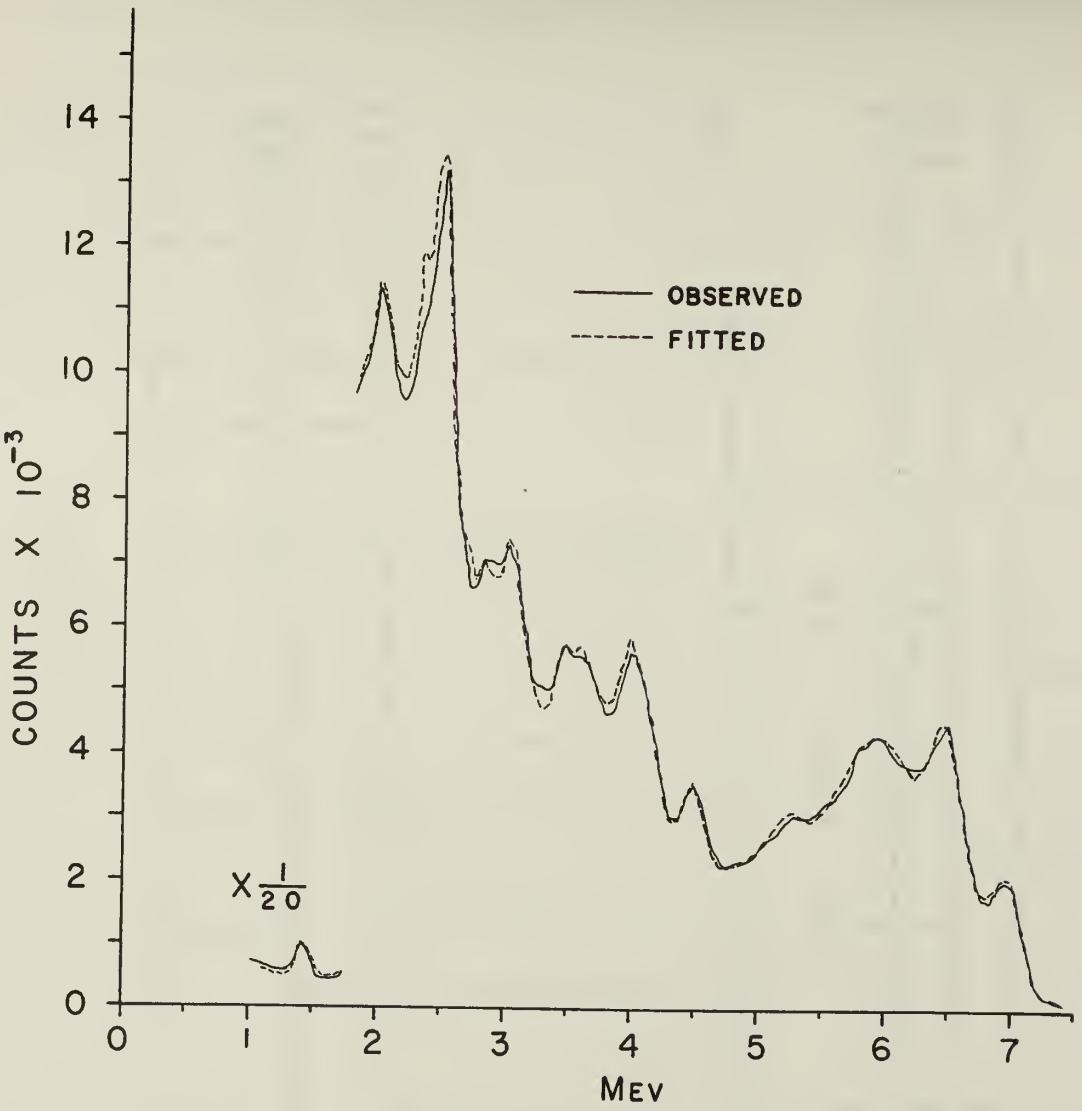

FIGURE 10. GAMMA-RAY SPECTRUM AT 1470 KEV

DECAY SCHEME AT 1470 KEV RESONANCE

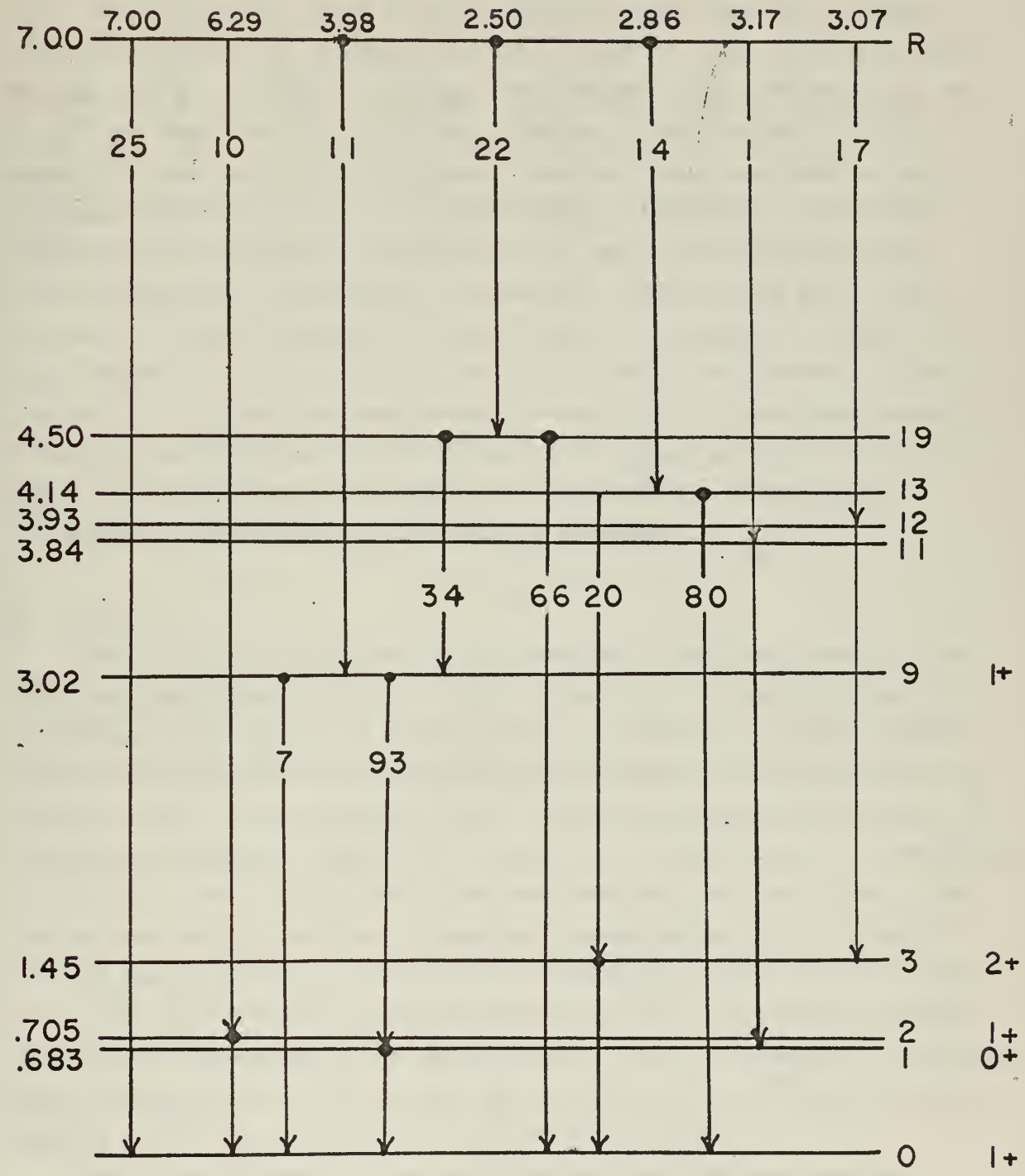

FIGURE 11.

observed. These ratios are in reasonably good agreement with ratios of 89:11 reported for level 9[22] and 88:12 reported for level 13[23].

Intensities of gamma rays observed in the angular correlation runs are shown in Table 6 along with intensities observed in reference 23 at 55^{o}. The intensities found in the correlation runs have been averaged over 4π steradians by weighting the mean values for each observation angle by the sine of that angle. Because the 1.46-Mev background radiation due to K^{40} was found to be quite strong relative to the 1.45-Mev gamma ray observed in the correlation runs, no attempt was made to analyze the gamma radiation of this or lower energy. Although the background radiation subtracts out, the statistics of the remaining counts do not allow extraction of significant information. The observed intensities are seen to agree reasonably well with those of reference 23 except for the 7.00-Mev radiation which is found to be considerably weaker in the present work. Since the experimental intensities are based upon reported values of intrinsic peak efficiencies[56] rather than an absolute spectrometer calibration, this discrepancy is not considered significant.

4. Angular Correlations at the 1470-kev Resonance

A. General

The correlation function coefficients which have been found in this experiment are given in Table 7. The values given are weighted means of the values found in each of the five sets of data taken. The chi-square values for each correlation coefficient have been calculated and show the different sets to be consistent, under the acceptance requirement that the cumulative chi-square probability be equal to or less than 0.9. Combining intensities from each data set, then analyzing for the coefficients gives values practically identical to the mean values quoted. This agreement to some degree serves as a check that computational errors have not crept in. Each experimentally observed spectrum has also been plotted together with the corresponding fitted spectrum, then visually examined to determine that a reasonable fit was obtained in each case. Fig. 12 shows a typical example of the fit obtained for the correlation runs.

The intensity analysis was performed both subtracting background radiation analytically and subtracting off-resonance background, with essentially the same results being obtained in each case. The standard

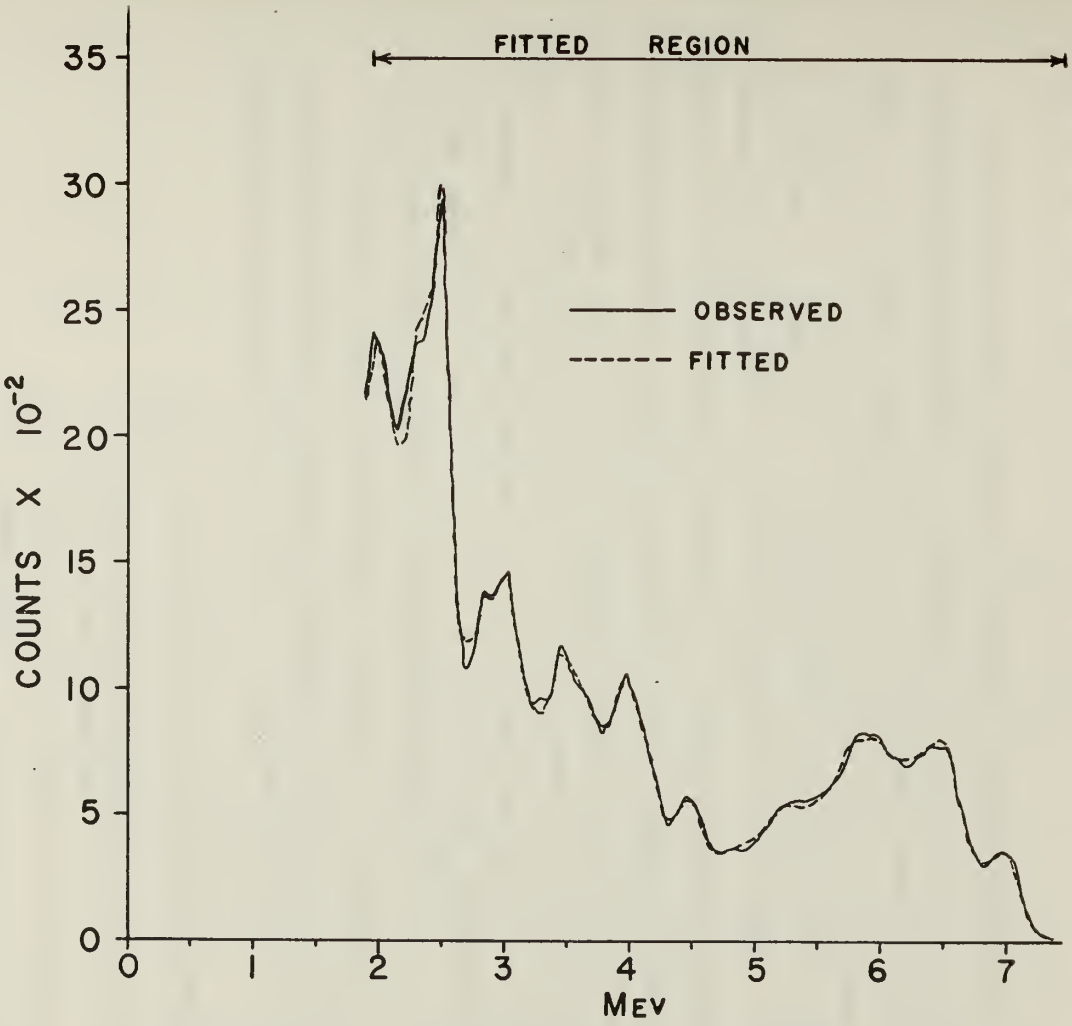

FIGURE 12. GAMMA RAY SPECTRUM FOR CORRELATION RUN 3-5 AT 90°

deviations in the mean coefficient values have been calculated from

$$1/\sigma^2 = \sum_{i=1}^{n} 1/\sigma_i^2$$

and have been compared with the values given by

$$\frac{1}{n(n-1)} \sum_{i=1}^{n} (x_i - \bar{x})^2$$

which agree closely.

The most obvious feature of the data is the anisotropy of the 4.50-Mev gamma ray which is incompatible with a spin of zero for this level. It is also noteworthy that the 4.50-Mev gamma ray is the only radiation to show a statistically significant $P_4(\cos\theta)$ term (notation is defined in Appendix 1). Fig. 13 shows the correlation coefficient values for this gamma ray obtained from each set of data. In this figure M denotes mean values and C denotes values obtained by combining intensities from each data set before computing coefficients. Fig. 14 shows the fit to the Legendre series both with and without P_4 terms. Although the existence of the P_4 term is not incontrovertible it permits a markedly better fit to the data and gives a smaller value of the parameter ϵ which serves as a guide to the appropriate number of terms which should appear in the Legendre series.[41]

In order to deduce spin-parity values it is necessary to examine the possible particle and radiation mixing ratios for this reaction. The notation used herein to refer to these mixing ratios is as follows:

δ_1 = Proton-partial-wave mixing parameter

δ_2 = The multipole mixing ratio of an intermediate unobserved gamma ray

δ_3 = The multipole mixing ratio of an observed gamma ray

δ_4 = Channel-spin mixing parameter

Appendix 1 defines these parameters more fully and describes how they enter into the expression for the theoretical correlation function. For the $Si^{29}(p,\gamma)P^{30}$ and $Si^{29}(p,x\gamma)P^{30}$ (intermediate unobserved) reactions,

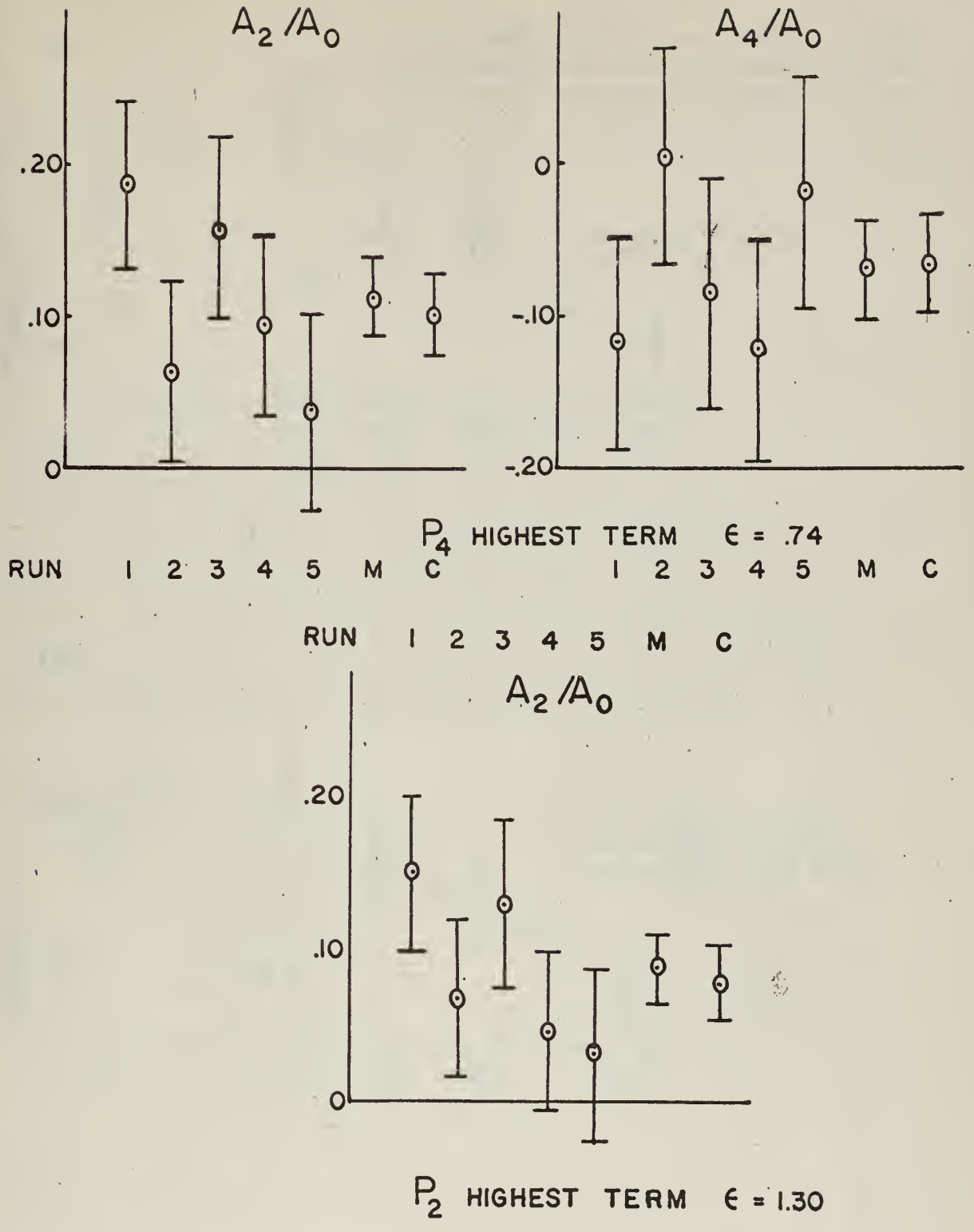

FIGURE 13. DISTRIBUTION COEFFICIENTS FOR THE 4.50 MEV GAMMA RAY

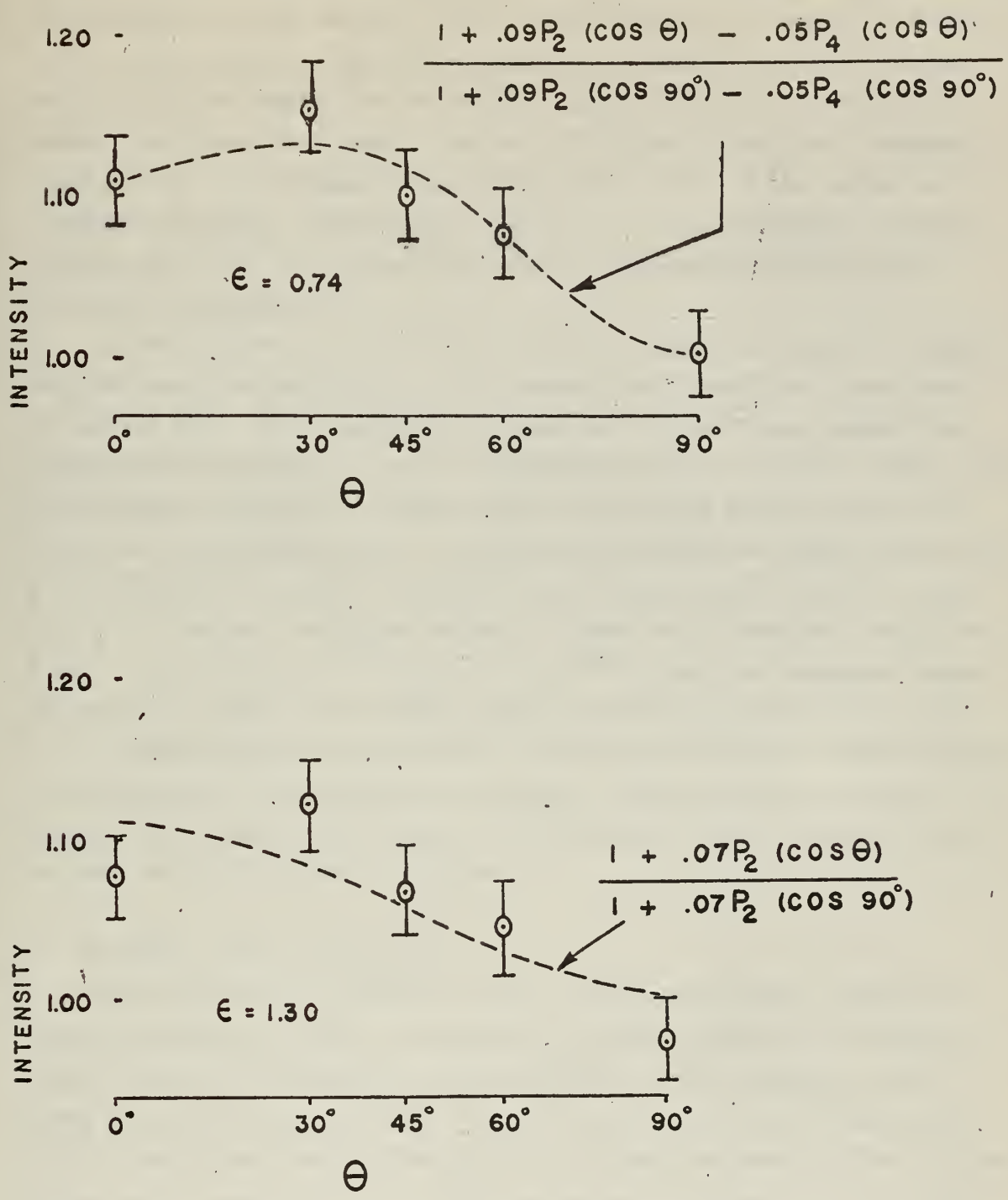

FIGURE 14. FITS OF COMBINED EXPERIMENTAL DATA TO LEGENDRE SERIES - 4.50-MEV GAMMA RAY (UNCORRECTED FOR FINITE SOLID ANGLE)

the correlation coefficients A_2/A_0 and A_4/A_0 are describable as functions of a maximum of three mixing ratios. Level curves, or contours, of constant A_i/A_0 values may be plotted against any two of the mixing ratios. Actually the arctangents of the mixing ratios are used as variables for convenience since they remain finite. If a third mixing ratio appears, changing its value changes these contour plots only to the extent of changing the A_i/A_0 values for all contours by a multiplicative constant. Contour plots for this analysis have been programmed and plotted as described in Appendix 2.

In the following discussion it will be assumed that only E1 radiation or E2/M1 mixtures are likely to be observed for transitions from levels of several Mev. This simplifying assumption is based upon transition probabilities estimated from the independent particle model [42] and is commonly made in analysis of gamma radiation following proton capture in light and intermediate nuclei. Although suppression or inhibition of dipole radiation is possible because of the isotopic spin selection rule, $\Delta T = \pm 1$ for self conjugate nuclei,[43] there are an adequate number of lower levels of both T = 0 and T = 1 in P^{30} so that the resonance level can decay by either E1 or E2/M1 radiation without violating this rule.

In analyzing the experimental correlation coefficient values, tables from reference 23 have been quite helpful. This reference tabulates the maximum and minimum values which may be assumed by A_2/A_0 and A_4/A_0 for a variety of postulated spin sequences.

B. Resonance level spin-parity

The observed A_2/A_0 terms of about -0.40 for the 7.00, 6.29, and 3.98 Mev gamma rays, which all proceed to known 1+ levels, are found to be most useful in determining the spin-parity of the resonance level. Among possible values through 4 for this level, it is found that only 1+, 2+, and 2- can lead to the A_2/A_0 coefficient measured for the 7.00-Mev ground state transition. The same conclusion is supported by the A_2/A_0 values observed for the 6.29 and 3.98 Mev radiations.

If one inspects the contour plot, Fig. 15, for the $1+ \rightarrow 1+$ transition it is seen that a d-s proton-angular-momentum mixing ratio of over 0.90 is required to produce the observed A_2/A_0 value for the 7.00-Mev gamma ray. Since the relative penetrability of d waves to s waves is about 3×10^{-2}, such a mixture is not a likely choice. The A_4/A_0 term observed

for the 4.50-Mev radiation supports this conculsion since A_4/A_0 terms do not result from resonance spins smaller than 2. Finally, the value of A_2/A_0 observed for the 2.34-Mev radiation will be shown to be incompatible with a 1+ resonance level spin. This radiation proceeds to the known 0+ level 1, at 0.68 Mev, from the known 1+ level 9, at 3.02 Mev. Level 9 is fed more than 50% from the resonance level and, secondarily, by the intermediate 1.48-Mev radiation from level 19. The A_2/A_0 value observed for this primary 3.98-Mev feeder restricts the ranges of δ_1 and δ_2 for the $R \rightarrow 9 \rightarrow 1$ transition. When these ranges are delineated on a contour plot for a $1+ \rightarrow 1+ \rightarrow 0+$ transition, it is found that A_2/A_0 for the second radiation is restricted to a range between -0.01 and +0.24. By an extension[48] of the formalism for intermediate unobserved cascades given in Appendix 1 it is possible to calculate the angular distribution coefficients for the $9 \rightarrow 1$ radiation which result from the $R \rightarrow 19 \rightarrow 9 \rightarrow 1$ cascade. It is found that, for a 1+ resonance level, the minimum possible value of A_2/A_0 occurs for an assumed spin of 2 for level 19. This minimum value has been calculated to be -0.175. Thus a 1+ resonance level leads to a minimum possible value for A_2/A_0 of about -0.093. Comparing this with the observed value of $-0.24 \pm .03$ for the 2.34-Mev gamma ray, 1+ can be ruled out as a possible spin-parity of the resonance level.

Having narrowed the possible resonance spin values to 2+ or 2-, the contour plots may be examined for the $2+ \rightarrow 1+$ and $2- \rightarrow 1+$ transitions, applicable to the 7.00-Mev radiation to the ground state. In the first case, channel-spin mixing may occur while in the second case proton-partial-wave mixing is permitted. For the $2+ \rightarrow 1+$ case Fig. 16a shows the contour plot with the experimental value of A_2/A_0 for the 7.00-Mev gamma ray delineated thereon by cross-hatching. Fig. 16b is a similar plot for A_4/A_0. The darker shading in Fig. 16b indicates the superposition of cross-hatching on both plots and defines the ranges and combinations of mixing parameters which can give rise to the observed coefficient values. For $\delta_3 \approx 0$ (i.e. M1 radiation), δ_4 is constrained to be less than $\approx \tan 50^\circ$. This must not be taken too seriously, however, since the A_4/A_0 contours are widely spaced at the top and bottom boundaries of the permitted region, so that a very slight increase in the error for the experimental A_4/A_0 value would allow δ_4 to range up to 90°. The small region at $\delta_3 \approx \tan(-67^\circ)$ and $\delta_4 \approx \tan 49^\circ$ also fits the observed corre-

lation. The plots for the 2- → 1+ case, shown in Figs. 17a and 17b, are quite similar to the 2+ → 1+ case and show that there is no restriction on f-p proton-wave mixing for $\delta_3 \approx 0$ (E1 radiation). The two small permitted regions at $\delta_3 \approx \tan 67^\circ$ may be ruled out since they require an M2/E1 mixture. It is seen that an unlikely but small M2/E1 mixture with $\delta_3 \approx 0.026$ or greater is required for this transition for the case of resonance formation by pure p waves. As will be shown, the 2- resonance level assignment is also less probable than 2+ based on mixing ratios which are required by experimentally observed coefficients for the 4.50-Mev radiation.

As a result of the above considerations, a spin-parity of 2+ is proposed for the resonance level with 2- as a less likely possibility.

C. R → 13 → 0 cascade

There are only two cascades which allow cross checking of mixing parameters as a method of eliminating possible spin sequences. These are the cascade through level 19 and that through level 13 both of which levels have undetermined spins. The latter cascade will be considered first. The existence of an A_4/A_0 term which has been observed in the distribution of the 4.14-Mev radiation from level 13 at the 1686-kev resonance[23] is evidence that level 13 must have a spin greater than or equal to 2. Of the likely possible spins for this level, $2\pm$, $3\pm$, and 4-, only 2+ and 2- can result in the negative value of A_2/A_0 observed for the 4.14-Mev gamma ray. An examination of the contour plots for the four sequences $2\pm \rightarrow 2\pm \rightarrow 1+$ for the R → 13 → 0 cascade shows compatibility in all cases with the observed coefficients for the 2.86-Mev gamma ray and the 4.14-Mev gamma ray. For the sequence 2+ → 2- → 1+ the parameter δ_4 is constrained to be larger than $\tan 70^\circ$ but the other possible sequences are compatible with a full range of values for either δ_1 or δ_4 as the case may be. The only finding is that, for all cases, the R → 13 transition must be relatively pure dipole radiation. The observed coefficient values for the weak 2.69-Mev gamma ray, which also is believed to deexcite level 13, are also compatible with all four possible spin sequences with reasonable choices for δ_3.

D. R → 19 → 0 cascade

Since no requirements on parameters applicable to this cascade are imposed by transitions already considered it becomes necessary to consider

the R →19 →0 sequence with no prior restrictions on the deltas involved. We find, furthermore, that no information is forthcoming from the R→19, 2.50-Mev gamma-ray correlation coefficient since this radiation is indistinguishable from the 12→3, 2.48-Mev gamma ray.

A survey of maxima and minima of A_2/A_0 coefficients shows, if we allow 2- as a possible resonance level spin, that the following sequences for the R→19→0 transition are consistent with the experimental coefficients for the 4.50-Mev radiation:

2+ 1+ 1+	2+ 1- 1+
2- 1+ 1+	2- 1- 1+
2+ 2+ 1+	2- 2- 1+
2- 2+ 1+	2- 3- 1+
2+ 3+ 1+	2+ 3- 1+

It has been found in the analysis that a better fit (see Fig. 14) to the data is given by the series including a P_4 term. Then, provided this term is not spurious, which is not to be excluded as a possibility, the list can be reduced by eliminating sequences not giving rise to A_4/A_0 terms.

The following possibilities then remain:

2+ 2+ 1+
2- 2+ 1+
2+ 3+ 1+
2+ 3- 1+
2- 3- 1+

The last two transitions shown require E3/M2 radiation so, adhering to the hypothesized E1 and E2/M1 radiative transitions as practical candidates, the spin of the 4.50-Mev level is limited to either 2+ or 3+. Of the three remaining possibilities, the 2- →2+ →1+ sequence is perhaps least likely. Figs. 19a and 19b show that this sequence for R →19→ 0 requires an f to p wave mixing parameter of over 0.10 with a large E2/M1 mixing ratio of nearly 12.0. For a 2+ →3+ →1+ sequence, Figs. 20a and 20b show that an E2/M1 ratio of over 1.7 is required for the 4.50-Mev

radiation in order to fit the data. Because large E2/M1 mixing parameters are not commonly seen in the lighter nuclei, this sequence, though more likely than $2- \rightarrow 2+ \rightarrow 1+$, does not appear as probable as a $2+ \rightarrow 2+ \rightarrow 1+$ sequence, as will be seen. For the $2+ \rightarrow 2+ \rightarrow 1+$ sequence Figs. 18a and 18b show that for an assumed channel-spin mixing ratio of zero, an E2/M1 mixing ratio of 0.27 will fit the observed coefficients for the 4.50-Mev gamma ray with a considerable latitude permitted for δ_2. Alternate choices for δ_4 will also permit acceptable choices of mixing parameters for this sequence though in general δ_2 and δ_3 will be required to be larger.

Summarizing, level 19 is found to have a spin of 2+ or 3+ under the assumptions which have been made, with 2+ being more probable.

E. Comparison with other results

Concurrently with the present work, an investigation of triple angular correlations at the 1470-kev resonance has been undertaken at Wright-Patterson Aeronautical Laboratories.[40] The angular distribution of the 7.00-Mev gamma ray was also examined in this experiment. An A_2/A_0 value of $-0.38 \pm .02$ was observed for this gamma ray in good agreement with the value shown in Table 7. Preliminary results of this experiment have indicated restriction of the resonance level spin to a value of 1 or 2 and show that a zero spin for the 4.50-Mev level is not compatible with such a restriction.[62] The preliminary analysis of the triple-correlation experiment is seen to be in agreement with the present work. It is to be hoped that the complete analysis of this work which is now in progress, will lead to a firmer indication of the spin-parity of the 4.50-Mev level since the 2+ (3+) value proposed herein depends upon the somewhat debatable A_4/A_0 term observed and upon the hypothesis that only E1 or E2/M1 radiation is present.

F. T = 1 character of level 19

The prediction of 0+ for the spin-parity of level 19 is based on the premise that this level is the T = 1 analog of the 3.80-Mev level of Si^{30} in the isotopic spin multiplet formalism.[42] A spin of 0 has been suggested for the 3.80-Mev level in Si^{30} based on observations of cascade gamma rays following the $Si^{30}(p,p')Si^{30}$ reaction.[63] A spin of 0+ results also from

calculations made by Thankappen and Pandya of collective vibrational states in a weakly-coupled collective model of the nucleus.[6] The spin-parity of level 19 in P^{30} is thus expected both on experimental and theoretical grounds. The finding of non 0+ spin-parity for this level then appears to be good evidence that either the level is complex (e.g. a doublet) or that it is not the isotopic spin multiplet analog of the 4.80-Mev state in Si^{30} as has been accepted. Some evidence has been reported that the 3.80-Mev level in Si^{30} is a doublet, based upon observations of protons from the reactions $Si^{28}(t,p)Si^{30}$ and $Si^{30}(p,p')Si^{30}$.[59,44] It is possible, therefore, that the analogous 4.50-Mev level in P^{30} is a doublet, although no other evidence so suggests. The other possible explanation is that a nearby level in P^{30}, such as that at 4.42 Mev, may be the T = 1 level rather that the 4.50 Mev level. This does not appear unlikely, since the T = 1 character attributed to the 4.50-Mev level is a probable rather than a firm assignment which was deduced from the investigation of the $S^{32}(d,\alpha)P^{30}$ reaction by Endt and Paris.[18] It is based upon a correction of the 3.80-Mev level in Si^{30} for the Coulomb energy and neutron-proton mass difference which yields a predicted energy of 4.47 Mev for the excitation energy in the P^{30} nuclide. The assignment is strengthened by the fact that the alpha-particle group from $S^{32}(d,\alpha)P^{30}$ corresponding to a residual excitation in P^{30} of $4.501 \pm .010$ Mev has only about half the intensity of neighboring groups. This has been interpreted as being due to operation of the selection rule conserving isotopic spin in this reaction.

On the basis of the energy predicted for the T = 1 level in P^{30} the 4.42-Mev level is seen to be nearly as likely a candidate as the 4.50-Mev level, particularly since the energy prediction is not expected to be exact. Similarly in the T conservation argument, the observed lower intensity of the alpha group for the 4.50-Mev level can hardly be considered conclusive evidence of the T = 1 character of the level, since some T = 0 levels are associated with alpha-particle groups of even lower intensity (e.g. the 3.84-Mev level). Unfortunately, the 4.42-Mev level in P^{30} is not known to be excited in radiative capture, so that spin-parity of this level will probable have to be determined from a different reaction.

5. Summary of Results

Excitation curves for the $Si^{29}(p,\gamma)P^{30}$ reaction have been obtained over the proton energy region from 1420 through 2160 kev. Four previously unreported

resonances have been detected and confirmed at proton energies of 1975, 2033, 2075, and 2117 kev with experimental uncertainties of ± 4 kev. Gamma-ray spectra at these resonances show that inelastic scattering predominates over radiative capture, except at 2117 kev where no inelastic scattering is evident. Some information concerning the radiative decay schemes at the 1975, 2075, and 2117 kev resonances was obtained by spectral analysis with the assistance of sum-coincidence spectra.

The gamma-ray spectrum at the 1470-kev resonance has been analyzed and found to be in agreement with the decay scheme proposed by Moore.[23] The angular distributions of gamma rays observed at this resonance have been measured in a series of five experimental observations, each consisting of gamma-ray spectra obtained at five angles relative to the proton beam. Analysis of this data, under the assumption that E1 and E2/M1 radiation deexcite P^{30} energy levels of several Mev, has shown that the 1470-kev resonance level has a spin-parity of 2+ or, less probably, 2-. The spin-parity of level 13 at 4.14 Mev has also been found to be limited to 2+ or 2-. Level 19 at 4.50 Mev was found not to have a spin-parity of 0+ which had been predicted.[6] Under the above-mentioned assumption, an apparent A_4/A_0 term observed in the angular distribution of this radiation leads to the conclusion that the spin-parity for level 19 is 2+ or, less probably, 3+.

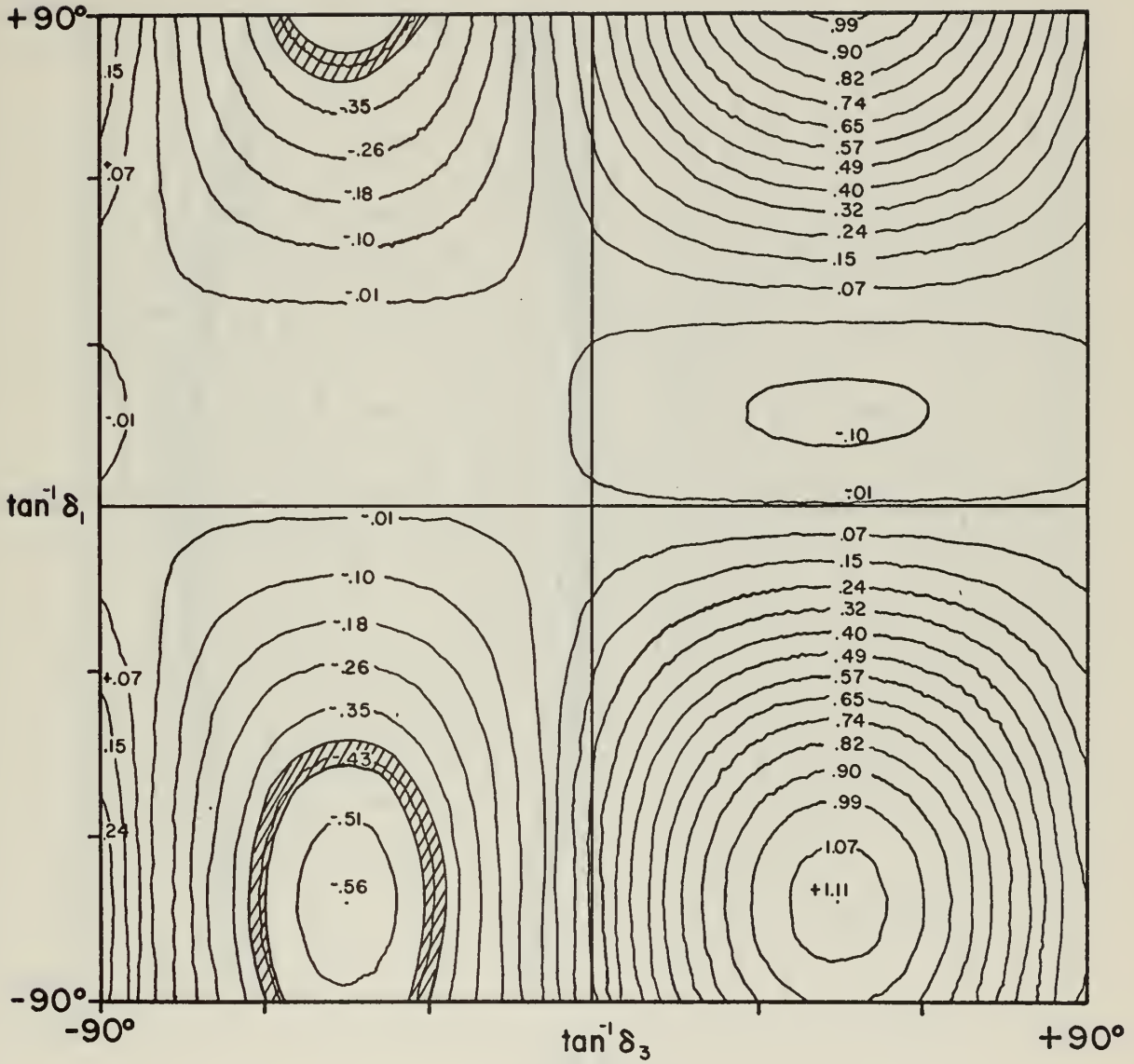

$1+1+A_2/A_o$

FIGURE 15

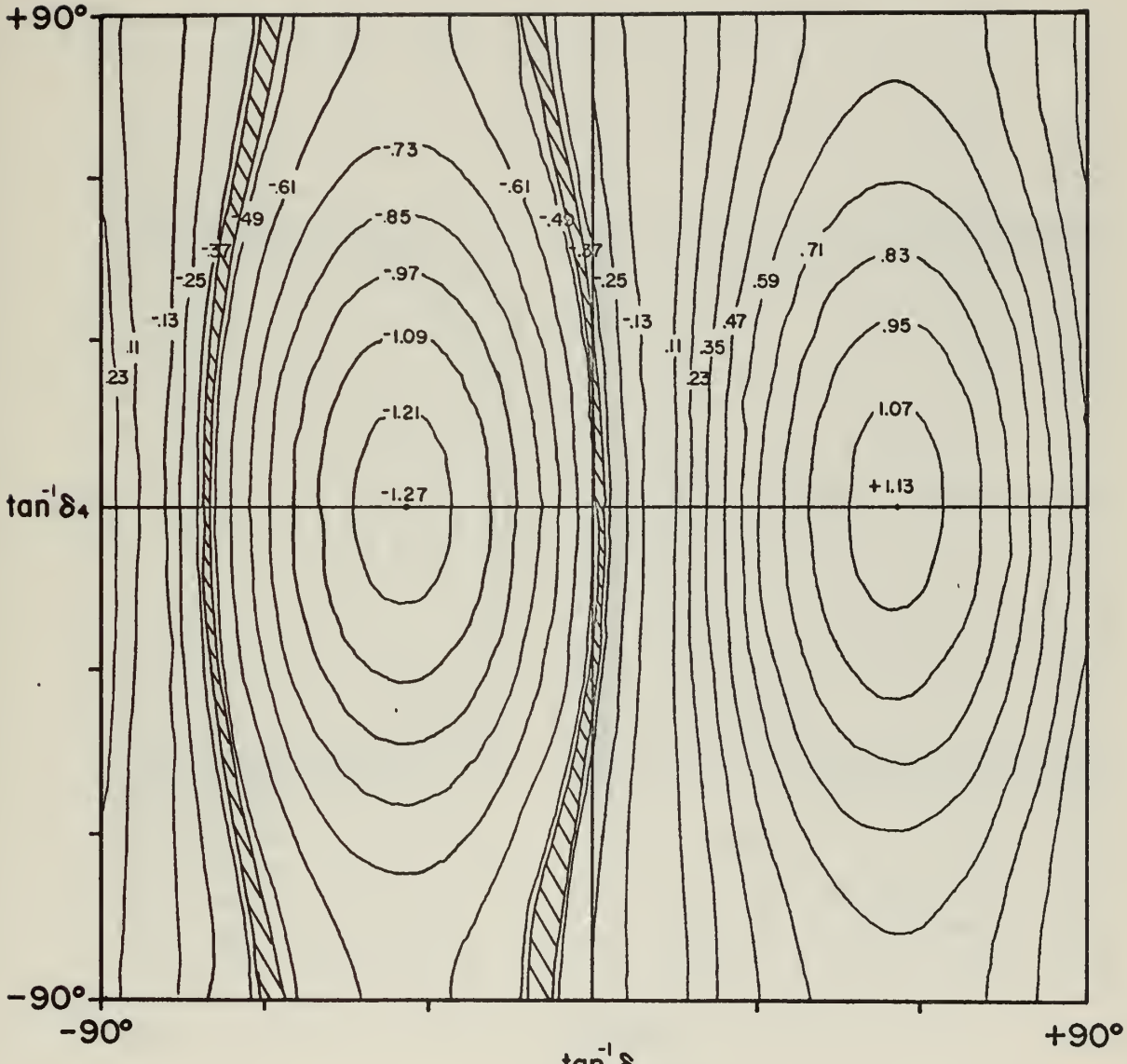

2+1+ A_2/A_o

FIGURE 16a

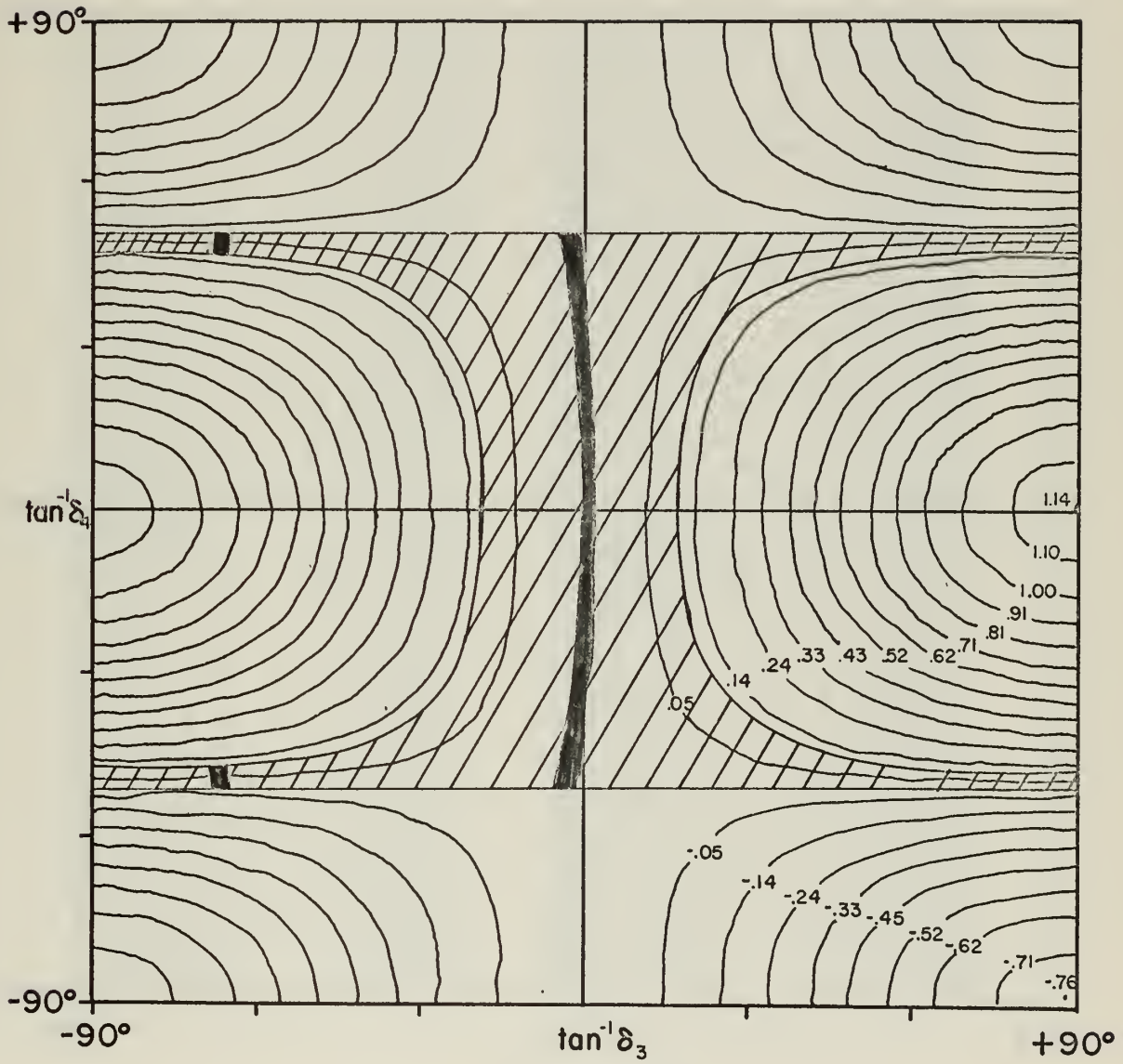

2+1+ A_4/A_o

FIGURE 16b

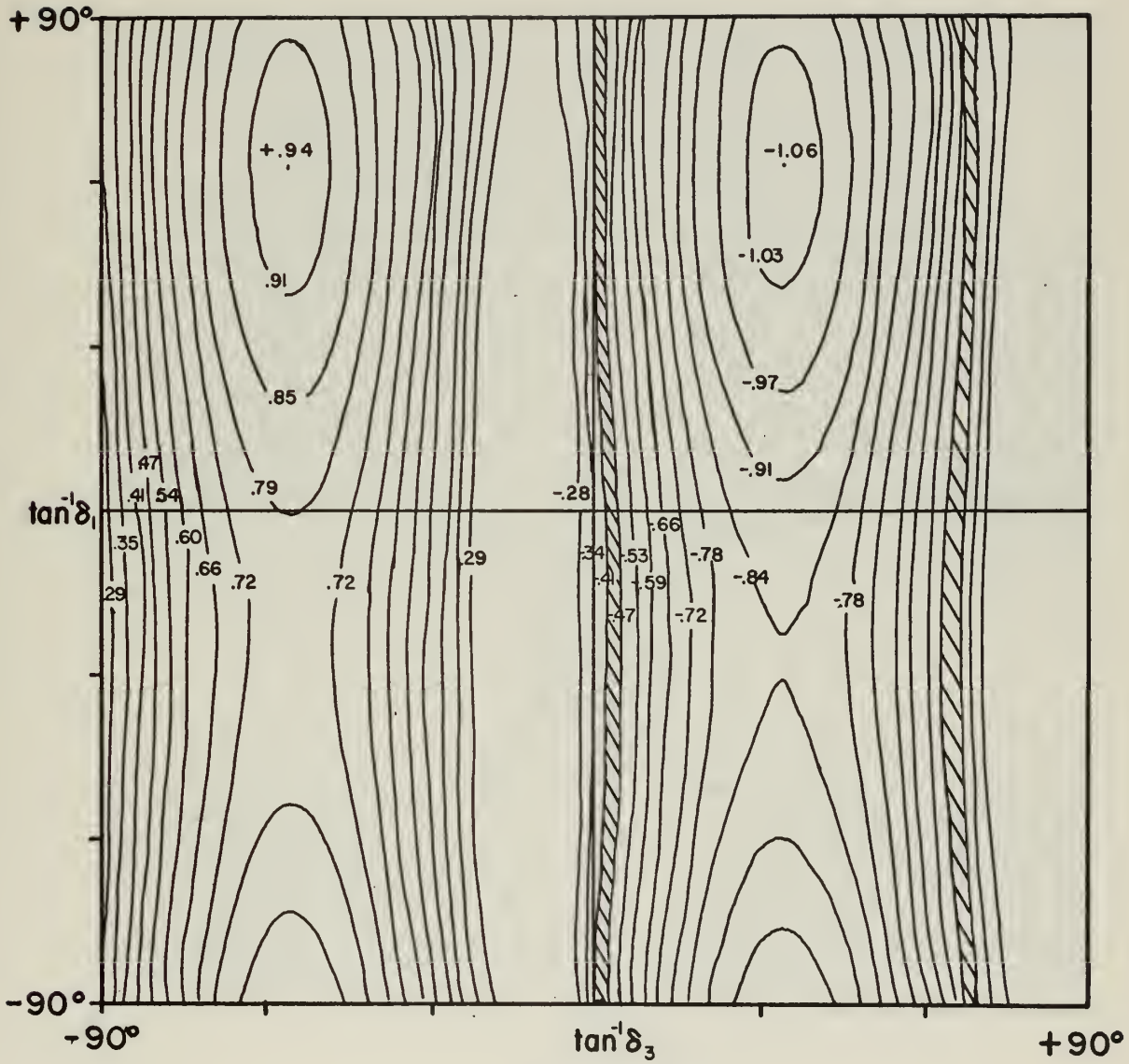

$2-1+A_2/A_o$

FIGURE 17a

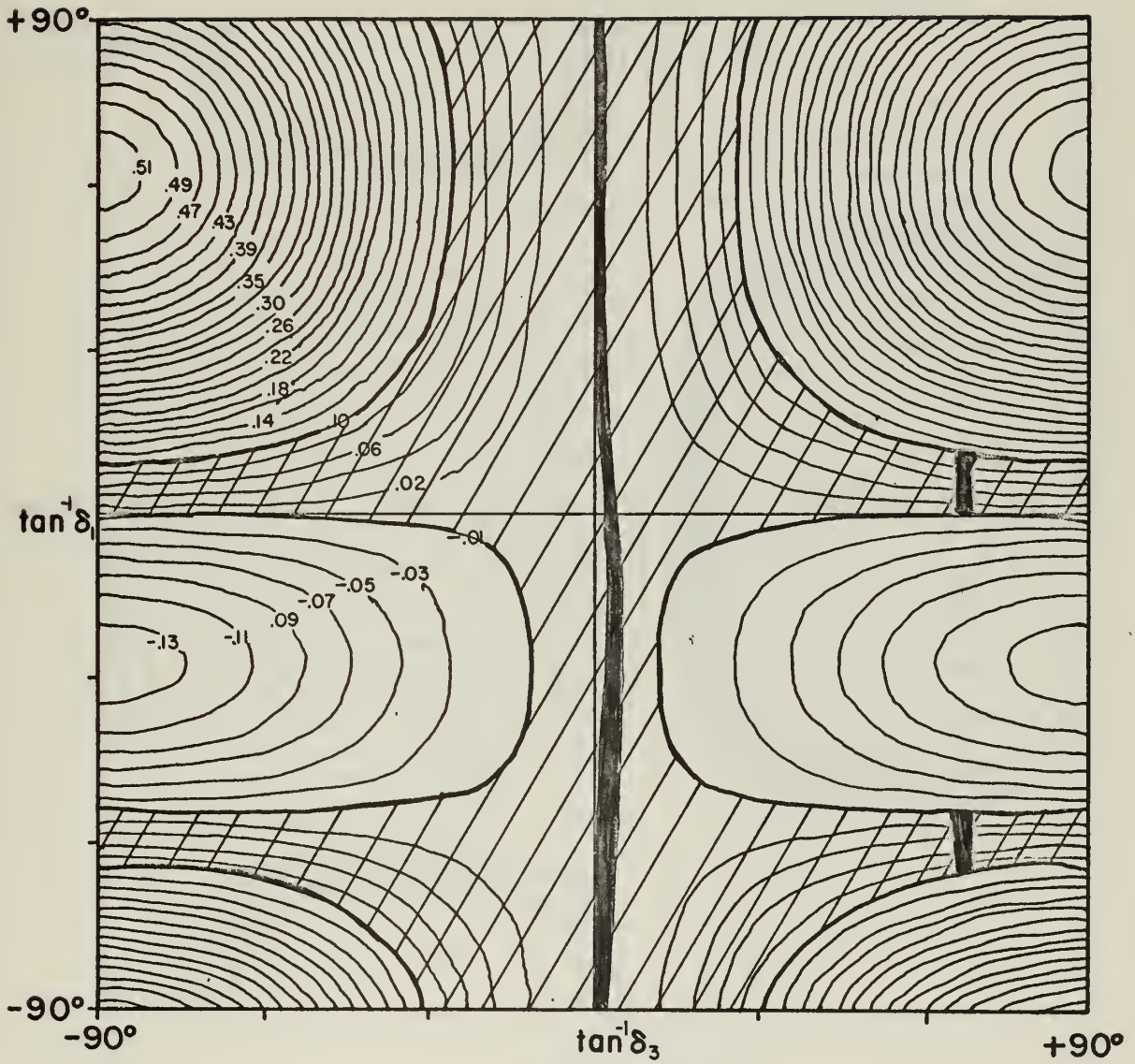

2-1+A_4/A_o
FIGURE 17b

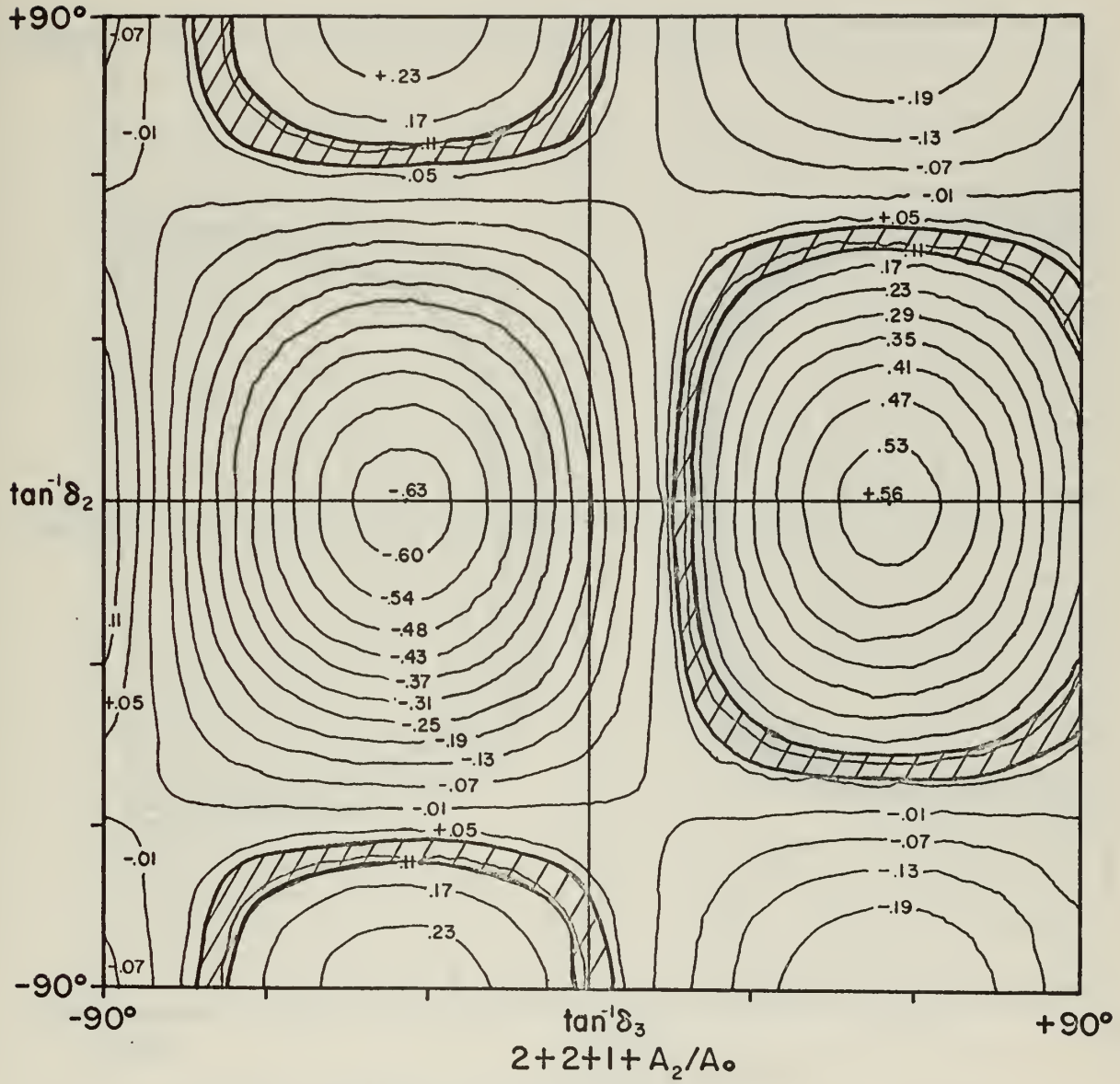

$2+2+1+A_2/A_0$

CASE SHOWN FOR $\delta_4 = 0$

CONTOUR MULTIPLIER = $.75+.25\sin(2\tan^{-1}\delta_4+90°)$

FIGURE 18a

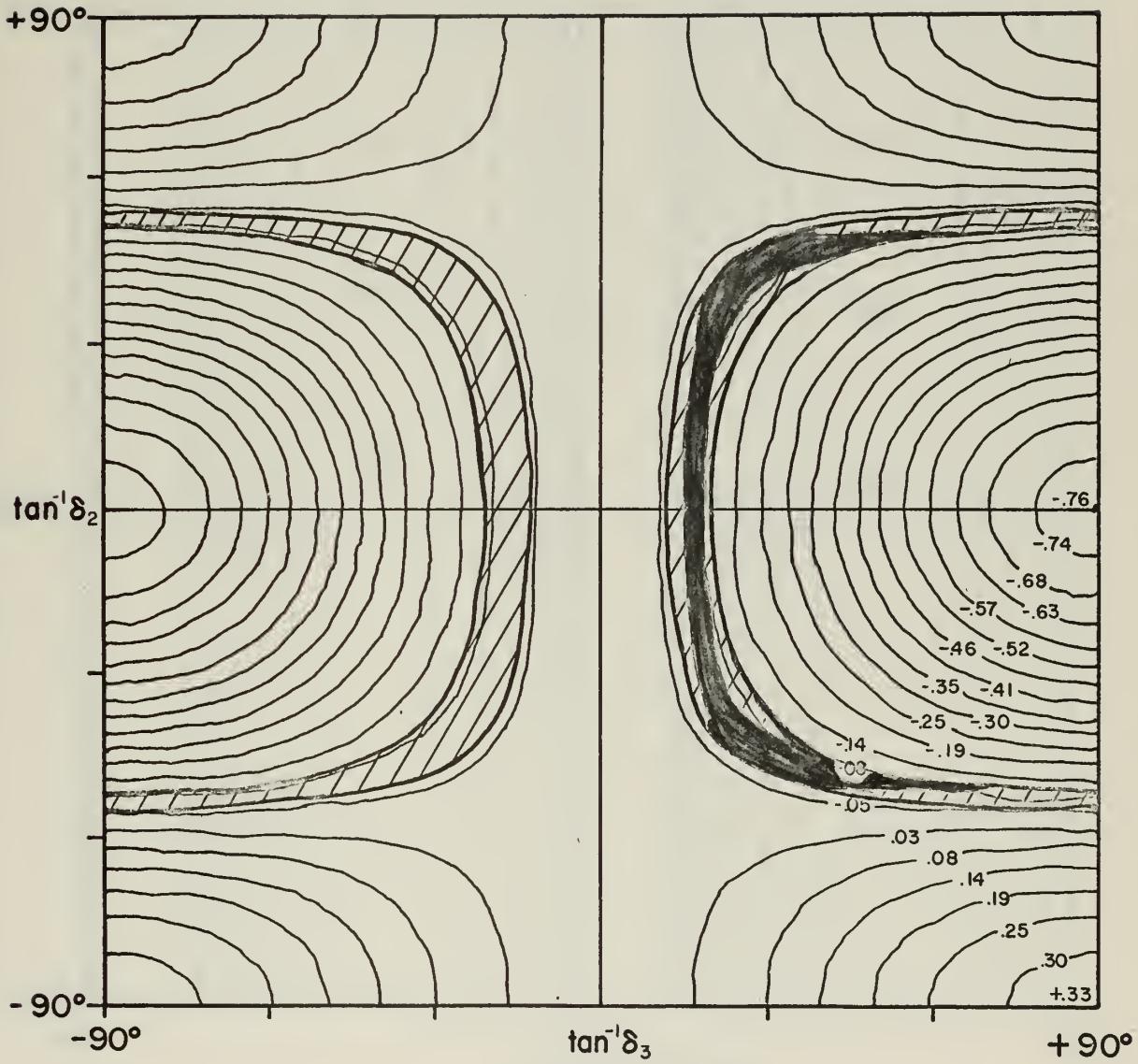

2+2+1+A_4/A_o

CASE SHOWN FOR $\delta_4 = 0$

CONTOUR MULTIPLIER = $-.127 + .635 \sin(2\tan^{-1}\delta_4 - 90°)$

FIGURE 18b

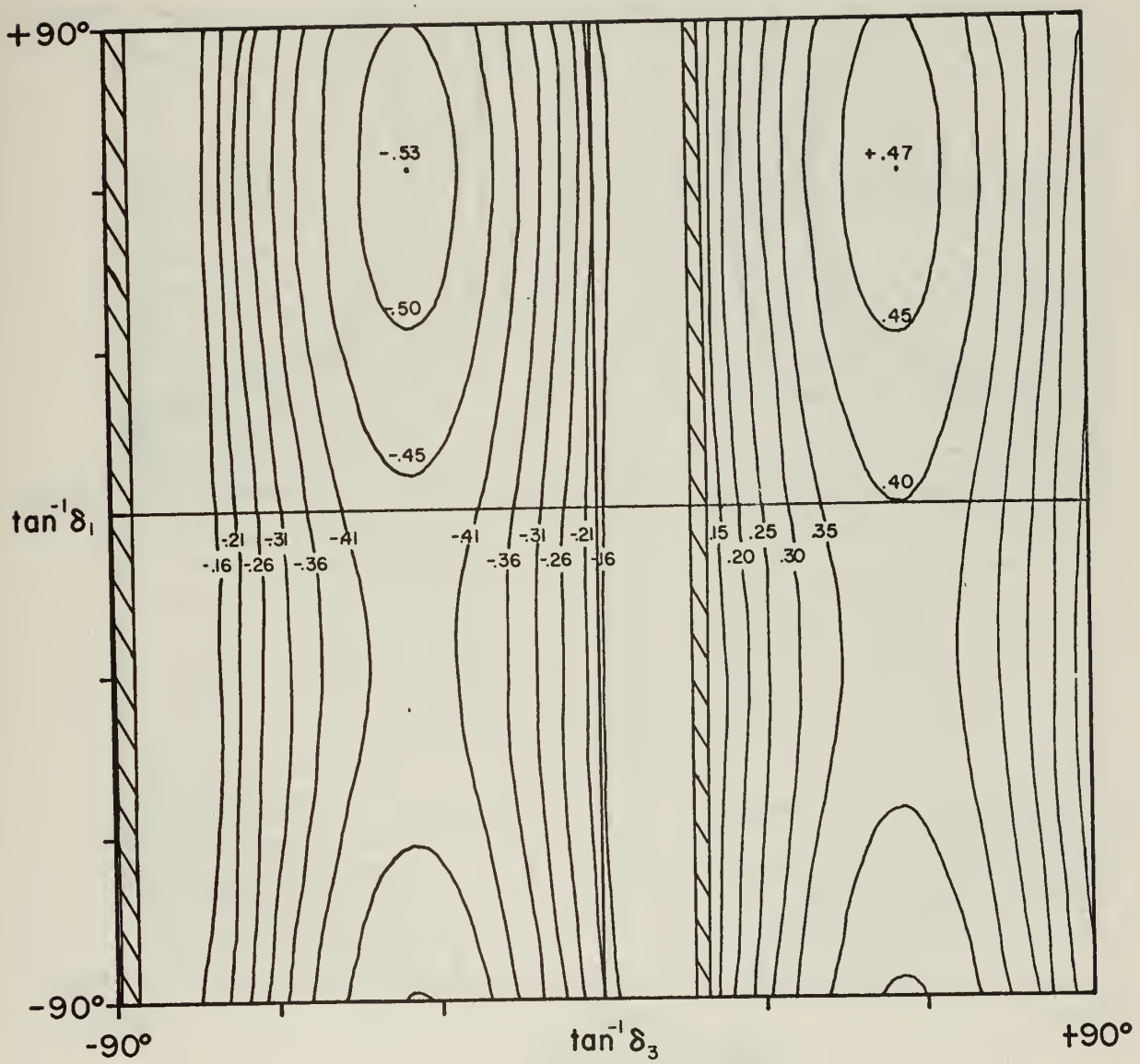

2-2+1+ A_2/A_o

FIGURE 19a

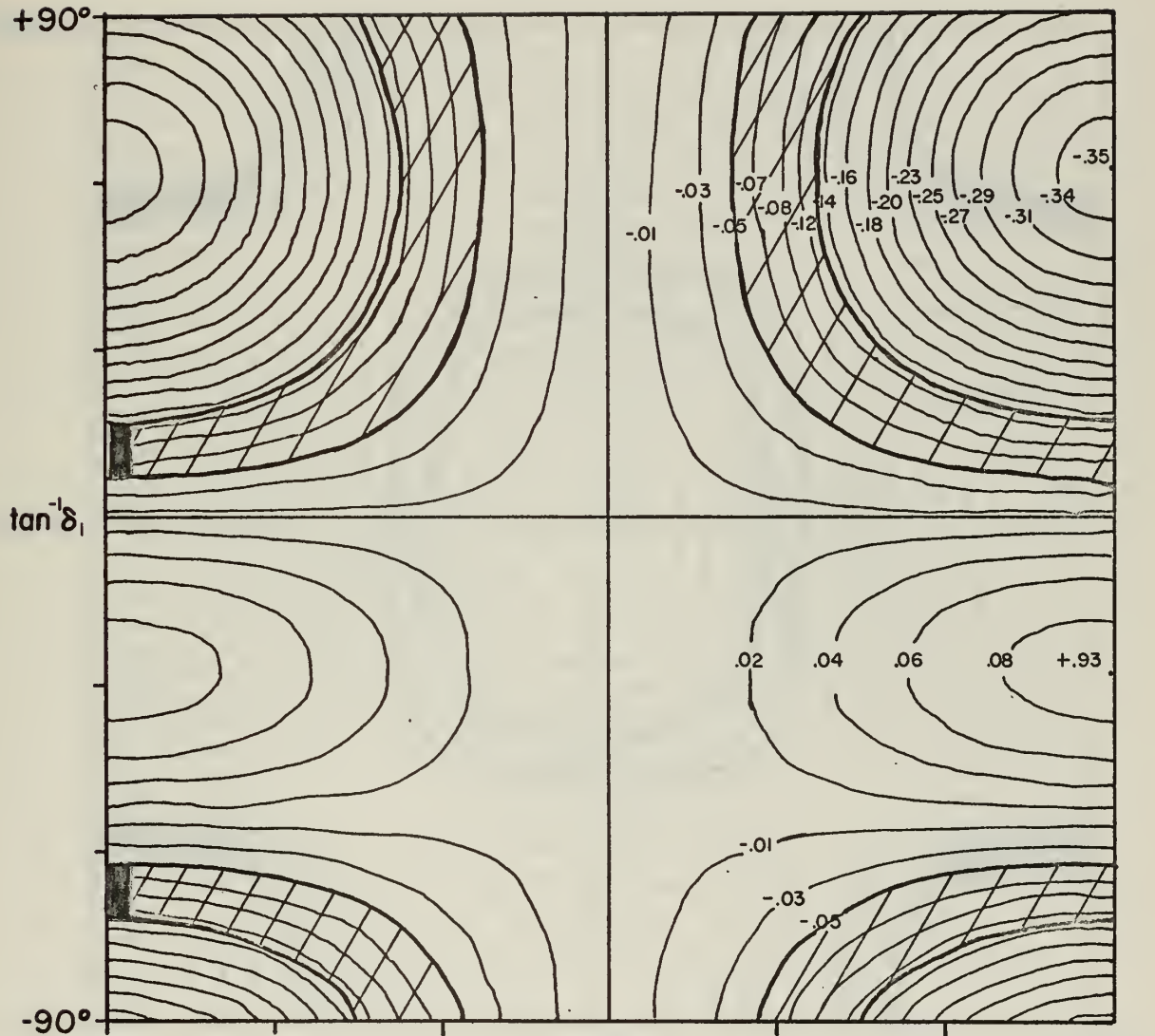

2-2+1+A_4 /A_o

FIGURE 19b

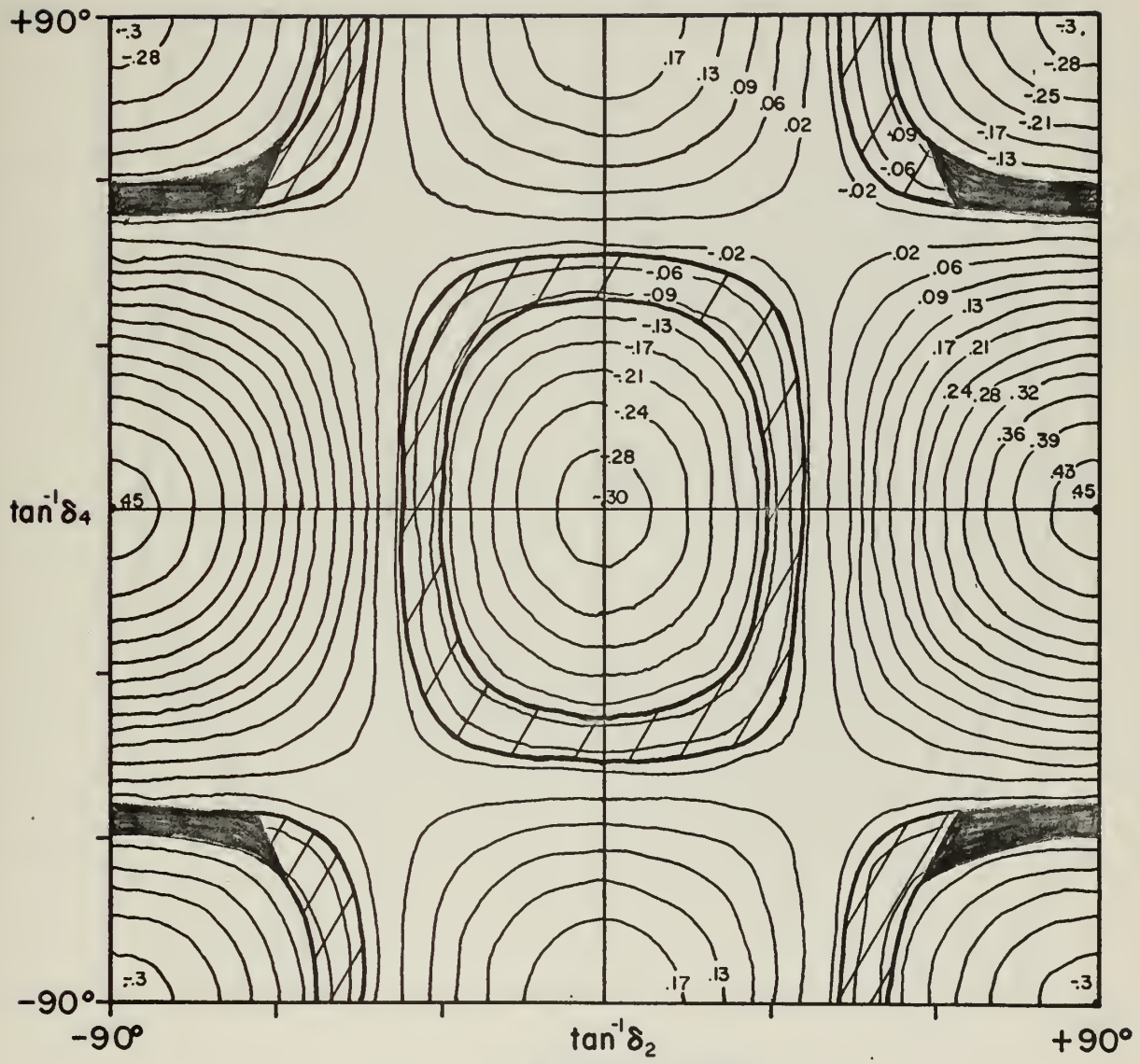

2+3+1+ A_4/A_o

FIGURE 20a

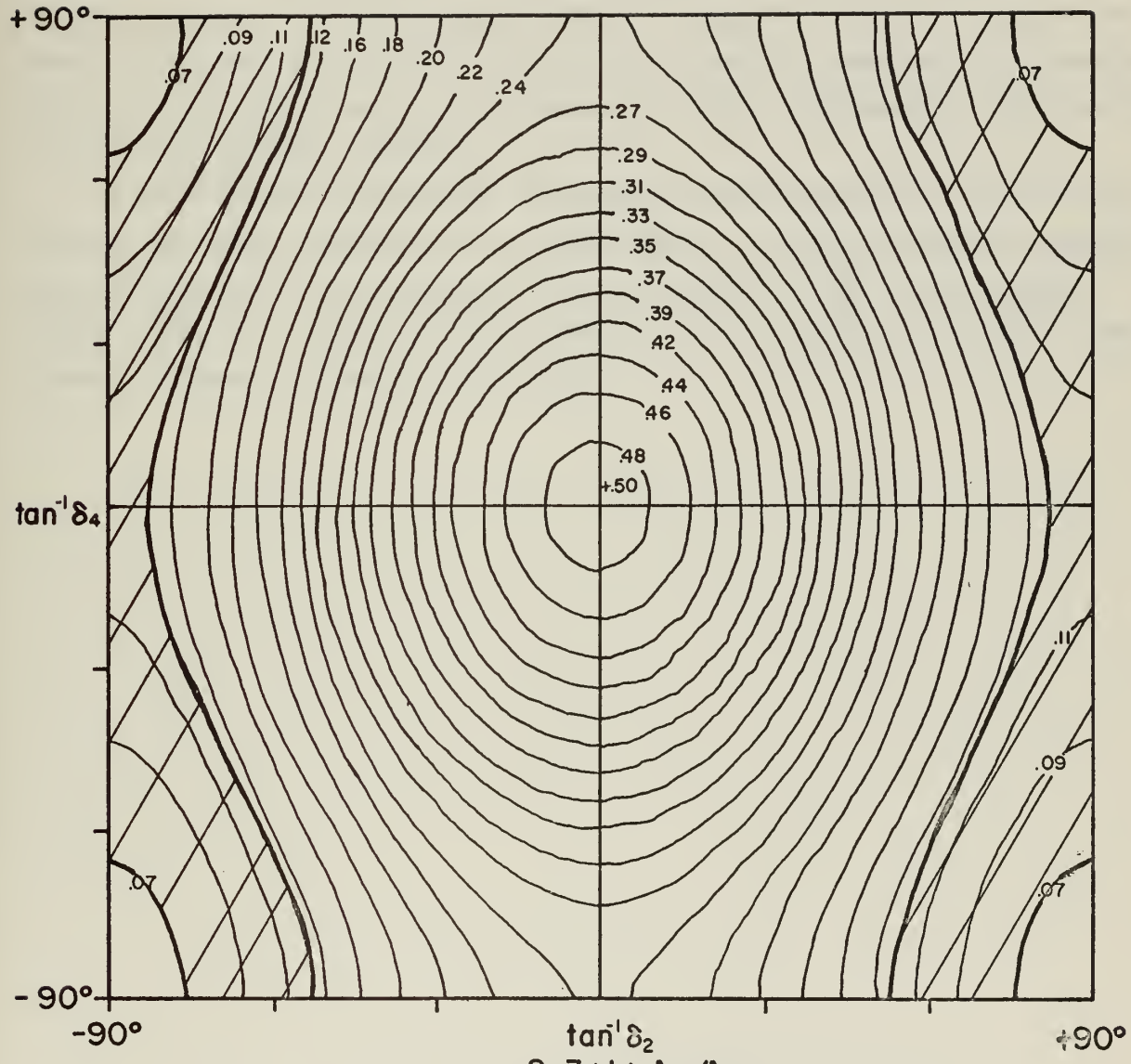

2+3+1+ A_2 /A_o

FIGURE 20b

V ACKNOWLEDGEMENTS

I wish to thank my advisors, Professor H.E. Handler and Professor E.A. Milne for their encouragement, guidance, and advice offered during the course of this work. I also am most grateful to Dr. L.W. Seagondollar and Dr. R.A. Moore of the University of Kansas for pointing out the significance of the 4.50-Mev level spin determination and to Dr. Moore for furnishing results of his experimental work. Among the many other people who have helped make this experiment possible, I wish to thank Mr. R.C. Moeller, Mr. M.A. Brillhart, and Mr. R.A. Garcia for their indispensible contributions to the experimental equipment.

I also wish to acknowledge the help and understanding of my wife Lois during the years consumed by this undertaking. I wish, finally, to express my appreciation of the cooperation and confidence of the Civil Engineer Corps of the U.S. Navy which have made possible my absence from more normal duties in order to complete this work.

Appendix 1 - Theoretical Description of Double Angular Correlations

A. General

There has been abundant literature coverage of the theory of angular correlations of successive nuclear radiations since Hamilton first predicted the effect and developed theoretical expressions for successive emission of quanta. [45] A comprehensive review of the subject has been published by Biedenharn and Rose [46] and recent articles useful in experimental applications have been published by Gove [47] and by Biedenharn. [48] The following notation is essentially that of Biedenharn. In all cases a primed symbol represents a larger value than the same symbol without a prime.

In the case of a (p,γ) reaction in which the direction of a primary gamma ray deexciting a resonance level is observed relative to the direction of an incident proton beam, the angular correlation is referred to as a double correlation. The function describing the relative probability of the gamma decay as a function of the angle between the beam direction and the emitted gamma ray can be written as an expression in the even Legendre polynomials:

$$W(\Theta) = \sum_{\nu=0}^{\nu_{max}} A_\nu(1)A_\nu(2)P_\nu(\cos\Theta) \quad , \quad \text{even} \qquad (1)$$

where $A_\nu(i) = a_\nu(L_iL_i)F_\nu(L_iL_ij_iJ) + 2\delta_h a_\nu(L_iL_i')F_\nu(L_iL_i'j_iJ)$

$$+ \delta_h^2 a_\nu(L_i'L_i')F_\nu(L_i'L_i'j_iJ)$$

and $F_\nu(LL'j_iJ) = (-1)^{j_i-J-1}\left[(2L+1)(2L'+1)(2J+1)\right]^{\frac{1}{2}} \cdot$

$$(LL'1\ -1|\nu 0)W(JJLL';\nu j_i)$$

The index h is related to the index i by:

$$h = i^2 - i + 1$$

$(LL'1\ -1|\nu 0)$ and $W(JJLL';\nu j_i)$ are respectively the Clebsch-Gordon coefficients and the Racah coefficients which are commonly used to describe systems involving coupling of angular momenta. The F functions, for which an extensive tabulation is available, [49] are defined in terms of a Clebsch-Gordon and a Racah coefficient by Biedenharn and Rose. [46] Arguments of the coefficients are angular momenta of the sequence:

$$j_1\begin{pmatrix}L_1'\\L_1\end{pmatrix}J\begin{pmatrix}L_2'\\L_2\end{pmatrix}j_2 \qquad (2)$$

j_1 = channel spin = proton spin $\oplus$ target spin

L_1, L_1' = interfering proton orbital angular momenta

J = spin of resonance level

L_2, L_2' = interfering gamma ray multipolarities

j_2 = spin of final state (not necessarily a ground state)

δ_1 = mixing parameter representing the ratio of the reduced matrix element for the transition involving L_1' proton waves to that for L_1 waves

δ_3 = mixing parameter representing the ratio of the amplitude of gamma rays of multipolarity L_2' to those of multipolarity L_2

$$a_\nu(LL') = \cos(\xi_L - \xi_{L'}) \cdot \frac{2[L(L+1)L'(L'+1)]^{\frac{1}{2}}}{L(L+1)+L'(L'+1) - \nu(\nu+1)} \qquad (3)$$

is a particle parameter in which ξ_L and $\xi_{L'}$ are the phases at the nuclear surface of the particle partial wave functions of multipolarity L and L'. The coherent interference between partial waves is expressed by the $\cos(\xi_L - \xi_{L'})$ term. The factor ξ includes the coulomb phase shift due to electrostatic potential for charged particles and the phase shift occurring in "hard sphere" scattering. The $a_\nu(L_2L_2')$ terms for photons as opposed to particles are equal to unity. In the case where mixing of channel spins j_1 and j_1' occur, W(θ) may be expressed as an incoherent mixture:

$$W(\theta) = W_{j_1}(\theta) + \delta_4^2 W_{j_1'}(\theta) \qquad (4)$$

where δ_4^2 is a mixing parameter expressing the ratio of probability of channel spin j_1' entering the reaction to that of channel spin j_1, $(j_1' \; j_1)$. The maximum order of Legendre polynomials appearing in (1), ν_{max}, is determined by conditions imposed on the W (abcd; ef) coefficients by conservation of angular momentum which may be expressed by the so-called triad relationships. These require each of the triads of values (acf), (bdf), (abe), and (cde) to form a possible triangle. Restriction to the case of intermediate states of well defined parity (i.e. no interferring intermediate states of opposite parities) leads to the further simplification that ν may take on only even values.

In the case of the reaction (p,xγ), in which x represents an unobserved intermediate gamma ray, the correlation is expressed as an incoherent mixture of multipoles occurring in the unobserved transition, i.e. in

the sequence:

$$j_0\begin{pmatrix}L_0\\L_0'\end{pmatrix}J_1\begin{pmatrix}L_1\\L_1'\end{pmatrix}J_2\begin{pmatrix}L_2\\L_2'\end{pmatrix}j_2 \tag{5}$$

$W(\theta)$ can be expressed: $W(0) = W_{L_1}(\theta)+\delta_2^2 W_{L_1'}(\theta)$ (6)

where:

j_0 = channel spin

L_0, L_0' = interfering proton orbital angular momenta

J_1 = spin of resonance level

L_1, L_1' = interfering gamma ray multipolarities of unobserved radiation

J_2 = spin of intermediate level

L_2, L_2' = interfering gamma ray multipolarities of observed radiation

j_2 = spin of final state

δ_2^2 = ratio of intensity of the unobserved gamma ray of higher multipolarity to the intensity of the lower multipolarity gamma ray.

The correlation function now contains an additional part expressing the connection between the two intermediate levels by the unobserved radiation as follows:

$$W(\theta) \sum_{\nu}^{\nu_{max}} A_\nu(0)C_\nu(1)A_\nu(2)P_\nu(\cos\theta) \tag{7}$$

where the $A_\nu(i)$ are the same as in (1) and

$$C_\nu(1) = (-1)^\nu \left[(2J_1+1)(2J_2+1)\right]^{\frac{1}{2}} W(J_1\ L_1 J_2;\ J_1 J_2)$$

It is seen that for the general double correlation case four mixing parameters may occur (barring the further complication of mixed intermediate states).

In the present investigation the Si^{29} target nucleus has a ground-state spin of $1/2+$, with the simplifying result that channel-spin mixing and proton-partial-wave mixing may not occur simultanously. The number of δ's is thus limited to a maximum of three. Explicitly, for resonance levels of $1+$, $2-$, $3+$, $4-$, etc. orbital angular momentum mixing of two partial waves may occur but channel-spin mixing is prohibited. For the resonance level spins of opposite parities from those listed only channel-spin mixing is permitted.

When three mixing parameters occur in the general case of intermediate unobserved radiation $(p,x\gamma)$ with a spin sequence

$$\begin{pmatrix} j_0' \\ j_0 \end{pmatrix} L_0 J_1 \begin{pmatrix} L_1' \\ L_1 \end{pmatrix} J_2 \begin{pmatrix} L_2' \\ L_2 \end{pmatrix} j_2 \quad \text{or} \quad j_0 \begin{pmatrix} L_0' \\ L_0 \end{pmatrix} J_1 \begin{pmatrix} L_1' \\ L_1 \end{pmatrix} J_2 \begin{pmatrix} L_2' \\ L_2 \end{pmatrix} j_2 \tag{8}$$

the normalized correlation function can be expressed as

$$W(\theta) = 1/A_0 \sum_{\nu} A_\nu P_\nu(\cos\theta) \tag{9}$$

where each A_ν/A_0 is a product of the form:

$$A_\nu/A_0 = \prod_{\mu} g_{\nu\mu}(\delta_\mu) \tag{10}$$

with $\mu = 1,2,3$ or $2,3,4$

and $$g_{\nu\mu} = \frac{a_{\nu\mu} + \delta_\mu \varphi_\mu b_{\nu\mu} + \delta_\mu^2 c_{\nu\mu}}{(1+\delta_\mu^2)}$$

(It is to be noted that the coefficient A_ν appearing in (9) is a conventional representation of the more complete forms shown in (1) and (7). A distinction must also be made, of course, between the correlation function $W(\theta)$ and the Racah coefficient $W(abcd; ef)$.

The coefficients a, b, and c can be expressed as follows:

proton wave mixing

$$a_{\nu 1} = \frac{2L_0(L_0+1)}{2L_0(L_0+1) - \nu(\nu+1)} F_\nu(L_0 J_0 J_1)$$

$$b_{\nu 1} = \frac{4\left[L_0(L_0+1)L_0'(L_0'+1)\right]^{\frac{1}{2}}}{L_0(L_0+1) + L_0'(L_0'+1) - \nu(\nu+1)} F_\nu(L_0 L_0' J_0 J_1) \qquad (11)$$

$$c_{\nu 1} = \frac{2L_0'(L_0'+1)}{2L_0'(L_0'+1) - \nu(\nu+1)} F_\nu(L_0' J_0 J_1)$$

unobs. gamma mixing

$$a_{\nu 2} = (-1)^\nu \left[(2J_1+1)(2J_2+1)\right]^{\frac{1}{2}} W(J_1 \nu L_1 J_2; J_1 J_2)$$

$$b_{\nu 2} = 0$$

$$c_{\nu 2} = (-1)^\nu \left[(2J_1+1)(2J_2+1)\right]^{\frac{1}{2}} W(J_1 \nu L_1' J_2; J_1 J_2)$$

gamma mixing

$$a_{\nu 3} = F_\nu(L_2 J_2 J_2)$$

$$b_{\nu 3} = 2F_\nu(L_2 L_2' J_2 J_2)$$

$$c_{\nu 3} = F_\nu(L_2' J_2 J_2)$$

chan. spin mixing

$$a_{\nu 4} = \frac{2L_0(L_0+1)}{2L_0(L_0+1) - \nu(\nu+1)} F_\nu(L_0 J_0 J_1)$$

$$b_{\nu 4} = 0$$

$$c_{\nu 4} = \frac{2L_0(L_0+1)}{2L_0(L_0+1) - \nu(\nu+1)} F_\nu(L_0 J_0' J_1)$$

$$\rho_1 = \cos(\xi_{L_0} - \xi_{L_0'})$$

$$\rho_2 = \rho_3 = \rho_4 = 1$$

For the (p,γ) case the only changes required are: $a_{\nu 2} = 1$, $b_{\nu 2} = 0$, $c_{\nu 2} = 0$ and $J_1 = J_2 = J$.

The angular correlation function, as an alternative, may be expressed in terms of the coefficients Z and Z_1, instead of the F coefficients:

proton wave mixing

$$\begin{aligned} a_{\nu 1} &= (-1)^{j_0} Z(L_0 J_1 L_0 J_1, j_0 \nu) \\ b_{\nu 1} &= 2(-1)^{j_0} Z(L_0 J_1 L_0' J_1, j_0 \nu) \\ c_{\nu 1} &= (-1)^{j_0} Z(L_0' J_1 L_0' J_1, j_0 \nu) \end{aligned} \qquad (12)^{*}$$

unobs. gamma mixing

$$\begin{aligned} a_{\nu 2} &= (-1)^{-L_1} W(J_1 J_2 J_1 J_2; L_1 \nu) \\ b_{\nu 2} &= 0 \\ c_{\nu 2} &= (-1)^{-L_1'} W(J_1 J_2 J_1 J_2; L_1' \nu) \end{aligned}$$

gamma mixing

$$\begin{aligned} a_{\nu 3} &= (-1)^{j_2} Z_1(L_2 J_2 L_2 J_2, j_2 \nu) \\ b_{\nu 3} &= 2(-1)^{j_2} Z_1(L_2 J_2 L_2' J_2, j_2 \nu) \\ c_{\nu 3} &= (-1)^{j_2} Z_1(L_2' J_2 L_2' J_2, j_2 \nu) \end{aligned}$$

chan. spin mixing

$$\begin{aligned} a_{\nu 4} &= (-1)^{j_0} Z(L_0 J_1 L_0 J_1, j_0 \nu) \\ b_{\nu 4} &= 0 \\ c_{\nu 4} &= (-1)^{j_0'} Z(L_0 J_1 L_0 J_1; j_0' \nu) \end{aligned}$$

For (p,γ) reactions $J_1 = J_2 = J$, $a_{\nu 2} = (2J+1)^{-1}$, $b_{\nu 2} = 0$, $c_{\nu 2} = 0$

* (The two formalisms (11) and (12) are to some extent incompatible. Not only may the coherent mixing parameter phases differ by ± 1 [50,51] but also for $L_0 = 0$ the parameter δ_1 doesn't represent the same matrix element ratio in both notations. The notation above, (12), has been used for most calculations in the present work. These expressions are in agreement with Sharp [52] except that the sign of $b_{\nu 3}$, for the $(p,x\gamma)$ case only, has been changed to agree with the part of Huby's correction applying to the observed gamma ray.[50,51] For the "unnatural" radiation mixtures (M1/E2, E3/M2, etc.) the sign of $b_{\nu 3}$ should be reversed. This sign convention permits the use of Moore's tabulated values [23] where the same convention is used.)

The Z and Z_1 coefficients and Racah and Clebsch-Gordon coefficients have been tabulated by Sharp et al. [52] Using this tabulation Moore [23] has prepared a convenient table of the a, b, and c coefficients applicable to radiative proton capture by Si^{29}.

In order to fit experimental data on angular correlation coefficients to theory, it is desirable to first eliminate as many spin sequences as possible on the basis of any evidence which may be available. In cases where only two mixing parameters enter, contour plots [47] showing contours of constant theoretical values of the coefficients A_2/A_0 can be plotted against the inverse tangents of the two mixing parameters for all possible spin sequences. If three mixing parameters enter, one of them may be held constant for the purpose of plotting the correlation coefficient contours against the inverse tangents of the other two parameters. It is seen from (10) that the contour values for different values of the fixed parameter differ only by a multiplicative constant.

When experimental values of correlation coefficients are delineated on the contour plot, some spin sequences can be eliminated and the possible combinations of mixing parameters are restricted for other sequences. The observed values of several correlation coefficients in one decay scheme may then fix or highly restrict values of the spin-parities of resonance and intermediate levels, and determine the values of the mixing parameters.

B. Application to 1470-kev resonance

For the resonance occurring at a laboratory proton energy of 1470 kev, the phase factor $\cos(\xi_L - \xi_{L'})$ has been calculated using the expression $\xi_L = \sigma_L + \phi_L$ where σ_L represents the phase shift due to the point coulomb potential and ϕ_L is the "hard sphere" phase shift.

σ_L is defined [42] by $\exp(2i\sigma_L) = \dfrac{\Gamma(L+1+i\eta)}{\Gamma(L+1-i\eta)}$ (13)

where $\eta = \dfrac{ZZ'e^2}{\hbar v}$ which leads to:

$$\sigma_{L+2} - \sigma_L = \tan^{-1}\left(\frac{\eta}{L+2}\right) + \tan^{-1}\left(\frac{\eta}{L+1}\right) \quad (14)$$

The value for ϕ_L defined by

$$\exp(2i\phi_L) = \frac{G_L(\eta,kR) - iF_L(\eta,kR)}{G_L(\eta,kR) + iF_L(\eta,kR)} \quad (15)$$

where F and G are the regular and irregular solutions to the radial wave equation for the coulomb potential. The value for ϕ_L can be found from the graphs of Sharp et al. [53] (these graphs actually list $-\phi_L$) and employing $R = 1.5A^{1/3}f$. as an estimate of the nuclear radius. These graphs have also been used to calculate the relative pentration factors

$$v_L/v_{L-2} = \frac{F_{L-2} + G_{L-2}}{F^2_L + G^2_L} \quad (16)$$

which are useful as a guide to the expected mixing parameter of interfering partial proton waves. [42] Results of these calculations appear in Tables 8 and 9.

TABLE 8

Relative Penetration Factors for 1470-Kev Protons

d/s	f/p	g/d
3.1×10^{-2}	5.0×10^{-3}	1.3×10^{-3}

TABLE 9

Coulomb Phase Factors for 1470-Kev Protons

$\xi_2 - \xi_0$	$\xi_3 - \xi_1$	$\xi_4 - \xi_2$
104°	73°	56°

Appendix 2 - Computer Programs and Analysis

A. General

In order to analyze experimental data in the form of gamma-ray spectra recorded by the 128-channel analyzer, two computer programs were developed. The first and more extensive program entitled program SPECFIT computes experimental correlation coefficients, while program CONTOUR is designed to utilize a California Computer Products Model 565 graph plotter as an output medium to automatically plot contours of constant angular correlation coefficient values against the inverse tangents of two mixing parameters. Both programs are written in fortran language and were run on a CDC-1604 digital computer.

B. Program SPECFIT

The output pulses of a photomultiplier tube viewing a scintillation crystal upon which monoenergetic photons impinge do not all have the same voltage. Instead, the three fundamental processes of photoelectric absorption, Compton scattering and pair production, which occur in the crystal with probabilities dependent upon gamma-ray energy, lead to a response pulse-spectrum which is characteristic of each particular gamma-ray energy. Experimental geometry, crystal size, shielding, various line-broadening effects, and characteristics of individual crystal-photomultiplier tube combinations influence the response also, so that response functions are in general unique for each spectrometer in a given experimental arrangement.

An experimentally observed spectrum is, of course, usually composed of a number of gamma rays, the spectrum being the sum of the constituent radiations each multiplied by its intensity. The problem of deciphering such an observed spectrum to obtain the energies and intensities of component gamma rays is of fundamental importance in gamma ray spectroscopy and has not yet been satisfactorily solved in complete generality.

Using notation, which is appropriate for the discrete pulse height intervals into which multi-channel analyzers sort pulses, and also appropriate for the discrete number of gamma ray energies composing resonance deexcitation spectra, one can write:

$$S_i = \sum_{j=1}^{m} R_{ij} I_j$$

where S_i = observed number of counts in channel i

R_{ij} = probability that a photon of energy E_j originating at a particular source will produce a pulse falling in pulse height channel i (usually referred to as the response matrix)

I_j = the number of photons of energy E_j originating at the source

m = the number of gamma ray energies which occur in the spectrum under consideration

A rather fundamental and obvious approach to this problem is to assume no knowledge of gamma-ray energies is available, divide the gamma ray energy range into a number of discrete intervals equal to the number of channels, then solve for:

$$I_i = \sum_j \sum_k R_{ik}^{-1} R_{kj} I_j = \sum_k R_{ik}^{-1} S_k$$

In fact, the first attempt to unfold experimental spectra in the present work utilized a modification of a program[54] which employed an iterative technique developed by Schofield[55] to solve the above equation. This attempt failed for two reasons which are rather instructive. First, the analytical expression used to approximate the response matrix did not adequately represent the true spectrometer response, and second, the technique proved inadequate with experimental counting statistics attainable to handle the analysis of approximately 100 channels.

In order to avoid the first problem resort was had to the technique of interpolating between experimentally-determined monoenergetic calibration curves in order to obtain the response matrix. In order to overcome the second objection it was decided to use information on the gamma ray energies available from preliminary "stripping" of spectra and from other sources. Having thus reduced the number of gamma rays to be considered, a linear combination of the selected response matrix elements was then fitted to the observed spectrum by a least squares process. This procedure was followed by another least squares analysis to obtain

correlation function coefficients from the gamma ray intensities calculated for a series of runs at different experimental angles. The steps in the computation procedure in program SPECFIT as finally developed are as follows:

1. Load data. (See section D of this Appendix)

2. Subtract any constant background from calibration spectra. This background represents the Compton "tails" of higher energy gamma rays contaminating certain of the calibration gamma rays.

3. Normalize each calibration spectrum to a photopeak height of one unit.

4. Include a straight line in the response matrix if this option is selected. This step is essentially a refinement of step 2.

5. Correct the input and background spectra for dead time of the pulse height analyzer. For this purpose the dead time given by the manufacturer is 38 + 0.5i microseconds where i is the pulse height channel number. This leads to an expression for corrected counts:

$$N'_j = \frac{N_j}{1 - 1/T \sum_{i=2}^{127} N_i (38 + 0.5i) \cdot 10^{-6}}$$

where N_i = the number of counts observed in channel i

T = counting time in seconds

6. Calculate energies in Mev corresponding to each channel number of the input spectrum.

7. Adjust energy scale and number of channels of background spectrum to match the input spectrum. Multiply by ratio of run times to get the proper background to be subtracted from the input spectrum and perform the subtraction.

8. Using the monoenergetic calibration spectra, calculate a matrix of response curves for the gamma rays which the spectrum is to be decomposed into. This calculation is performed in a subroutine entitled RESPONS as follows:

   a. Find the two calibration curves bracketing a gamma ray energy desired as a response matrix element.

b. Shift the lower-energy calibration curve found in a. so that its photopeak falls in the same channel as the higher energy photopeak. Fill in bottom of shifted curve as determined by the slope between the bottom two unshifted channels. Match energy calibration of the lower-energy curve to the upper. (For this step, and elsewhere where interpolation is necessary, cubic interpolation is performed using the four nearest points to the desired value.)

c. Interpolate linearly between each pair of points of the bracketing calibration curves to obtain a response curve for the desired gamma-ray energy. (A "curve" in this description is meant to imply the vector consisting of a 1 X n array of values, n being the number of channels used in the description).

d. Using the input spectrum channel energies calculated in 6., interpolate to get a response curve with channels and channel energies corresponding to those of the input data.

e. Normalize the response curve for the given gamma-ray energy so that the ordinate corresponding to each channel represents the probability that one photon leaving the source will produce a count in that channel. For this calculation the experimentally-determined intrinsic peak efficiency data of Lazer[56] have been used to derive the following approximate expression for intrinsic peak efficiency as a function of source distance:

$$\epsilon = AE^{-x}$$

where $A = .165 + .0067h$

$x = .9699 - .00918h$

h = source to crystal distance in centimeters

E = gamma ray energy in Mev

Assuming an accurately gaussian photopeak, and that the crystal resolution is approximately inversely proportional to the square root of gamma ray energy, (an assumption which was experimentally verified) the ratio of photopeak height to area can be expressed:

$$\alpha = \frac{1}{6\sqrt{2\pi}} = \frac{2}{WR}\sqrt{\frac{\ell n 2}{.662\pi E}} = \frac{1}{.866WR\sqrt{E}}$$

where R is the usual resolution definition of peak width at one half maximum amplitude divided by energy for the Cs^{137} gamma ray, and W is the spectrometer calibration in pulse height channels per Mev. When α is multiplied by the appropriate solid angle fraction and attenuation coefficient, the value obtained represents the probability of recording one count in the photopeak channel when one photon originates at the source.

f. Return to main routine.

9. Fit the experimental spectrum with a linear combination of the selected monoenergetic response curves, the coefficients representing absolute intensities because of the method of normalizing the response matrix. The weighted sum of the squares of the differnces between observed channel counts and fitted counts is minimized in order to arrive at this fit. The normal equations resulting from the minimization are:

$$\sum_j S_j R_{jk} w_j = \sum_{ij} R_{ji} R_{jk} I_i w_j = 0 \qquad i \leqslant j$$

where S_j = Observed counts in channel j

R_{jk} = Response matrix element giving probability of a count in channel j due to one photon of energy E_k originating at the source

w_j = Weight assigned to the squared error in channel j

I_i = Number of photons of energy E_i which leave the source during the counting period

j summations are over the channels for which a fit is desired

i summation is over the number of gamma ray energies E_i used to fit the observed spectrum

For calculation the I_i are expressed: $I_i = \sum_k A_{ki}^{-1} B_k$

with $A_{ki} = \sum_j R_{ji} R_{jk} w_j$ and $B_k = \sum_j S_j R_{jk} w_j$

A standard subroutine (GAUSS3) is used to invert A. Mention should be made of the weights w_j which have been used. Normally, for a Poisson distribution the weight is taken as $1/\sigma^2$ where the number of observed counts in a channel are used as an estimate of the variance σ^2. Ferguson,[57] who has pointed out that this procedure overweights statistically low counts, identifies the Poisson distribution variance, which rightly is the mean number of counts, with the fitted number of counts for each channel. This procedure is adopted here with a modification to account for statistical error arising from the subtraction of background counts. We have $S_i' = S_i - b_i$, where S_i are observed channel counts corrected for dead time and b_i are background counts to be subtracted. Then,

$$\sigma^2(S_i') = \sigma^2(S_i) + \sigma^2(b_i)$$

$$\approx S_i + (T/T_b)b_i = S_i' + (1 + T/T_b)b_i$$

where T = counting time for data and T_b = counting time for background run. Identifying S_i' with the computed number of counts, S_i'', then gives $S_i'' + (1 + T/T_b)b_i$ for the channel variances. To avoid overweighting of very small values of fitted counts an arbitrary minimum value of σ^2 is chosen to be two per cent of the average value of σ_i^2 over the fitted channels. Since no fitted count values are initially available, an initial weight of one is assigned to each channel and the solution is then iterated to convergence, stopping when

$$\sum_i \left(\frac{\delta Ii}{Ii}\right)^2 \quad \text{is smaller than } 10^{-6}.$$

(This series of iterations, usually five in the present work, accounts for most of the program running time and can be abbreviated for preliminary analyses; see reference 57 in this regard.) $\delta I_i/I_i$ is the fractional change in the computed intensity of the i^{th} gamma ray between successive iterations.

10. The computed intensities are examined for algebraic sign. Since only positive intensities have a physical basis any negative intensities are discarded and the problem resolved to this point.

11. For each gamma ray calculate the fitted total number of counts in the channels above the channel representing 40 per cent of the photopeak energy.

(This is an arbitrary calculation used only for checking results obtained in manual unfolding). The fractional error assigned to these counts is set equal to the fractional error in the corresponding intensity. The statistical variance estimators of the intensities have been taken to be the diagonal elements of the inverse of the matrix A in 9.[41] In addition to statistical intensity errors there is an error due to gain and discriminator drifts in the monitor counts channel which must be accounted for as well as error due to eccentricity of the beam spot on the target. These fractional errors have been estimated to be 3.3 per cent and 1.2 per cent respectively in the present experiment. The three errors are combined according to:

$$1/\epsilon^2 = \sum_j 1/\epsilon_j^2 .$$

Two other possible sources of error should be noted here. First, the errors in the experimentally determined response matrix, which can considerably complicate the error calculations for the intensities, are kept to a minimum by obtaining good counting statistics in the calibration spectra. The other source of error is gain drift which tends to smear spectral peaks. Fortunately, the main effect of such drift seems to be an increase in the mean squared errors in the curve fitting process and intensity determinations are apparently not too sensitive to the effect.

12. The intensities and their errors calculated in 11 are read out and stored for use in the subsequent determination of correlation coefficients and mean values.

13. The absolute values of differences between observed and fitted counts are summed over fitted channels and divided by total input spectrum counts over the same range to give a measure of the fit which has been achieved in the analysis. This measure is then read out.

14. The input and fitted spectra are plotted in a graph output.

15. The above process is repeated for each run in the data set until the data for all the experimental angles has been processed.

16. When the preceding analysis is completed for a set of data a subroutine entitled LEASTSQ may be called, if appropriate, to compute the correlation coefficients. For each gamma ray in the spectrum a least squares fit of the counts computed at the experimental angles is made to the usual series:

$$W(\theta) = \sum_i^l A_i P_i(\cos\theta), \quad i \text{ even}$$

where P_i are the even Legendre polynomials. The fit is first made to $A_0 + A_2P_2 + A_4P_4$ then $A_0 + A_2P_2$. (Provision has been made for fitting to the series terminating with P_6 by simply changing the initial value of NP to 4; however, see reference 61 concerning accuracy of P_6 terms). The computation, which follows the procedure given by Rose[41], proceeds as follows:

a. Table gamma ray absorption coefficients[58] in copper and corresponding energies in Mev. Correct intensities and sigmas for attenuation in copper target backing.

b. Set up matrix P_{ij} of Legendre polynomials for experimental angles.

c. Do least squares calculation to find coefficients using the reciprocal of the estimated intensity variances from 11 as weights.

d. Normalize coefficients and correct for the effect of the finite solid angle subtended by the scintillation crystal. These latter corrections are precomputed in an auxiliary program using the expressions given by Rose.[41] Estimated variances of the coefficient ratios, A_2/A_0, etc., are computed from the expression given by Reich et al.[61] (After computation variances were increased by a factor $1/\epsilon^2$ in all cases where the computed value of ϵ^2 was less than unity.)

e. Calculate anisotropy.

f. Compute the criterion ϵ^2. This quantity, defined by Rose's analysis, is a measure of non-statistical errors in the data. If such errors are eliminated the value of ϵ^2 serves to indicate whether the appropriate number of polynomials has been used in the correlation function expression, with values of ϵ^2 greater than unity indicating an inappropriate choice. It is pertinent here that non-statistical errors have already been introduced into the problem in 11 above so that this criterion is valid only to the extent that an accurate estimate of the true variance of the counts has been achieved. The computed values of ϵ^2 in general are near unity and seem to verify that the estimated variances can be considered to be reasonably good.

g. Selected values of the normalized calculated correlation function, and values of a comparison theoretical function if desired, are read out, and similarly normalized experimental points are read out. (Experimental values are uncorrected for solid angle, the correction being applied to the theoretical function for comparison with experimental results.)

h. Iterate for each gamma-ray energy.

i. Reduce number of polynomials if orders higher than P_2 have been used and iterate solution. (The program also calculates coefficients for the cosine series:

$$W(\theta) = 1/A_0 \sum_{1}^{m} A_{2n} \left[\cos(\theta)\right]^{2n})$$

j. Return to main routine.

16. Repeat entire analysis for as many sets of data as indicated.

17. Combine coefficients to get weighted mean values and Chi square values if more than one set of data is analyzed. Read out these values.

18. Combine intensities at each angle from all sets of data and re-analyze for coefficients using this combined data set.

C. Glossary of names of selected variables and constants appearing in program SPECFIT. An asterisk indicates an input quantity.

A(I,J)	The matric product of the response matrix with its transpose, weighted with the WT values.
AINV(I,J)	The inverse of A(I,J).
ANISO(I)	Anisotropy for Legendre series solution (I = 1), and for cosine series solution (I = 2).
ARGP(I)	Vector containing cosines of the angles B3(I).
*B(I)	A vector representing the product of the inverse of the response matrix and the observed spectrum.
*BACK(I)	A number representing background counts to be subtracted from calibration curve I.
BACKGND(I)	The calculated background spectrum to be subtracted from an input spectrum.
*BCHAN	The lower of the channel pair described under TCHAN

FIN(I,J,K)	Storage for FINTENS(I), data set J, run K.
FMU(I)	Mass absorption coefficient in copper for EMU(I) Mev gamma ray Units in cm^2/gm.
*HCM	Distance from source to crystal face in centimeters.
HOLD(I)	A temporary storage vector.
LPKS	Same as NPKS but not including any straight line component. (See NBAOPT)
*MAXCHAN	An upper channel limit in loading CALB data. Between MAXCHAN and MINT, CALB(I) values are filled in with the value of CALB(MAXCHAN).
*MESH	The number of channels in input spectrum.
*MINT	Number of channels in calibration spectra.
*MINTB	Number of background channels.
MPKS	Initial value of NPKS for restoring the value.
MPKS2	Initial value of LPKS for restoring the value.
*NBAOPT	Background option selector. NBAOPT = 0 No background read in nor subtracted from SPEC NBAOPT = 1 Background spectrum is read in and SPEC is corrected for this background NBAOPT = 2 Same as NBAOPT = 1 and in addition a straight line is included in the response matrix.
*NCUT	A channel number below which the graph output values are divided by a scale factor SCALE.
NERFL	An output of matrix inversion subroutine. A value of 1 indicates matrix is non singular, and 2 indicates a singular matrix.
*NHIEST	The upper channel of the range over which a fit is made in SPECFIT.
*NLOWEST	The lower channel of the range over which a fit is made in SPECFIT.
*NOCALB	Number of calibration spectra.
*NPHOTO	The photograph number of the observed spectrum; for identification only.

*NPKS	The number of spectral components with which the observed spectrum is to fitted. Program will increase this value by one if option is chosen to include a straight line in R (See NBAOPT).
*NRUNS	Number of runs in a set of data.
NP	Number of Legendre polynomials to be fitted in first pass through LEASTSQ.
*NPRINT	Print suppression index NPRINT = 0 All printouts and graphs are made NPRINT = 1 Suppress printouts of spectrum values and cosine series coefficients NPRINT = 2 Same as 1 and also suppress graph outputs NPRINT = 3 Same as 2 with briefer more compact arrangement of correlation coefficients NPRINT = 4 Same as 3 but graphs plotted
*NSETS	Number of sets of data.
OMEGA(I,J)	Used for temporary storage in SPECFIT and diagonal elements used for weights in LEASTSQ.
*PKSEP(I)	The number of channels corresponding to 1.022 Mev for energy calibration of CALB curves. Taken as channel distance from photo peak to pair peak for higher energy calibration gammas.
*PHOT(I)	The channel of calibration curve I in which the photopeak occurs. (May be an interpolation between two integral channels numbers).
*PKEN(I)	Energy in Mev of a spectral component.
POLY(I,J)	The matrix of Legendre polynomials of order 2(J-1) evaluated at angle B3(I).
R(I,J)	The response matrix.
RED	A normalizing factor for 3" x 3" unshielded NaI(Tl) crystal representing the probability that one photon at the source will produce one count in the photopeak channel.
*RES	The proton energy in kev at the resonance being investigated (for identification only).
SAN(I)	Estimate of standard deviation of ANISO(I).
SAVE(I,J)	An auxiliary matrix.

SBB(I)	Coefficient for renormalizing input spectrum with counts from an auxiliary monitor (optional; if not entered values are unity).
*SCALE	A scale factor for graph output. See NCUT.
SCOEFT(I)	The standard deviation in COEFT(I).
SIGCTS(I)	The calculated error in COUNTS(I).
SIGTENS(I)	The error for calculated spectral intensity INTENS(I).
SIN(I,J,K,)	Storage for errors in FIN(I,J,K)
*SPEC(I)	The vector representing the counts in the observed spectrum.
STC(I,J,K)	Storage for accumulating calculated correlation coefficients of order I, for gamma ray J and data set K.
STORE(I,J)	A temporary storage matrix for A while it is being inverted.
STSC(I,J,K)	Standard deviation of STC(I,J,K).
STW(I,J)	Temporary storage.
STSW(I,J)	Temporary storage.
SUM7(I)	Temporary storage.
*TBACK	Duration of background run in units of seconds x 60
TC(I)	The weighted mean value of correlation coefficient of order I.
*TCHAN	The upper of a pair of input spectrum channels to be used for sensing energy calibration of the input spectrum.
TEMP(I)	Temporary storage.
*TOPEN	Energy of TCHAN in Mev.
TS(I)	Standard deviation of TC(I)
*TX60SEC	Duration of a run in units of seconds x 60.
WT(I)	The weight assigned to channel I in least squares solution for intensities.
XI(I)	The matric product of POLY and B1 weighted with the diagonal elements of OMEGA.

XS(I)	A vector representing the energy in Mev of each channel of the input spectrum.
Z(I)	A temporary storage vector.
*ZERO	The number which if any diagonal element of matrix A is smaller than, A will be considered singular.

D. DATA INPUT SEQUENCE FOR PROGRAM SPECFIT

Input	Number of sets	Number of cards in set	Input name	Remarks
1	1	1	NSETS, NPRINT	4
2	1	1	EL, ECC, HCM	
3	1	1	NOCALB, MINT	
4	NOCALB	1	BACK(J), PHOT(J), ENCALB(J), MAXCHAN, PKSEP(J)	
		MAXCHAN/7	CALB(I,J)	
5	1	1	NPKS, NBAOPT	
6	1	NPKS	PKEN(I)	
7	1	1	BSL, BEN, BPHOT, MINTB, TBACK	1
8	1	MINTB/7	BTGT(I)	
9	1	1	NRUNS, CTSNORA, NLOWEST, NHIEST, NCUT, SCALE, ZERO	2
10	1	1	RES, NPHOTO	3
11	1	1	MESH, TCHAN, TOPEN, BCHAN, BOTEN, B3(NRUNDEX), T60XSEC	
12	1	1	CTSNORB	
13	1	MESH/7	SPEC(I)	
14	1	4	Graph data cards	5

REMARKS:

1.) Read in only for NBAOPT greater than 1.

2.) Input resumes here for each successive data set.

3.) Input resumes here for each successive run within a data set.

4.) All loading formats are multiples of F10.3 and I10 except that ZERO is E10.1 and TBACK is F20.3.

5.) Blank cards may be loaded if graph option not used.

E. Description of program CONTOUR

As described in appendix 1 the correlation function coefficients for (p,γ) and $(p,x\gamma)$ intermediate unobserved reactions for spin 1/2 target nuclides can be described as a product of, at most, three functions of the form:

$$g_{ik} = \frac{a_{ik} + b_{ik}\delta_k + c_{ik}\delta_k^2}{1 + \delta_k^2}$$

where i denotes the order of the coefficient and k is the index of the mixing parameter δ. For computation the substitution $\delta = \tan Y$ is commonly used, and leads[60] to $g = \alpha + \beta \sin(2Y + \gamma)$

with $\alpha = \frac{a + c}{2}$

$$\beta = + \frac{s}{2}\left[b^2 + (a - c)^2\right]^{1/2}$$

$$\gamma = \tan^{-1}\left(\frac{a - c}{b}\right)$$

$$s = b/|b|$$

where indices have been dropped for clarity.

This program computes sets of possible values of two mixing parameters for various fixed values of correlation coefficients. Using a graph plotter output medium available through a locally developed subroutine, these sets of values are plotted to form a set of contours along which the value of the correlation coefficient is constant. Steps in the computation are as follows:

1. Read in data for one possible spin sequence to be examined. Compute values of α, β and γ for the lowest order coefficient which occurs. If three mixing parameters occur simultaneously, read out the expression for the fixed g as a function of the fixed mixing parameter. (All loading formats are standardized to be F10.3 and I10 for floating and fixed point variables respectively.)
2. Find and read out the maximum and minimum possible values of the coefficient and the corresponding values of the Y's.

3. Fix the coefficient at an initial value within its range. Assign values to one of the Y's in equal increments throughout the range -90° to $+90^{\circ}$ and solve for the corresponding values of the remaining Y, which in general will be double valued over the region selected.
4. Read out pairs of Y values for the selected coefficient value both to the print medium and to the graph plotter.
5. Repeat steps three and four for successively larger values of the coefficient until a specified number of contours has been plotted.
6. Repeat steps two through five until contour plots for coefficients of all orders permitted by the given spin sequence have been produced.

F. Input variables for CONTOUR

NSETS	Number of spin sequences for which plots are to be made.
JFIND	Index of the mixing parameter to be solved for. (Y values on graph). 1 = proton partial wave mixing 2 = unobserved gamma multipolarity mixing 3 = observed gamma multipolarity mixing 4 = channel spin mixing
JSTEP	Index of mixing parameter assigned successive values (x values on graph) See JFIND.
JFIX	Index of mixing parameter to be held constant when three parameters occur simultaneously. (Set to five for (p,γ) reaction where only two parameters occur.)
IMAX	Index specifying the highest order coefficient occurring in the spin sequence. (Order = 2*IMAX)
JMAX	Largest value which the index of mixing ratio assumes for use in reading input data. (Usually set at four.)
NCONTS	Number of contours to be plotted on each graph.
NPTS	Number of pairs of points to be computed for each branch of one contour.
DELTA(JFIX)	Fixed value assigned to the third mixing parameter during a calculation.

RHO	Energy dependent Coulomb phase factor to be multiplied into the b coefficients for proton-partial-wave mixing.
A(I,J) B(I,J) C(I,J)	The a, b, and c factors occurring in the expression for g. I denotes the coefficient order (order = 2I) and J the mixing parameter index. See FIND.

G. Fortran Listing of Program SPECFIT

```
..JOB*PHELPS NO GRAPHS - 35 MIN RUNNING TIME
      PROGRAM SPECFIT
      DIMENSION  SPEC(130), XS(130),CALB(530, 09), PHOT(09), ENCALB(09)
     1 ,TEMP(530), BACK(09), HOLD(530), Z(20), DIF(530), PKEN(20), PKCTS
     2 (20), R(130,20), FINTENS(20), E(20), A(20,20), AINV(20, 20), STOR
     3 E(20,20), B(20), SIGTENS(20), SIGCTS(20), COUNTS(20), WT(130), SA
     4 VE(20), POLY(20,4), OMEGA(20,20), CEE(4,4),CEEINV(4,4),PART1(9),
     5 XI(4), COEFT(4), SCOEFT(4), ARGP(20), B1(20), B2(20), B3(20),
     6 SUM7(4), ANISO(2), SBB(20), STW(20,20), STSW(20,20), BTGT(530)
     7 , FMU(20), EMU(20), PKSEP(10), BACKGND(130), STC(4, 20, 6),
     8 STSC(4,20,6), TC(4), TS(4), FIN(20,5,5), SIN(20,5,5)
      COMMON SPEC, XS, CALB, PHOT, ENCALB, TEMP, BACK, HOLD, Z, DIF,
     1 PKEN, PKCTS, R, FINTENS, E, A, AINV, STORE, B, SIGTENS, SIGCTS,
     2 COUNTS, WT, SAVE, POLY, OMEGA, PART1, CEE, CEEINV, XI, COEFT,
     3 SCOEFT, ARGP, B1, B2, B3, SUM7, ANISO, SBB, STW, STSW, BTGT,
     4 MESH, MINT, GAMEN, ZERO, NERFL, NPKS, NRUNS, PKSEP, LPKS
     5 , NSETDEX, STC, STSC, NPRINT, HCM
      NSETDEX  =  1
C     LOAD DATA
      READ INPUT TAPE 2, 831, NSETS, NPRINT
      READ INPUT TAPE 2, 8  , EL, ECC, HCM
      READ INPUT TAPE 2, 820, NOCALB, MINT
      DO 830 J=1, NOCALB
      READ INPUT TAPE 2, 835, BACK(J), PHOT(J), ENCALB(J), MAXCHAN,
     1 PKSEP(J)
      READ INPUT TAPE 2, 815, (CALB(I,J), I=1, MAXCHAN)
      DO 830 I = MAXCHAN, MINT
  830 CALB(I, J) = CALB(MAXCHAN, J)
C     SUBTRACT CONSTANT BACKGROUND FROM CALIBRATION SPECTRA
   12 DO 13  J  =  1  , NOCALB
      DO  13  I  =  1,  MINT
   13 CALB(I, J) = CALB(I,J) - BACK(J)
C     NORMALIZE CALIBRATION SPECTRA TO PHOTOPEAK HEIGHTS
  505 DO  20  J  =  1, NOCALB
      NPHX  =  PHOT (J)
      IF (CALB (NPHX + 1, J) - CALB(NPHX,  J))  507, 507, 509
  507 CB  =  CALB(NPHX, J)
      GO TO 510
  509 CB  =  CALB ( NPHX + 1, J)
  510 DO 20  I  =  1, MINT
   20 CALB(I, J)  =  CALB(I, J) / CB
      READ INPUT TAPE 2, 840, NPKS, NBAOPT
      LPKS  =  NPKS
      MPKS  =  NPKS
```

```
      MPKS2  =  LPKS
      DO 845 I=1, NPKS
      READ INPUT TAPE 2, 825, PKEN(I), PKCTS(I)
  845 E(I) = PKEN(I)
C     INCLUDE CONST VECTOR IN RESPONSE FOR NBAOPT OVER 1
      IF(NBAOPT - 1)806,846, 90
   90 NPKS  =  NPKS + 1
      MPKS  =  NPKS
      PKEN(NPKS)  =  9.999
      E(NPKS)  =  PKEN(NPKS)
      DO 91 I  =  1, 130
   91 R(I, NPKS)  =  0.002
C     LOAD BACKGROUND FOR NBAOPT OVER 0
  846 READ INPUT TAPE 2, 848, BSL, BEN, BPHOT, MINTB, TBACK
      READ INPUT TAPE 2, 816, (BTGT(I), I  =  1, MINTB)
      FMINTB  =  MINTB
      IF (FMINTB - 200.0 ) 847, 847, 849
  847 XDEAD  =  0.50
      GO TO 850
  849 XDEAD  =  0.125
  850 SUMD  =  0.0
      DO 851  I  =  2,  MINTB
      FLI  =  I
  851 SUMD  =  SUMD + BTGT(I) * (38.0 + XDEAD * FLI )
      SUMD  =  SUMD * (6.0E-05/TBACK)
      DO 852  I  =  1,  MINTB
  852 BTGT(I)  =  BTGT(I)/(1.0 - SUMD)
  806 WRITE OUTPUT TAPE 3, 832, NSETDEX
      WRITE OUTPUT TAPE 3, 1073
C     LOAD DATA
      READ INPUT TAPE 2, 842, NRUNS, CTSNORA, NLOWEST, NHIEST, NCUT,
     1 SCALE, ZERO
      ZERO  =  1.0E-15
      NCUT  =  23
      NRUNDEX  =  1
  807 READ INPUT TAPE 2, 805, RES, NPHOTO
      READ INPUT TAPE 2, 810, MESH,TCHAN, TOPEN, BCHAN,BOTEN,B3(NRUNDEX)
     1 , T60XSEC
      READ INPUT TAPE 2, 817, CTSNORB
      IF(  CTSNORA  -  1.0 ) 837, 837, 836
  836 IF ( CTSNORB - 1.0 ) 837, 837, 838
  838 SBB(NRUNDEX)  =  CTSNORA/CTSNORB
      WRITE OUTPUT TAPE 3, 841, SBB(NRUNDEX)
      GO TO 839
```

```
  837 SBB(NRUNDEX)  =  1.0
  839 READ INPUT TAPE 2, 814, (SPEC(I) ,I=1,MESH)
C     CORRECTFOR DEAD TIME OF ANALYZER
      SUMD  =  0.0
      DO 808  I  =  2,  MESH
      FLI  =  I
  808 SUMD  =  SUMD  +  SPEC(I)  *  (38.0 + 0.5 * FLI )
      SUMD  =  SUMD * (6.0E-05/T60XSEC )
      DO 809  I  =  1,  MESH
  809 SPEC(I)  =  SPEC(I)/(1.0 - SUMD)
      TF  =  1.0 + T60XSEC/TBACK
      KITER  =  0
C     CALCULATE INPUT SPECTRUM CHANNEL ENERGIES
      SPSLOPE = (TOPEN - BOTEN)/(TCHAN - BCHAN)
      DO 855 I=1,MESH
      ENDEX = I
  855 XS(I) = BOTEN + (ENDEX - BCHAN) * SPSLOPE
      WRITE OUTPUT TAPE 3, 860, NRUNDEX
      WRITE OUTPUT TAPE 3, 865, RES, NPHOTO
      IF ( NPRINT - 1 ) 853, 883, 883
  853 WRITE OUTPUT TAPE 3, 870
      WRITE OUTPUT TAPE 3, 875,(XS(J), J=1, MESH)
      WRITE OUTPUT TAPE 3, 880
      WRITE OUTPUT TAPE 3, 875, (SPEC(J), J=1, MESH)
C     ADJUST ENERGY CALIBRATION AND CHANNELS OF BACKGROUND IF USED
  883 IF(NBAOPT - 1) 885, 884, 884
  884 DO 10  I = 1, MINTB
   10 TEMP(I)  =  BTGT(I) * (T60XSEC/TBACK)
  406 DO 675 K = 1, MESH
      CHX = BPHOT  + (XS(K) - BEN) * BSL
      IF (CHX - 1.0) 520, 525, 525
  520 VAL  =  TEMP(1)
      GO TO 675
  525 IF(CHX - FMINTB) 535, 530, 530
  530 VAL  =  TEMP(MINTB)
      GO TO 675
  535 I    = CHX
      FLNCHX = I
      FRACT = CHX - FLNCHX
      IF (I - 1) 381, 381, 374
  374 DEL 1=  TEMP(I) - TEMP(I-1)
      DEL2=  TEMP(I+1) - TEMP(I) - DEL1
      DEL3=  TEMP(I+2) - TEMP(I+1) - DEL2 -DEL2 - DEL1
      U1 = 1.0 + FRACT
      U2 = U1*(U1 - 1.0)/2.0
      U3 = U2*(U1 - 2.0)/3.0
```

```
  380 VAL = TEMP(I-1) + U1*DEL1 + U2*DEL2 + U3*DEL3
      IF  ( VAL - 0.0 ) 390, 391, 391
  390 VAL = 0.0
  391 GO TO 675
  381 I = I + 1
      DEL1=  TEMP(I) - TEMP(I-1)
      DEL2=  TEMP(I+1) - TEMP(I) - DEL1
      DEL3=  TEMP(I+2) - TEMP(I+1) - DEL2 -DEL2 - DEL1
      U1 = FRACT
      U2 = U1*(U1 - 1.0)/2.0
      U3 = U2*(U1 - 2.0)/3.0
      GO TO 380
  675 BACKGND(K)  =  VAL
C     SUBTRACT BACKGROUND FROM SPECTRUM FOR NBAOPT = 1 OR GREATER
  887 DO 886 I  =  1, MESH
  886 SPEC(I)  =  SPEC(I)  -  BACKGND(I)
      IF (NPRINT - 1) 888, 885, 885
  888 WRITE OUTPUT TAPE 3, 889
      WRITE OUTPUT TAPE 3, 875 (BACKGND   (J), J  =  1, MESH  )
      WRITE OUTPUT TAPE 3, 881
      WRITE OUTPUT TAPE 3, 875 (SPEC(J), J=1, MESH  )
C     CALCULATE RESPONSE MATRIX
  885 CALL RESPONS
C     SOLVE LEAST SQUARES PROBLEM FOR RELATIVE INTENSITIES
      DO 854  I  =  1, MESH
  854 WT(I) = 1.0
  102 DO 105  I = 1, NPKS
      DO 105  K = 1, NPKS

      SUM=0.0
      DO 100  J =  NLOWEST , NHIEST
  100 SUM = R(J,I) * WT(J) * R(J,K) + SUM
      A(I, K) = SUM
  105 STORE(I,K)=  A(I,K)
      CALLPGAUSS3( NPKS, ZERO , STORE , AINV ,NERFL)
      DO 115  K = 1, NPKS
      SUM = 0.0
      DO 110  J = NLOWEST, NHIEST
  110 SUM = SPEC(J) * WT(J) * R(J,K) + SUM
  115 B(K) = SUM
      DO 125  L = 1, NPKS
      SUM = 0.0
      DO 120  K = 1, NPKS
  120 SUM = AINV(K, L) * B(K) + SUM
  125 FINTENS(L) = SUM
```

```
      DO 135  I = 1, NPKS
  135 SIGTENS(I)  =  SQRTF(ABSF(AINV(I, I)))
C     ITERATE SOLUTION TIL CONVERGENCE WITH WTS FROM COMPUTED SPECTRUM
  136 DO 137  I  =  1, MESH
      DIF(I)  =  0.0
      DO 137  J  =  1, NPKS
  137 DIF(I)  =  R(I,J) * FINTENS(J) + DIF(I)
      SUMB = 0.0
      DO 260 I = NLOWEST, NHIEST
  260 SUMB = DIF(I) + SUMB +  TF  * BACKGND(I)
      FMESH  =  MESH
      RMESH  =  NHIEST - NLOWEST + 1
      SUMB  =  50.0 * RMESH/SUMB
      DO 275  I = 1, MESH
      IF((1.0/ (DIF(I) +   TF  * BACKGND(I))) - SUMB)265,265,270
  265 WT(I)  =  1.0/(DIF(I)  +  TF  * BACKGND(I))
      GO TO 275
  270 WT(I) = SUMB
  275 CONTINUE
      SUMC = 0.0
      DO 280 I = 1, NPKS
      SUMC = ((SAVE(I) - FINTENS(I))/FINTENS(I))**2  + SUMC
  280 SAVE(I) = FINTENS(I)
      KITER = KITER + 1
      IF (KITER  -  10) 281, 290, 290
  281 IF(SUMC - 1.0E-06) 290,290,102
  290 WRITE OUTPUT TAPE 3, 295, KITER
C     CHECK MATRIX INVERSION
      IF (NERFL  -  1) 219, 219, 1056
C     DISCARD ANY NEGATIVE INTENSITIES AND RESOLVE
  219 I  =  1
  220 IF (I  -  NPKS) 224, 224, 298
  224 IF (FINTENS(I) - 0.0) 230, 225, 225
  225 I = I + 1
      GO TO 220
  230 IF (PKEN(I) - 9.999 ) 232, 225, 232
  232 NPKS =  NPKS- 1
      LPKS  =  LPKS - 1
      PKENP  =  PKEN(I)
      DO 235 J = I, NPKS
      DO 231 K = 1, MESH
  231 R(K, J) =R(K, J + 1)
      PKEN(J) = PKEN(J+ 1)
  235 E(J) = PKEN(J)
      PKEN(NPKS + 1 )  =  PKENP
      E(NPKS + 1)    = PKENP
```

```
      KITER  =  0
      GO TO 102
C     READ OUT SYNTHETIC SPECTRUM
  298 IF ( NPRINT - 1 ) 291, 299, 299
  291 WRITE OUTPUT TAPE 3, 300
      WRITE OUTPUT TAPE 3, 875, (DIF(I),  I  =  1, MESH  )
C     NORMALIZE AND STORE INTENSITIES
  299 SUMA = 0.0
      DO 140  I  =  1, LPKS
  140 SUMA= FINTENS(I) + SUMA
      DO  141  I  =  1, NPKS
      FIN(I, NSETDEX, NRUNDEX)  =  FINTENS(I) * SBB(NRUNDEX)
      DOG= SIGTENS(I)**2 + (FIN(I, NSETDEX, NRUNDEX)**2)*(EL**2+ECC**2)
      SIN(I, NSETDEX, NRUNDEX)  =  SQRTF(DOG) * SBB(NRUNDEX)
      FINTENS(I) = FINTENS(I)/SUMA * 100.0
  141 SIGTENS(I) = SIGTENS(I)/SUMA * 100.0
      WRITE OUTPUT TAPE 3, 143, SUMA
      WRITE OUTPUT TAPE 3,145, NLOWEST, NHIEST
      WRITE OUTPUT TAPE 3,150
```



```
C     CALCULATE COUNTS AND NORMALIZE TO MONITOR COUNTS RATIO
      DO 168   K  =  1, NPKS
      CUTCOUN  =  E(K) * 0.4
      IA  =  1
      XSDIF  =  XS(2) - XS(1)
  155 XSP  =  XS(IA) - XSDIF/2.0
      IF ( XSP  -  CUTCOUN) 162, 166, 166
  162 IA  =  IA + 1
      GO TO 155
  166 FRACT  = (XSP - CUTCOUN)*XSDIF
      SUM  =  R(IA - 1, K) * FRACT
      DO 170 I  =  IA, MESH
  170 SUM  =  R(I, K) + SUM
      COUNTS(K)  =  SUM * FINTENS(K) * ( 0.01 * SUMA)
      SIGCTS(K)  =  ( 0.01 * SUMA ) *  SIGTENS(K)*SUM
      SIGCTS(K) = SIGCTS(K)**2 + (COUNTS(K)**2)*(EL**2 + ECC**2)
      SIGCTS(K) = SQRTF(SIGCTS(K))
C     STORE  INTENS  SIGMAS AND ENERGIES FOR ALL RUNS
      OMEGA(NRUNDEX, K)  = (FINTENS(K)/100.0) * SBB(NRUNDEX)
      DOG  =  SIGTENS(K)**2 + (FINTENS(K)**2) * (EL**2+ECC**2)
      STW(NRUNDEX, K)  = (SQRTF(DOG)/100.0 )*SBB(NRUNDEX)
C     READ CUT AND GRAPH RESULTS
  168 WRITE OUTPUT TAPE 3, 165, PKEN(K),  COUNTS(K) , SIGCTS(K),
     1IA,CUTCOUN,            FINTENS(K), SIGTENS(K)
      TOTP  =  0.0
```

```
      TOT =C.0
      FITMEAS = 0.0
      DO 31C  I   =  NLOWEST, NHIEST
      FITMEAS = ABSF( SPEC(I) - DIF(I)) + FITMEAS
      TOT = SPEC(I) + TOT
  310 TOTP= DIF(I)  + TOTP
      FITMEAS =(FITMEAS/TOT)* 100.0
      WRITE OUTPUT TAPE 3, 320, TOT, TOTP, FITMEAS
      DO 311  I   =  1,  NCUT
      SPEC(I)  =  SPEC( I)/SCALE
  311 DIF(I)  =  DIF(I)/SCALE
      IF (NPRINT - 2) 314, 309, 309
  309 IF (NPRINT - 4) 316, 314, 316
  314 CALL GRAPH(MESH,XS,SPEC, 8)
      CALL GRAPH(MESH,XS, DIF, 8)
      DO 313  I   =  1, MESH
  313 DIF(I)  =  DIF(I)  +  1000.0
      CALL GRAPH(MESH,XS,DIF,8)
      GO TO 292
  316 READ INPUT TAPE 2,1085, ID1, ID2, ID3, ID4, ID5
C     IF CONST VECTOR USED(9.999 MEV) RESTORE AS LAST ELEMENT OF PKEN
  292 DO 293 I = 1, MPKS2
      I2 = I + 1
      IF(PKEN(I) - 9.999) 293, 297, 293
  293 CONTINUE
      GO TO 289
  297 DO 294 I = I2, MPKS
      PKEN ( I - 1 ) = PKEN(I)
  294 E( I - 1 ) =  PKEN(I - 1)
      PKEN(MPKS) = 9.999
      E(MPKS) = PKEN(MPKS)
      DO 296 I   =  1, MESH
  296 R(I , MPKS) = 0.0C2
  289 NPKS  =  MPKS
      LPKS  =  MPKS2
      IF  (NRUNDEX  -  NRUNS)  940,  945,  945
  940 NRUNDEX  =  NRUNDEX  +  1
      WRITE OUTPUT TAPE 3, 1090
      GO TO 807
  945 DO 7004  J = 1, MPKS
      DO 7004  I = 1, NRUNS
      A(I,J)  =  FIN(J, NSETDEX, I)/100.0
 7004 AINV(I,J)  =  SIN(J, NSETDEX, I)/100.0
      WRITE OUTPUT TAPE 3, 1035
C     GO TO COEFFICIENT ANALYSIS
      CALL LEASTSQ
```

```
      GO TO 1058
 1056 WRITE OUTPUT TAPE 3, 1057, NSETDEX, NRUNDEX
      WRITE OUTPUT TAPE 3, 1051, ((A(I,J), I=1,NPKS), J=1,NPKS)
      GO TO 316
 1058 IF (NSETDEX - NSETS) 1053, 1052, 1052
 1053 NSETDEX  =  NSETDEX  +  1
      NRUNDEX  =  1
      GO TO 806
 1052 IF (NSETS - 1) 106, 106, 1054
C     FIND WEIGHTED MEAN DISTRIBUTION COEFFICIENTS

 1054 WRITE OUTPUT TAPE  3, 1060
      DO 1064  I  =  1, 3
      KB  =  I**2 - 3*I + 4
      DO 1064  J  =  1, NPKS
      SUM1  =  0.0
      SUM2  =  0.0
      DO 1063  K  =  1, NSETS
      SUM1  =  SUM1 + STC(I, J, K) * (1.0/(STSC(I, J, K)**2))
 1063 SUM2  =  SUM2 + 1.0/(STSC(I, J, K)**2)
      TC(I) = SUM1/SUM2
      TS(I)  = SQRTF( 1.0/SUM2)
      IF ( I - 2 ) 1068, 1066, 1068
 1066 IF(J-1) 1067, 1067, 1068
 1067 WRITE OUTPUT TAPE 3, 1061
 1068 CHISQ  =  0.0
      SSQ  =  0.0
      DO 1065  K  =  1, NSETS
      IF(STSC(I,J,K)-0.00001) 1071, 1080, 1080
 1080 CHISQ  =  CHISQ  +  ((STC(I,J,K)-TC(I))/STSC(I,J,K)  )**2
 1065 SSQ  =  (STC(I,J,K) - TC(I))**2 + SSQ
      FNS  =  NSETS
      SSQ  =  SQRTF( SSQ/((FNS - 1.0)*FNS) )
      GO TO 1064
 1071 CHISQ  =  999.99
      SSQ  =  999.99
 1064 WRITE OUTPUT TAPE 3, 1062, E(J), KB, TC(I), TS(I), CHISQ, SSQ
C     SUMMARY OF DISTRIBUTION COEFFICIENTS
      WRITE OUTPUT TAPE 3, 1093
      WRITE OUTPUT TAPE 3, 1094
      DO 1096  J  =  1, NPKS
      DO 1096  I  =  1, 3
      KB  =  I**2 - 3*I + 4
      NP  =  ( -I**2 + 5*I )/2
 1096 WRITE OUTPUT TAPE 3, 1095, PKEN(J), NP, KB, (STC(I,J,K), STSC(I,J,
```

```
     1 K), K = 1, 5)
       DO 1120 I = 1, 20
       B1(I) = 0.0
 1120  B2(I) = 0.0
C      FIND WEIGHTED MEAN INTENSITIES
       DO 1105 K = 1, NRUNS
       SUM = 0.0
       DO 1102 I = 1, LPKS
       SUM1 = 0.0
       SUM2 = 0.0
       DO 1101 J = 1, NSETS
       IF(SIN(I,J) - 1.0      ) 1106, 1100, 1100
 1106  WRITE OUTPUT TAPE 3, 1107, I, J
       GO TO 1108
 1100  SUM1 = SUM1 + FIN(I,J,K)/(SIN(I,J,K)**2)
 1101  SUM2 = SUM2 + 1.0/(SIN(I,J,K)**2)
       B(I) = SUM1/SUM2
       E(I) = 1.0/SQRTF(SUM2)
       A(K,I) = B(I)/100.0
       AINV(K,I) = E(I)/100.0
       B1(I) = B1(I) + B(I) * SINF(B3(K) / 57.2958 )
       B2(I) = B2(I) + (E(I)**2 ) * SINF(B3(K) / 57.2958 )
 1102  SUM = SUM + B(I)
       SUM = SUM/100.0
 1108  WRITE OUTPUT TAPE 3, 1103, B3(K)
       DO 1105 I = 1, LPKS
       B(I) = B(I)/SUM
       E(I) = E(I)/SUM
 1105  WRITE OUTPUT TAPE 3, 1104, PKEN(I), B(I), E(I)
       SUM = 0.0
       DO 1130 I = 1, LPKS
 1130  SUM = SUM + B1(I)
       WRITE OUTPUT TAPE 3 , 1140
       WRITE OUTPUT TAPE 3, 1170
       DO 1150 I = 1, LPKS
       B1(I) = (B1(I)/SUM ) * 100.0
       B2(I) = 100.0 * SQRTF(B2(I))/SUM
 1150  WRITE OUTPUT TAPE 3, 1160, PKEN(I), B1(I), B2(I)
       CALL LEASTSQ
       WRITE OUTPUT TAPE 3, 1113
    8  FORMAT( 3F10.3     )
  106  FORMAT(31HOCHECK MATRIX INVERSION ERFL =     I2 /)
  143  FORMAT(31HOSUM OF ABSOLUTE INTENSITIES =     F15.4  / )
  145  FORMAT(58 HORELATIVE INTENSITIES FROM LEAST SQUARE FITTING CHANNEL
     1S   I3, 9H THROUGH I3  //)
  150  FORMAT(92HO  ENERGY    COUNTS    SIGMA              CUTOFFCHAN. CUTO
```

```
     1FFEN   INTENS     SIGMA                    //)

  165 FORMAT(   F8.3,   F12.1,   F9.1  , I17,F11.3,   F10.2, F9.2     )
  295 FORMAT(25HONUMBER OF ITERATIONS  =  I2 /)
  300 FORMAT (23HOSYNTHESIZED SPECTRUM       /)
  320 FORMAT(/16HOINPUT COUNTS = F9.1, 18H  FITTED COUNTS = F9.1,      15
     1 H  FITMEASURE = F7.1, 10H  PERCENT    /)
  805 FORMAT(F10.3,   I10 )
  810 FORMAT( I10, 6F10.3)
  814 FORMAT(7F10.3)
  815 FORMAT( 7F10.3)
  816 FORMAT( 7F10.3)
  817 FORMAT( F10.3 )
  820 FORMAT(2I10    )
  825 FORMAT(2F10.3)
  831 FORMAT(2I10)
  832 FORMAT( 18H1DATA SET NUMBER        I3  /)
  835 FORMAT(3F10.3, I10, F10.3)
  840 FORMAT ( I10, F10.3 )
  841 FORMAT(26HONORMALIZING COEFFICIENT =    F7.4  /)
  842 FORMAT( I10, F10.3, 3I10, F10.3, E10.1     )
  848 FORMAT(   3F10.3,   I10  , F20.3 )
  860 FORMAT(42HOUNFOLDING OF GAMMA SPECTRUM - RUN NUMBER  I3 /)
  865 FORMAT(11HORESONANCE F10.3, 20H KEV   PHOTO NUMBER  I4 /)
  870 FORMAT(18HOCHANNEL ENERGIES  /)
  875 FORMAT( 8F12.3)
  880 FORMAT(18HOINITIAL SPECTRUM  /)
  881 FORMAT(38HOINITIAL SPECTRUM MINUS BACKGROUND        /)
  889 FORMAT ( 12HOBACKGROUND    /)
  895 FORMAT(14HOCURVE NUMBER   I2, 15H TO BE STRIPPED     /)
  900 FORMAT(40HOSPECTRUM AFTER STRIPPING CURVE NUMBER   I2  / )
  920 FORMAT(/  80H  COMPONENT NUMBER          ENERGY              RELATIVE
     1 INTENSITY      COUNTS                /)
  930 FORMAT (I10, F22.3, F20.3, F28.3  )
 1020 FORMAT(10HOENERGY =   F6.3,   5H MEV   /)
 1030 FORMAT( 1P10E11.2)
 1035 FORMAT ( 40H1ANALYZE FOR DISTRIBUTION COEFFICIENTS    //)
 1051 FORMAT( 1P13E9.1  /)
 1057 FORMAT( 29HOMATRIX A SINGULAR DATA SET     I4, 7H  RUN     I4 /)
 1060 FORMAT( 70HOFIND WEIGHTED MEAN COEFFICIENTS FOR CORRECTED  LEGENDR
     1E SERIES NP=2        /)
 1061 FORMAT( 25HOSAME FOR NP=3 SERIES    /)
 1062 FORMAT(F6.3, 8H MEV - A I1, 7H/A0 =  F6.4, 9H SIGMA = F6.4 ,14H  C
     1HISQUARE =  F7.2  , 8H SSQ =   F6.4  /)
 1073 FORMAT (26 HOWED 31 JUL AM DECK 1            /)
```

```
 1085 FORMAT  (A1)
 1090 FORMAT(2HO      //////)
 1093 FORMAT(39HOSUMMARY OF DISTRIBUTION COEFFICIENTS    /)
 1094 FORMAT(103HO  MEV     NP      COEFT      SET1    SIGMA     SET2    SIGMA
     1     SET3    SIGMA     SET4    SIGMA     SET5    SIGMA     /)
 1095 FORMAT( F6.2, I6, 6H      A I1, 3H/A0  F9.3, 9F8.3     /)
 1103 FORMAT(19HOMEAN INTENSITIES     F5.1, 9H DEGREES     / 28HOENERGY
     1INTENSITY  SIGMA    /)
 1104 FORMAT(  F6.2, F12.2, F9.2  /)
 1107 FORMAT( 5HOSIN(  I1, 1H,  I1, 6H) = 0     /)
 1113 FORMAT( 42HOEND OF PROGRAM SPECFIT                          /)
 1140 FORMAT(30HOAVERAGE INTENSITY OVER 4 PI          /)
 1160 FORMAT (3F10.3    /)
 1170 FORMAT(34HO   ENERGY      INTENS      SIGMA       /)
 5500 FORMAT (15HOHANGUP PRINT       I2    /)
      END
      SUBROUTINE RESPONS
      DIMENSION  SPEC(130), XS(130),CALB(530, 09), PHOT(09), ENCALB(09)
     1 ,TEMP(530), BACK(09), HOLD(530), Z(20), DIF(530), PKEN(20), PKCTS
     2 (20), R(130,20), FINTENS(20), E(20), A(20,20), AINV(20, 20), STOR
     3 E(20,20), B(20), SIGTENS(20), SIGCTS(20), COUNTS(20), WT(130), SA
     4 VE(20), POLY(20,4), OMEGA(20,20), CEE(4,4),CEEINV(4,4),PART1(9),
     5 XI(4), COEFT(4), SCOEFT(4), ARGP(20), B1(20), B2(20), B3(20),
     6 SUM7(4), ANISO(2), SBB(20), STW(20,20), STSW(20,20), BTGT(530)
     7 , EMU(20), EMU(20), PKSEP(10), BACKGND(130), STC(4, 20, 6),
     8 STSC(4, 20, 6)
      COMMON SPEC, XS, CALB, PHOT, ENCALB, TEMP, BACK, HOLD, Z, DIF,
     1 PKEN, PKCTS, R, FINTENS, E, A, AINV, STORE, B, SIGTENS, SIGCTS,
     2 COUNTS, WT, SAVE, POLY, OMEGA, PART1, CEE, CEEINV, XI, COEFT,
     3 SCOEFT, ARGP, B1, B2, B3, SUM7, ANISO, SBB, STW, STSW, BTGT,
     4 MESH, MINT, GAMEN, ZERO, NERFL, NPKS, NRUNS, PKSEP, LPKS
     5 , NSETDEX, STC, STSC, NPRINT, HCM
      DO 675   J  =  1, LPKS
      DO 602  I  =  1, MINT
      HOLD(I)  =  0.0
  602 TEMP(I)  =  0.0
      JP  =  25
      JJ = 2

  605 IF(ENCALB(JJ)-E(J)  ) 610,620,620
  610 JJ = JJ + 1
      GO TO 605
  620 NSHFT =       PHOT(JJ) - PHOT(JJ-1)
C     SHIFT LOWER UNDER UPPER
      KK = MINT- NSHFT
```

```
      DO  630   I = 1 , KK
  630 TEMP(I+NSHFT) =  CALB(I, JJ-1)
      KK = NSHFT + 1
      SLC = CALB(2, JJ - 1) - CALB(1, JJ - 1)
      DO 640 I = 1, KK
      FLX = I - 1 - NSHFT
  640 TEMP(I) = CALB(1, JJ - 1) + SLC * FLX
      IF (J -JP)641 , 400  ,641
  400 WRITE OUTPUT TAPE 3, 410 , E(J)
  641 PH  =  NSHFT
      FRACT = (PHOT(JJ)- PHOT(JJ-1)) - PH
      HOLD(1)  =  TEMP(1)
      HOLD(2)  =  TEMP(2)
      KK  =  MINT - 2
      GFACTOR = (PKSEP(JJ - 1) - PKSEP(JJ))/PKSEP(JJ - 1)
      DO 315 II =  3, KK
      I  =  II
      X  =  I
      FRACT2  =  FRACT - GFACTOR*( X - PHOT(JJ))
  642 Y  =  I  -  II
      Y  =  Y + FRACT2
      IF( Y + 0.0 ) 644, 648, 643
  643 IF( Y - 1.0 ) 648, 648, 647
  644 I  =  I + 1
      GO TO 642
  647 I  =  I - 1
      GO TO 642
  648 FRACT2  =  Y
      IF ( I - 2 ) 652, 652, 649
  649 IF ( I - MINT + 1 ) 653, 652, 652
  652 HOLD(II)  =  TEMP(II)
      GO TO 315
  653 CONTINUE
      DEL1  =  TEMP(I-1) - TEMP(I-2)
      DEL2  =  TEMP(I) - TEMP(I-1) -DEL1
      DEL3  =  TEMP(I+1) - TEMP(I) -DEL2 - DEL2 -DEL1
      U1 =  2.0  -  FRACT2
      U2 =  U1*(U1 - 1.0)/2.0
      U3 =  U2*(U1 -2.0)/3.0
      HOLD(II)= TEMP(I-2) + U1*DEL1 + U2*DEL2 + U3*DEL3
  315 CONTINUE
      DO 320 I =1, MINT
      IF  (HOLD (I) - 0.0 )  319, 320, 320
  319 HOLD (I)  =  0.0
  320 TEMP(I) = HOLD(I)
C     INTERPOLATE BETWEEN CURVES
```

```
  646 DO 650  I  =  1,  MINT
      EFRACT  =  (E(J)  -  ENCALB(JJ-1))/(ENCALB(JJ) - ENCALB (JJ-1))
  650 TEMP(I) = TEMP(I) + (CALB(I,JJ) - TEMP(I))*EFRACT
      SL  =  PKSEP(JJ)/1.022
  406 AMP  =  0.165  +  0.00667 * HCM
      PKHTFAC  =  (1.0/ (0.866 * 0.089*SQRTF(PKEN(J))))*(XS(2)-XS(1))
      SOLIDA  =  (7.62/(4.0 * HCM))**2
      ATTEN  =  0.9935
      EXP  =  0.9699  -  0.00918 * HCM
      RED  =  AMP * PKHTFAC * SOLIDA * ATTEN * (PKEN(J) **(-EXP))
      DO 675 K=1,MESH
      CHX   =PHOT(JJ)+  (XS(K) - E(J)) * SL
      NPHOB = PHOT(JJ)
      NCHX  =  CHX
      I = NCHX
      FLNCHX = NCHX
      FRACT  =  CHX  -  FLNCHX
      IF(I-1) 390, 381,  374
  374 IF(I - MINT ) 371, 390, 390
  371 DEL1=   TEMP(I) - TEMP(I-1)
      DEL2=   TEMP(I+1) - TEMP(I) - DEL1
      DEL3=   TEMP(I+2) - TEMP(I+1) - DEL2 -DEL2 - DEL1
      U1 = 1.0 + FRACT
      U2 =  U1*(U1 - 1.0)/2.0
      U3 =  U2*(U1 - 2.0)/3.0
  380 VAL =  TEMP(I-1) + U1*DEL1 + U2*DEL2 + U3*DEL3
      IF  ( VAL  -  0.0 )  390, 391, 391
  390 VAL  =  0.0
  391 GO TO 675

  381 I = I + 1
      DEL1=   TEMP(I) - TEMP(I-1)
      DEL2=   TEMP(I+1) - TEMP(I) - DEL1
      DEL3=   TEMP(I+2) - TEMP(I+1) - DEL2 -DEL2 - DEL1
      U1 = FRACT
      U2 =  U1*(U1 - 1.0)/2.0
      U3 =  U2*(U1 - 2.0)/3.0
      GO TO 380
  675 R(K, J)  =  VAL * RED
  410 FORMAT(20HORESPONSE READOUTS        ,F5.2  ,4 H MEV  /)
  679 FORMAT(2H0 /(1P8E12.3))
 5500 FORMAT (15HORANGUP PRINT      I2   /)
      RETURN
      END
      SUBROUTINE  PGAUSS3(N,EP,A,X,KER)
```

```
      DIMENSION A(20,20),X(20,20)
      DO 1  I=1,N
      DO 1  J=1,N
    1 X(I,J)=0.0
      DO 2  K=1,N
    2 X(K,K)=1.0
   10 DO 34 L=1,N
      KP=0
      Z=0.0
      DO 12 K=L,N
      IF(Z-ABSF(A(K,L)))11,12,12
   11 Z=ABSF(A(K,L))
      KP=K
   12 CONTINUE
      IF(L-KP)13,20,20
   13 DO 14 J=L,N
      Z=A(L,J)
      A(L,J)=A(KP,J)
   14 A(KP,J)=Z
      DO 15 J=1,N
      Z=X(L,J)
      X(L,J)=X(KP,J)
   15 X(KP,J)=Z
   20 IF(ABSF(A(L,L))-EP)50,50,30
   30 IF(L-N)31,34,34
   31 LP1=L+1
      DO 36 K=LP1,N
      IF(A(K,L))32,36,32
   32 RATIO=A(K,L)/A(L,L)
      DO 33 J=LP1,N
   33 A(K,J)=A(K,J)-RATIO*A(L,J)
      DO 35 J=1,N
   35 X(K,J)=X(K,J)-RATIO*X(L,J)
   36 CONTINUE
   34 CONTINUE
   40 DO 43 I=1,N
      II=N+1-I
      DO 43 J=1,N
      S=0.0
      IF(II-N)41,43,43
   41 IIP1=II+1
      DO 42 K=IIP1,N
   42 S=S+A(II,K)*X(K,J)
   43 X(II,J)=(X(II,J)-S)/A(II,II)
      KER=1
      RETURN
```

```
   50 KER=2
      END
      SUBROUTINE LEASTSQ
      DIMENSION  SPEC(130), XS(130),CALB(530, 09), PHOT(09), ENCALB(09)
     1 ,TEMP(530), BACK(09), HOLD(530), Z(20), DIF(530), PKEN(20), PKCTS
     2 (20), R(130,20), FINTENS(20), E(20), A(20,20), AINV(20, 20), STOR
     3 E(20,20), B(20), SIGTENS(20), SIGCTS(20), COUNTS(20), WT(130), SA
     4 VE(20), POLY(20,4), OMEGA(20,20), CEE(4,4),CEEINV(4,4),PART1(9),
     5 XI(4), COEFT(4), SCOEFT(4), ARGP(20), B1(20), B2(20), B3(20),
     6 SUM7(4), ANISO(2), SBB(20), STW(20,20), STSW(20,20), BTGT(530)
     7 , FMU(20), EMU(20), PKSEP(10), BACKGND(130), STC(4, 20, 6),
     8 STSC(4, 20, 6), SAN(2)
      COMMON SPEC, XS, CALB, PHOT, ENCALB, TEMP, BACK, HOLD, Z, DIF,
     1 PKEN, PKCTS, R, FINTENS, E, A, AINV, STORE, B, SIGTENS, SIGCTS,
     2 COUNTS, WT, SAVE, POLY, OMEGA, PART1, CEE, CEEINV, XI, COEFT,
     3 SCOEFT, ARGP, B1, B2, B3, SUM7, ANISO, SBB, STW, STSW, BTGT,
     4 MESH, MINT, GAMEN, ZERO, NERFL, NPKS, NRUNS, PKSEP, LPKS
     5 , NSETDEX, STC, STSC, NPRINT, HCM
      NP   =  3
      JNN  =  1
```



```
      NN = NPKS
      L  =  NRUNS
      RA  =  57.2957795
      ALPHA1  =  1.0
      ALPHA2  =  0.0
      ALPHA3  =  0.0
      ALPHA4  =  0.0
      B(1) = 1.0
      B(2) = 0.9295
      B(3) = 0.7780
      B(4) = 0.4955
C     LIST GAMMA ABSORPTION COEFFICIENTS AND CORRESPONDING ENERGIES
      FMU(1)  =  .0834
      FMU(2)  =  .0760
      FMU(3)  =  .0658
      FMU(4)  =  .0588
      FMU(5)  =  .0475
      FMU(6)  =  .0416
      FMU(7)  =  .0356
      FMU(8)  =  .0328
      FMU(9)  =  .0316
      FMU(10)  = .0309
      FMU(11)  = .0306
      FMU(12)  = .0309
```

```
      EMU(1)  =   0.5
      EMU(2)  =   0.6
      EMU(3)  =   0.8
      EMU(4)  =   1.0
      EMU(5)  =  1.5
      EMU(6)  =   2.0
      EMU(7)  =   3.0
      EMU(8)  =   4.0
      EMU(9)  =   5.0
      EMU(1C) =   6.0
      EMU(11) =   8.0
      EMU(12) =  10.0
      IF (NPRINT-3) 201,199,199
  199 WRITE OUTPUT TAPE 3, 7111
C     CLEAN  STORAGE
  201 DO 7021 I = 1,  20
      B1(I)   =  A(I, JNN)
      B2(I)   =  AINV(I, JNN)
      DO 7021  J = 1,  20
      OMEGA(I,J) = 0.0
      STW(I,J)   = 0.0
 7021 STSW(I,J)  = 0.0
      GAMEN  = PKEN(JNN)
      JK = 1                                                          003
C     CORRECT FOR ATTENUATION IN COPPER TARGET BACKING
      IF (NP - L) 1243, 1243, 1210
 1243 I  =  1
 1244 IF( I - 13)1245, 1251, 1251
 1245 IF(   EMU(I) - GAMEN)  1250, 1250, 1251
 1250 I = I +1
      GO TO 1244
 1251 CNUM    =   EMU(I) - EMU(I - 1)
      CDEM    =   EMU(I) - EMU(I - 1)
      FMUE    =   FMU(I - 1) + (CNUM/CDEM) * (GAMEN - EMU(I -1))
      FMUE    =  8.89 * FMUE
      IF (NPRINT-3) 1252, 1249, 1249
 1252 WRITE OUTPUT TAPE 3, 1235, GAMEN
 1249 DO 1260  I  =  1, L
      THICK  =  0.046 /  ( COSF ((B3(I) - 45.0)/57.29578))
      ATTENC  =  EXPF( - FMUE * THICK)
      B1(I)  =  B1(I) / ATTENC
      B2(I)  =  B2(I) / ATTENC
      IF(NPRINT-3) 1254, 1260, 1260
 1254 WRITE OUTPUT TAPE 3, 1253, B1(I), B2(I), B3(I)
 1260 CONTINUE
      WEUNCTF(A,B,C,G,D)  =  A + (B/4.0)*(3.0*COSF(2.0*D/RA)+ 1.0) +
```

```
     1 (0.015625*C)*(35.0*COSF(4.0*D/RA) + 20.0*COSF(2.0*D/RA) + 9.0) +
     2 (G/512.0)*(231.0*COSF(6.0*D/RA) + 126.0*COSF(4.0*D/RA) +
     3 105.C*COSF(2.0*D/RA)  + 50.0)
C      SET UP POLYNOMIAL MATRICES
       DO 203 I=1,L
       ARGP(I) = COSF((B3(I)/RA))
       POLY(I,1) = 1.0
       POLY(I,2) = 0.5*(3.0*(ARGP(I)**2)-1.0)
       POLY(I,4) = 0.0625*(231.0*ARGP(I)**6-315.0*ARGP(I)**4+105.0*
     1 ARGP(I)**2-5.0)
  203 POLY(I,3) = 0.125*(35.0*(ARGP(I)**4)-30.0*(ARGP(I)**2)+3.0)

       IF(JK-1)206,206,204
  204 DO 205 I = 1,L
       POLY(I,1) = 1.0
       POLY(I,2) = ARGP(I)**2
       POLY(I,4) = ARGP(I)**6
  205 POLY(I,3) = ARGP(I)**4
  206 IF(NP - 3) 1450, 1460, 1470
 1450 DO 1455 I   =   1, L
       POLY(I,3)   =   0.0
 1455 POLY(I,4)   =   0.0
       GO TO 1470
 1460 DO 1465 I = 1, L
 1465 POLY(I,4) = 0.0
 1470 CONTINUE
C      COMPUTE CEE MATRIX
       DO 215 I = 1, L
  215 OMEGA(I,I) = ((1.0)/B2(I))**2
       DO 225 I   =   1, NP
       DO 225 J   =   1, NP
       CEE(I,J)   =   0.0
       DO 225  K   =   1, L
  225 CEE(I,J)   = CEE(I,J) + OMEGA(K,K)*POLY(K,I)*POLY(K,J)
C      INVERT CEE
       DO 7020 I   =   1,20
       DO 7020 J   =   1, 20
       STORE(I,J)   =   0.0
 7020 STSW(I,J) = 0.0
       DO 7030 I = 1, NP
       DO 7030 J = 1, NP
 7030 STORE(I,J) =  CEE(I, J)
       CALLPGAUSS3(NP, ZERO, STORE, STSW  , NERFL)
       DO 230  I   =   1, NP
       DO 230  J   =   1, NP
```

```
  230 CEEINV(I,J)   =  STSW(I,J)
      IF (NERFL - 1 ) 241, 241, 1056
  241 FORMAT (3F20.12/)
      DO 246  J   =  1, NP
      XI(J)   =  0.0
      DO 246 I   =  1, L
  246 XI(J)   =  POLY(I,J)*OMEGA(I,I)*B1(I) + XI(J)
C     COMPUTE COEFFICIENTS AND THEIR SIGMAS
      DO 248 I = 1, NP
      SUM81 = 0.0
      DO 247 K = 1, NP
  247 SUM81 = CEEINV(I,K)*XI(K) + SUM81
  248 COEFT(I) = SUM81
      DIV = COEFT(1)
      DO 249 I = 1, NP
  249 COEFT(I) = COEFT(I)/DIV
      DO 260 I=1, NP
      SCOEFT(I)   =  SQRTF(ABSF(CEEINV(I,I)))/DIV
      SCOEFT(I)   =  SCOEFT(I)*(CEEINV(I,I)/ABSF(CEEINV(I,I)))
  260 TEMP(I) = COEFT(I)/B(I)
      VEESQ1   =  0.0
      DO 993 J   =  1,L
  993 VEESQ1   =  (B1(J)/B2(J))**2 + VEESQ1
      VEESQ2   =  0.0
      DO 994 K   =  1, NP
  994 VEESQ2   =  COEFT(K)*XI(K)*DIV + VEESQ2
      E2   =  L
      EP   =  NP
      EPSSQ   =  (VEESQ1 - VEESQ2)/(E2 - EP)
      DO 8100  I   =  1, NP
      BRA   = (COEFT(I)**2) * CEEINV(1,1) + CEEINV(I,I) - 2.0*COEFT(I)*
     1 CEEINV(I,1)
      BRA   =  BRA*EPSSQ
      SCOEFT(I)   =  (BRA/ABSF(BRA))*SQRTF(ABSF(BRA))/DIV
 8100 TEMP(I+10)   =  SCOEFT(I)/B(I)
C     COMPUTE ANISOTROPY
      IP   =  NP + 1
      DO 259  I   =  IP,  4
      COEFT(I)   =  0.0
      SCOEFT(I)   =  0.0
      TEMP(I + 10) = 0.0
  259 TEMP(I)   =  0.0
      IF (JK - 2)  261, 262, 262
  261 W0 = WFUNCTF(COEFT(1),COEFT(2),COEFT(3),COEFT(4), 0.0)
      W90= WFUNCTF(COEFT(1),COEFT(2),COEFT(3),COEFT(4),90.0)
      IF (NP - 3) 251, 252, 254
```

```
  251 STC(1, JNN, NSETDEX)  =  TEMP(2)
      STSC(1, JNN, NSETDEX)  =  TEMP(2 + 10)


      GO TO 264
  252 DO 253  KE  =  2, 3
      STC(KE, JNN, NSETDEX)  =  TEMP(KE)
  253 STSC(KE, JNN, NSETDEX)  =  TEMP(KE + 10)
  254 GO TO 264
  262 WO  =  0.0
      W90  = COEFT(1)
      DO 263  I=1, NP
  263 WO  =  WO +COEFT(I)
  264 ANISO(JK)  =  WO/W90 - 1.0
      P1  =  (1.0/W90)**2
      SAN(JK)  =  0.0
      DO 7110  I  =  1, NP
      Z(I)  =  (W90*POLY(1, I) - WO*POLY(L, I))**2
 7110 SAN(JK)  =  SAN(JK)  +  Z(I) * (SCOEFT(I)  **2)
      SAN(JK)  =  P1 * SQRTF(SAN(JK))
      IF (NPRINT-3) 265, 7107, 7107
  265 IF(JK-2) 274, 339, 339
  274 CONTINUE
      WRITE OUTPUT TAPE 3, 275
  280 WRITE OUTPUT TAPE 3, 342, (COEFT(I), SCOEFT(I), I = 1,NP)
      WRITE OUTPUT TAPE 3, 1370
      WRITE OUTPUT TAPE 3, 342,(TEMP(I), TEMP(I+10), I=1,NP)
 7107 IF (NPRINT-3) 7104, 7108, 7108
 7108 WRITE OUTPUT TAPE 3, 7112, GAMEN, NP, TEMP(1), TEMP(11), TEMP(2),
     1 TEMP(12), TEMP(3), TEMP(13), TEMP(4), TEMP(14), EPSSQ, ANISO
      GO TO 1058
 7104 WRITE OUTPUT TAPE 3, 295, EPSSQ
      IF ( NPRINT - 1 ) 298, 338, 338
  298 IF(B3(3)-180.0) 297, 297, 320
C     COMPUTE POINTS ON THEORETICAL AND EXPERIMENTAL CURVES
  297 WRITE OUTPUT TAPE 3, 296
      SUM9  =  0.00
  300 WFUNCT = WFUNCTF(COEFT(1), COEFT(2), COEFT(3), COEFT(4), SUM9)/
     1 WFUNCTF(COEFT(1), COEFT(2), COEFT(3), COEFT(4), 090.0)
  315 VFUNCT = WFUNCTF(ALPHA1, ALPHA2, ALPHA3, ALPHA4, SUM9)/WFUNCTF
     1 (ALPHA1, ALPHA2, ALPHA3, ALPHA4, 090.0)
      WRITE OUTPUT TAPE 3, 324, SUM9, WFUNCT, VFUNCT
      SUM9 = SUM9 +15.0
      IF (SUM9 - 090.0) 300, 300, 314
  314 WRITE OUTPUT TAPE 3,316
      WRITE OUTPUT TAPE 3, 1316
```

```
      ADIV = DIV*WFUNCTF(COEFT(1), COEFT(2), COEFT(3), COEFT(4), 090.0)
      DO 318 J = 1,L
      AB1 = B1(J)/ADIV
      AB2 = B2(J)/ADIV
  318 WRITE OUTPUT TAPE3, 317, B3(J), AB1, AB2
      GO TO  338
  320 WRITE OUTPUT TAPE 3, 296
      SUM10  =  270.0
  325 WFUNCT = WFUNCTF(COEFT(1), COEFT(2), COEFT(3), COEFT(4), SUM10)/
     1 WFUNCTF(COEFT(1), COEFT(2), COEFT(3), COEFT(4), 270.0)
  335 VFUNCT = WFUNCTF(ALPHA1, ALPHA2, ALPHA3, ALPHA4,SUM10)/WFUNCTF
     1 (ALPHA1, ALPHA2, ALPHA3, ALPHA4, 270.0)
      WRITE OUTPUT TAPE 3, 324, SUM10, WFUNCT, VFUNCT
      SUM10 = SUM10 +15.0
      IF (SUM10 - 360.0) 325, 325, 634
  634 WRITE OUTPUT TAPE 3,635
      WRITE OUTPUT TAPE 3, 1635
      ADIV = DIV*WFUNCTF(COEFT(1), COEFT(2), COEFT(3), COEFT(4), 270.0)
      DO 637 J = 1,L
      AB1 = B1(J)/ADIV
      AB2 = B2(J)/ADIV
  637 WRITE OUTPUT TAPE3, 636, B3(J), AB1, AB2
  338 JK = 2
      GO TO 204
  339 WRITE OUTPUT TAPE 3, 340
      WRITE OUTPUT TAPE 3,1241, ANISO(1), ANISO(2)
      WRITE OUTPUT TAPE 3,1340
      WRITE OUTPUT TAPE 3,1241, SAN(1), SAN(2)
      IF ( NPRINT - 1 ) 343, 344, 344
  343 WRITE OUTPUT TAPE 3, 341
      WRITE OUTPUT TAPE 3, 342, (COEFT(I), SCOEFT(I), I = 1,NP)
  344 WRITE OUTPUT TAPE 3, 336
      GO TO 1058
 1056 WRITE OUTPUT TAPE 3, 1057, E(JNN)
 1058 JNN  =  JNN  +  1
      JK  =  1
      IF(JNN - NN) 201,201,1210
 1210 IF(NP - 2) 1212, 1212, 1211
 1211 NP  =  NP - 1

      JNN  =  1
      GO TO 201
 1212 CONTINUE
      DO 351  I  =  1,  20
      DO 351  J  =  1,  20
```

```
      STORE(I,J)  =  0.0
      AINV(I,J)  =  0.0
  351 A(I,J)  =  0.0
      L=0
      RETURN
  275 FORMAT(72HOLEAST SQUARE FIT COEFFICIENTS OF LEGENDRE POLYNOMIALS A
     1ND THEIR SIGMAS                                                  /)
  292 FORMAT(F9.6/)
  295 FORMAT(18HOEPSILON SQUARE = , E20.6/)
  296 FORMAT(45HOEXPERIMENTAL FUNCTION   THEORETICAL FUNCTION/)
  316 FORMAT(42HONORMALIZED EXPERIMENTAL COUNTS AND SIGMAS   /)
  317 FORMAT(F20.2, 2F20.5/)
  324  FORMAT(F7.2, F10.6, F20.6/)
  336 FORMAT(2HO  /////)
  340 FORMAT(52HO      ANISOTROPY-P        ANISOTROPY-C                /)
  341 FORMAT(42HOCOEFFICIENTS AND SIGMAS FOR COSINE SERIES/)
  342 FORMAT(2F10.5/)
  635 FORMAT(42HONORMALIZED EXPERIMENTAL COUNTS AND SIGMAS   /)
  636 FORMAT(F20.2, 2F20.5/)
 1057 FORMAT ( 22HOMATRIX CEE SINGULAR       F6.3, 11H MEV GAMMA    /)
 1203 FORMAT( F10.6)
 1235 FORMAT (49 HOSTART ANALYSIS FOR DISTRIBUTION COEFFICIENTS OF  F7.3
     1 ,14H MEV GAMMA RAY /14HOINPUT COUNTS  /)
 1241 FORMAT( 2F20.12 /)
 1316 FORMAT   (81HO              ANGLE              COUNTS              SIG
     1MA                          /)
 1370 FORMAT( 50HOCOEFFICIENTS CORRECTED FOR SOLID ANGLE                 /)
 1340 FORMAT(52HO      SIGMA ANISO-P       SIGMA ANISO-C                 /)
 1635 FORMAT   (81HO                ANGLE                  COUNTS
     1 SIGMA                      /)
 1253 FORMAT ( 8HOCOUNTS= F10.1, 7H SIGMA= F10.1, 7H ANGLE=F6.1   )
     1NC,  F10.7/)
 7111 FORMAT( 115HOENERGY      NP        A0     SIGMA        A2     SIGM
     1A        A4     SIGMA        A6     SIGMA     EPSSQ     ANISO  /)
 7112 FORMAT( F7.3, I8, 10F10.3   /)
      END
      END
```

H. Fortran Listing of Program CONTOUR

```
..JOB*PHELPS CONTOUR - GRAPHS
      PROGRAM CONTOUR
      DIMENSION A(4,4)     , B(4,4),     C(4,4),     DELTA(4),
     1ALPHA( 4, 4), BETA( 4, 4), GAMMA( 4, 4), Y( 4), COEFT ( 4 ),
     2YP(900), XP(900) , YP2(1800), XP2(1800), LTITLE(10)
      SFX   =  30.0
      SFY   =  30.0
      MINOFFX=4
      MINOFFY=4
      LABLENO=0
      MODE=1
      MTITLE=4
      NODCURV =2
      LODCURV =3
      LABEL   =  0
      DO 10 I   =  1, 10
   10 LTITLE(I)   =  (8H          )
      LTITLE(1)   =  8H PHELPS
      LTITLE(2)   =  8H CONTOUR
      RA=57.2957795131
      PI=3.1415926536
      BSINF(A)   =  ATANF( A/SQRTF(1.0 - A**2))
      WRITE OUTPUT TAPE 3,180
      WRITE OUTPUT TAPE 3,190
   20 READ INPUT TAPE 2, 30, NSETS
      DO  270  MA   =  1, NSETS
      M   =  MA
      READ INPUT TAPE 2, 40, JFIND, JSTEP, JFIX, IMAX, JMAX, NCONTS,NPTS
      NGPS   =  NPTS * 2
      READ INPUT TAPE 2, 50, DELTA(JFIX), RHO
      READ INPUT TAPE 2, 60, ((A(I, J), B(I, J), C(I, J), J=1,JMAX),I=1,
     1 IMAX)
      IF (RHO - 0.0 ) 24, 26, 24
   24 DO 25  I   =  1,  IMAX
   25 B(I, 1)   =  B(I, 1)*RHO
   26 WRITE OUTPUT TAPE 3, 200
      WRITE OUTPUT TAPE 3, 210
      WRITE OUTPUT TAPE 3, 220,  ((N, J, A(N,J), B(N,J), C(N,J),J=1,JMAX
     1), N=1,IMAX)
      DO 270  IB   =  1, IMAX
      I   =  IB
 5005 WRITE OUTPUT TAPE 3, 5500, NHANG
      NHANG   =  NHANG   +  1
      MODCURV = 1
      II=   I * 2
      DO 85 J = 1, JMAX
```

```
      ALPHA(I, J) = (A(I, J) + C(I, J))/2.0
      IF( B(I, J) - 0.0 ) 80,70,80
   70 GAMMA(I, J) =(PI/2.0)  *  ((A(I,J)-C(I,J))/ABSF(A(I,J)-C(I,J)))
      S   =  1.0
      GO TO 85
   80 GAMMA(I, J) = ATANF((A(I,J)- C(I, J))/B(I, J))
      S   =  B(I,J)/ABSF(B(I,J))
   85 BETA(I, J)=S*0.5*   SQRTF( B(I, J)**2 + (A(I, J) -C(I, J))**2)
   90 IF(JFIX - 4) 100,100,110
  100 Y (JFIX) = ATANF(DELTA(JFIX))
      GFIX = ALPHA(I, JFIX) + BETA(I, JFIX) *SINF(2.0*Y(JFIX) + GAMMA
     1 (I, JFIX))
      GRA   =  GAMMA(I, JFIX) * RA
      WRITE OUTPUT TAPE 3, 87, JFIX,DELTA(JFIX)
      WRITE OUTPUT TAPE 3, 88, II, JFIX, ALPHA(JFIX), BETA(JFIX), GRA
      GO TO 120
  110 GFIX=1.0
  120 FLNC = NCONTS
      X11 = (ALPHA(I,JSTEP) + BETA(I,JSTEP))*(ALPHA(I,JFIND)+BETA(I,
     1 JFIND))
      X12 = (ALPHA(I,JSTEP) + BETA(I,JSTEP))*(ALPHA(I,JFIND)-BETA(I,
     1 JFIND))
      X21 = (ALPHA(I,JSTEP) - BETA(I,JSTEP))*(ALPHA(I,JFIND)+BETA(I,
     1 JFIND))
      X22 = (ALPHA(I,JSTEP) - BETA(I,JSTEP))*(ALPHA(I,JFIND)-BETA(I,
     1 JFIND))
      AMAX  = MAX1F(X11, X12, X21, X22) * GFIX
      AMIN  =-MAX1F(-X11, -X12, -X21, -X22) * GFIX
      DEL1  =  RA * (PI/2.0 - GAMMA(I, JSTEP)) * 0.5
      DEL2  =  RA * (PI/2.0 - GAMMA(I, JFIND)) * 0.5
      WRITE OUTPUT TAPE 3, 125, II, AMAX, II, AMIN, DEL1 , DEL2
      WRITE OUTPUT TAPE 3, 170, JFIND, JSTEP, JFIX, DELTA(JFIX), II
      DO 265  K  =  1 , NCONTS
      LDEX  =  1
      FLK = K


      K2  =  FLK/2.0
      COEFT(I)  =  AMIN +((FLK - 0.5)/FLNC) * (AMAX - AMIN)
      FLNPTS=NPTS
      DO 16C  N  =  1,  2
        AY1  =  2 - N
      AY2  =  N - 1
      LNA  =  NPTS*(N - 1) + 2 - N
      LNB  = NPTS * N
```

```
      DO 160 L  =  LNA,  LNB
      FLL=L - LNA
      Y(JSTEP) = (FLL/FLNPTS - 0.5) * PI
      GSTEP= ALPHA(I,JSTEP) + BETA(I,JSTEP)*SINF(2.0*Y(JSTEP) +
     1GAMMA(I,JSTEP))
      GFIND=COEFT(I)/(GFIX*GSTEP)
      YY=(GFIND-ALPHA(I,JFIND))/BETA(I,JFIND)
      IF(ABSF(YY)-1.0)130,130,140
  130 YY   =  AY1*BSINF(YY) + AY2*(PI - BSINF(YY))
      GO TO 150
  140 XP( L) =-95.0
      YP( L) =-95.0
      GO TO 160
  150 YY =      (0.5 * (YY - GAMMA(I, JFIND)))
      YY   =  TANF(YY)
      YP(L)   =  ATANF(YY) * RA
      XP(L)=Y(JSTEP)*RA
  160 CONTINUE
      WRITE OUTPUT TAPE 3,230,JSTEP
      WRITE OUTPUT TAPE 3,240, (XP(L), L=1,LNB , 10)
      WRITE OUTPUT TAPE 3,250,JFIND,II,COEFT(I)
      WRITE OUTPUT TAPE 3,260,(YP(L),L=1,LNB , 10)
      L2   =  1
  290 DO 265  L  =     1, NGPS
      IF ( YP(L)  + 95.0 ) 300, 310, 300
  300 YP2(L2)   =  YP(L)
      XP2(L2) = XP(L)
      IF (YP(L+1) +95.0) 318, 330, 318
  318 IF (ABSF(YP(L+1) - YP(L)) - 30.0) 319, 330, 330
  319 IF(ABSF(XP(L+1)-XP(L))-5.0) 320, 330, 330
  320 L2   =  L2  +  1
  310 GO TO 265
  330 IF (L2 - 1 ) 265, 265, 312
  312 CALL GRAPH2 (L2,XP2,YP2,8,MODCURV ,LABLE,LTITLE,SFX,SFY,
     1MINOFFX,MINOFFY,LABLENO,MODE,MTITLE,M)
      MODCURV   =  2
      L2   =  1
  265 CONTINUE
 5000 WRITE OUTPUT TAPE 3, 5500, NHANG
      NHANG   =  NHANG  +  1
      XP(1) = -95.0
      XP(2) = -95.0
      YP(1) = -95.0
      YP(2) = -95.0
      L2   =  2
      CALL GRAPH2 (L2,XP2,YP2,8,NODCURV ,LABLE,LTITLE,SFX,SFY,
```

```
     1MINOFFX,MINOFFY,LABLENO,MODE,MTITLE,M)
5001 WRITE OUTPUT TAPE 3, 5500, NHANG
     NHANG  =  NHANG  +  1
     CALL GRAPH2 (L2,XP2,YP2,8,LODCURV ,LABLE,LTITLE,SFX,SFY,
     1MINOFFX,MINOFFY,LABLENO,MODE,MTITLE,M)
5004 WRITE OUTPUT TAPE 3, 5500, NHANG
     NHANG  =  0
 270 CONTINUE
     WRITE OUTPUT TAPE 3,280
  30 FORMAT( I10)
  40 FORMAT(7I10)
  50 FORMAT(2F10.3)
  60 FORMAT( 3F10.3)
  87  FORMAT(45HOSINE CURVE FOR FIXED MIXING PARAMETER DELTA  I1,
     1 23H WHICH HAS BEEN SET TO  F6.3, 18H FOR COMPUTATION   /)
  88 FORMAT (2HOG 2I1, 3H = F7.3, 3H + F7.3, 9HSIN(2Y +  F7.3, 1H)  /.
 125 FORMAT (2HOA I1, 6HMAX =  F7.4,  3H  A I1, 6HMIN = F7.4,17H X AND
     1Y ANGLES=  2F9.4  /)
 170 FORMAT(  7HODELTA I1,21H IS DEPENDENT, DELTA I1,23H IS INDEPENDENT
     1, DELTA I1,10H FIXED AT F6.4, 18H LEGENDRE ORDER = I1  / )
 180 FORMAT(120H1PROGRAM CONTOUR - P A PHELPS - DELTA INDICES AS FOLLOW
     1S - 3 REFERS TO OBSERVED GAMMA MIXING, 1 REFERS TO PROTON PARTIAL)
 190 FORMAT(116HOWAVE MIXING, 4 REFERS TO CHANNEL SPIN MIXING, 2 REFERS
     1 TO UNOBSERVED GAMMA MIXING AND 5 MEANS  P-GAMMA TRANSITIONS / )
 200 FORMAT(35HO                INPUT COEFFICIENTS      /     )
 210 FORMAT( 90HOLEGENDRE ORDER  DELTA INDEX            A
     1    B                    C                /          )

 220 FORMAT(  I8, I16, 3F20.3   /  )
 230 FORMAT(37HO  VALUES IN DEGREES OF ARCTAN DELTA I1  /)
 240  FORMAT( 10F10.3  )
 250 FORMAT(26HO  VALUES OF ARCTAN DELTA I1, 2H A I1, 5H/A0= F5.3  /)
 260 FORMAT( 10F10.3  )
 268 FORMAT ( A1 )
 280 FORMAT(25HOEND OF PROGRAM CONTOUR  /)
5500 FORMAT(20HOHANG UP PRINT OUT     I3   /)
9001 FORMAT (6I4)
     END
     END
```

REFERENCES

1. A.E. Litherland, et al., Can. J. Phys. 36, 378 (1958)
2. R.K. Sheline, Nuclear Phys. 2, 382 (1957)
3. D.A. Bromley, et al., Can. J. Phys. 35, 1057 (1957)
4. P.C. Broude, et al., Proc. Phys. Soc. (London) 72, 1097 (1958)
5. V.K. Thankappan and S.P. Pandya, Nuclear Phys. 19, 303 (1960)
6. V.K. Thankappan and S.P. Pandya, Nuclear Phys. 39, 394 (1963)
7. N. Hole, et al., Zeitung fur Physik 181, 48 (1941)
8. M.R. Seiler, Phys. Rev. 99, 340 (1955)
9. S. Milani, et al., Phys. Rev. 99, 645 (1955)
10. S.P. Tsytko and Iu.P. Antuf'ev, Soviet Phys. -JETP 3, 993 (1957)
11. N.K. Green and R.F. Wiseman, M.S. Thesis, USNPGS (unpubl.) (1958)
12. L.W. Seagondollar, et al., Phys. Rev. 120, 251 (1960)
13. L.L. Lee and F.P. Mooring, Phys. Rev. 104, 1342 (1956)
14. H. Ohmura, et al., J. Phys. Soc. Japan 16, 593 (1961)
15. U.P. Wild, M.S. Thesis, Univ. of Kansas (unpubl.) (1962)
16. P.M. Endt, et al., Phys. Rev. 95, 580 (1954)
17. P.C. Broude, et al., Phys. Rev. 101, 1052 (1956)
18. P.R. Endt and C.H. Paris, Phys. Rev. 110, 89 (1958)
19. C. Van der Leun and P.M. Endt, Phys. Rev. 110, 96 (1958)
20. A.K. Val'ter, et al., Soviet Phys. -JETP 14, 1035 (1962)
21. Y.P. Antuf'ev, et al., Soviet Phys. -JETP 15, 268 (1962)
22. E.E. Baart, et al., Proc. Phys. Soc. 79, 237 (1962)
23. R.A. Moore, Ph.D. Thesis, Univ. of Kansas (1963)
24. Nuclear Data Sheets, National Research Council of the National Academy of Sciences, Wash., D.C.

25. P.M. Endt and G. Van der Leun, Nuclear Phys. 34, 151 (1962)

26. C.D. Moak, et al., Nucleonics p. 18, Sept., 1951

27. B. Kennedy, M.S. Thesis USNPGS (unpubl.) (1962)

28. J.E. Draper and A.A. Fleischer, Rev. Sci. Instr. 31, 49 (1960)

29. A.M. Hoogenboom, Nucl. Instr. and Meth. 3, 57 (1958)

30. J. Kantele and R.W. Fink, Nucl. Instr and Meth. 15, 69 (1962)

31. J.B. Garg, Nucl. Instr. and Meth. 6, 72 (1960)

32. H.P. Murbach and H. Wilman, Proc. Phys. Soc. (London) B 66, 905 (1953)

33. J.B. Marion, Revs. Modern Phys. 33, 139 (1961)

34. S.E. Hunt and K. Firth, Phys. Rev. 99, 786 (1955)

35. R.B. Murray, in Nuclear Instruments and Their Uses, ed. A.H. Snell, (John Wiley & Son, New York, 1962), Vol. I, p. 82.

36. K.J. Van Oostrum, et al., Nuclear Phys. 25, 409 (1961)

37. J.O. Newton, Nuclear Phys. 21, 529 (1960)

38. J. Vorona, et al., Phys. Rev. 116, 1563 (1959)

39. A.M. Romanov, Soviet Phys. -JETP 12, 1072 (1961)

40. L.W. Seagondollar, Private communication.

41. M.E. Rose, Phys. Rev. 91, 610 (1953)

42. J.M. Blatt and V.F. Weisskopf, Theoretical Nuclear Physics (John Wiley & Son, New York, 1953)

43. D.H. Wilkenson, in Nuclear Spectroscopy, ed. Fay Ajzenberg-Selove, Part B (Academic Press, New York, 1960)

44. R.E. White, Phys. Rev. 119, 767 (1960)

45. D.R. Hamilton, Phys. Rev. 59, 122 (1940)

46. L.C. Biedenhorn and M.E. Rose, Revs. Modern Phys. 25, 729 (1953)

47. H.E. Gove, in Nuclear Reactions ed. P.M. Endt, M. DeMeur, (North-Holland Pub. Co., Amsterdam, 1959) Vol. I.

48. L.C. Biedenhorn, in Nuclear Spectroscopy, ed. Fay Ajzenberg-Selove, Part B (Academic Press, New York, 1960).

49. M. Ferentz and N. Rosenzweig, Table of F Coefficients, ANL-5324, AEC 1955.

50. R. Huby, Proc. Phys. Soc., B 67, 1103 (1954)

51. R. Huby, Proc. Phys. Soc., A 72, 97 (1958)

52. W.T. Sharp, et al., Tables of Coefficients for Angular Dist. Analysis (AECL Chalk River Project Research & Development, CRT-556, Dec. 1953).

53. W.T. Sharp, et al., Graphs of Coulomb Functions (TPI - 70, AEC, Chalk River, 1953).

54. J.F. Mollenauer, UCRL - 9748, Univ. Calif., Aug. 1961

55. N.E. Scofield, U.S. Naval Rad. Def. Lab., TR-447, San Francisco (1960)

56. N.H. Lazar, IRE Trans. on Nuclear Science NS-5, 138 Dec. 1958

57. A.J. Ferguson, Atomic Energy of Canada Limited, CRP - 1055, (AECL-1398), Chalk River (1961)

58. C. Davisson, in Beta and Gamma-Ray Spectroscopy, ed. K. Sigbahn, (Interscience Pub. Inc., New York, 1955)

59. S. Hinds, et al., private communication reported by reference 25.

60. D.D. Watson, et al., Nucl. Instr. and Meth., 23, 157 (1963)

61. C.W. Reich, et al., Nucl. Instr. and Meth., 23, 36 (1963)

62. G.I. Harris, R.A. Moore and D.D. Watson, private communications.

63. C. Broude and H.E. Gove, Bull. Amer. Phys. Soc., 5, 248 (1960)